AN INVESTIGATIVE STUDY OF A SPECTRUM-MATCHING IMAGING SYSTEM

Final Report

By Donald S. Lowe, John Braithwaite, and Vernon L. Larrowe

October 1966

Prepared under Contract No. NAS 8-21000

by
INFRARED AND OPTICAL SENSOR LABORATORY
WILLOW RUN LABORATORIES
INSTITUTE OF SCIENCE AND TECHNOLOGY
THE UNIVERSITY OF MICHIGAN
Ann Arbor, Michigan

NATIONAL AERONAUTICS AND SPACE ADMINISTRATION
George C. Marshall Space Flight Center
Huntsville, Alabama

NOTICES

Sponsorship. The work reported herein was conducted by the Willow Run Laboratories of the Institute of Science and Technology for the National Aeronautics and Space Administration under Contract NAS 8-21000. Contracts and grants to The University of Michigan for the support of sponsored research are administered through the Office of the Vice-President for Research.

Distribution. Initial distribution is indicated at the end of this document.

Availability. Libraries of contractors and of other qualified requesters may obtain additional copies of this report by submitting NASA Form 492 directly to:

Scientific and Technical Information Facility
P. O. Box 5700
Bethesda, Maryland 20014

Final Disposition. After this document has served its purpose, it may be destroyed. Please do not return it to the Willow Run Laboratories.

AN INVESTIGATIVE STUDY OF A SPECTRUM-MATCHING IMAGING SYSTEM

Final Report

By Donald S. Lowe, John Braithwaite, and Vernon L. Larrowe

October 1966

Prepared under Contract No. NAS 8-21000
by
INFRARED AND OPTICAL SENSOR LABORATORY
WILLOW RUN LABORATORIES
INSTITUTE OF SCIENCE AND TECHNOLOGY
THE UNIVERSITY OF MICHIGAN
Ann Arbor, Michigan

NATIONAL AERONAUTICS AND SPACE ADMINISTRATION
George C. Marshall Space Flight Center
Huntsville, Alabama

FOREWORD

The work described in this report was conducted by the Infrared and Optical Sensors Laboratory (M. R. Holter, Head) of the Willow Run Laboratories, a unit of The University of Michigan's Institute of Science and Technology. D. S. Lowe was Principal Investigator and also the coordinating author of this report. Specific aspects of the work and the corresponding sections of the report were undertaken as follows

Data Processing: R. Legault and V. Larrowe

Airborne Subsystem: Optics and Mechanics, J. Braithwaite and E. Work
Electronics, L. Larsen
Performance Estimates, W. L. Brown

The work reported is consonant with and fulfills part of the objectives of a comparative multispectral remote-sensing program of the Laboratory. The goal of the program is to develop methods of improving and extending current remote-sensing capabilities by using the spectral characteristics of surface features of objects being sought. Improvements are sought in the kinds and quantities of data obtainable and in the quality, speed, and economy of the image-interpretation process.

In particular, the work reported is very closely related to and dependent upon that completed by the Willow Run Laboratories under contract to the U. S. Geological Survey, Contract No. 14-08-0001-10053 and that being carried out under the U. S. Geological Survey Contract No. 14-08-001-10108.

ABSTRACT

Techniques are discussed for the classification of remote objects and materials on the basis of the spectrum of the solar radiation they reflect and of the thermal radiation they emit. A specific system for optimizing and evaluating the most promising of these techniques is recommended and described. It consists of an analyzer, a processor, and an airborne data-collection subsystem. The airborne subsystem includes an optical-mechanical ground scanner with which has been integrated a multichannel spectrograph, a control console, and a multichannel tape recorder. This subsystem will collect multichannel spectral data from the strip of territory being overflown. (The video data in any one channel could be used to construct a monochromatic strip map.) These data are recorded on parallel channels, one for each spectral interval. The tapes are later fed to the analyzer, which performs a statistical analysis of selections of the data corresponding to particular classes of objects or materials. The reduced statistics can then be used as classification keys in the processor. By using keys corresponding to a target and appropriate backgrounds, the processor can then locate specific targets from new data obtained with the airborne subsystem. The output of the processor might be in the form of maps showing the distribution of the target(s) of interest or in the form of the statistics of such distributions.

CONTENTS

FIGURES

TABLES

AN INVESTIGATIVE STUDY OF A SPECTRUM MATCHING IMAGING SYSTEM

Final Report

1 INTRODUCTION

This report presents the results of a two-month investigative study of a multispectral scanner system to be used to automatically differentiate or enhance the appearance of selected terrestrial features on the basis of their spectral characteristics in the 0.33- to 13.5-μ region of the electromagnetic spectrum. The sensor would be used to conduct surveys of the earth's natural resources from an airborne platform with ultimate application from spacecraft. The study defines a program for construction and checkout of a laboratory model of the system and evaluation of this new concept.

This new sensor, which we call spectrum-matching imaging system (SMIS), is now within the state of the art because of a number of advances in solid-state components and decision theory. Basically, the sensor looks at each resolution element (scene point) of a scene in many spectral bands simultaneously. By use of pattern-recognition techniques, a decision is made as to whether or not the spectral radiance of each scene point belongs to a set known to exist for a particular terrestrial feature at the time of overflight. The tones in the resulting graphic presentation can then be made to represent how well the spectral radiance or brightness of a given scene point corresponds to a reference or known spectral radiance. A graphic presentation permits the data user to interpret the resulting image or pattern, but in some applications it is visualized that the output can be numerical, e.g., the acreage planted in wheat or the percent vegetative ground cover. It should be noted that this is a radically new imaging-sensing concept since all current imaging sensors observe and display the magnitude of radiance of each scene point in a given spectral interval (cameras, radars, and electro-optical sensors) or the thermal emission (infrared and passive microwaves). SMIS observes the spectral properties of each scene point, makes a decision as to whether or not these properties are common with those being sought, and then displays graphically the results of this decision.

Optical-mechanical scanners are generally used to generate imagery in the spectral regions where photographic or photoemissive detectors are not responsive. In most instances,

these scanners use the sensitive area of a detector element as the scanning aperture. The operating principles of airborne optical-mechanical scanners have been discussed by Holter and Wolfe [1] and are illustrated in figure 1. When mounted in an aircraft or spacecraft, the scanning mirror sweeps the scanning aperture (instantaneous field of view) in lines perpendicular to the flight path, and the forward motion of the vehicle provides scan line advance. With suitable processing and printing the resulting image is a strip map of the scene below, not unlike a television picture with an endless frame. Since the signals from the detectors in an optical-mechanical scanner are electrical, they are amenable to electronic processing in real time prior to display or generation of imagery.

While most scanners use the detector (or a field stop in front of or imaged on the detector) to define the field of view, the entrance slit of a multichannel spectrometer can be used as the field stop, as shown schematically in figure 2. In such a system, each detector of the spectrometer observes the same resolution element of the scene but in a different wavelength region. The output signal from each detector element is a video signal corresponding to the scene brightness in the particular wavelength region of operation. This video signal can be used to generate an image of the scene in the wavelength region as defined by the position of the detector in the spectrometer. The output signals from multiple detectors can be combined to determine the spectral distribution of the radiation from each scene point. This spectral information then can be used selectively to enhance or suppress the brightness of objects or materials in a scene on the basis of their spectral radiance. Thus, the multichannel video data can be fed to a signal processor that is designed to generate a single video signal whose intensity, for example, might be proportional to the probability that the spectrum measured indicates the object or material being sought.

The possibility of material selection on the basis of the spectral distribution of its radiation is quite reasonable. Numerous investigators have made or are making spectral measurements of natural features in situ to optimize single-band imagery, but only a few are attempting to determine the feasibility of recognizing landscape features from their spectral reflectance [2-8]. These measurements are largely confined to the photographic region or are being made by nonimaging sensors. Only in recent programs has the idea of combining spectral and spatial information been considered [2, 4]. An optical-mechanical scanner is not limited to the photographic region and can operate in many bands between 0.33 and 2.5 μ where reflected solar radiation predominates. The discrimination potential of a multispectral scanner is enormous. Assume for the moment that an object's tone can be determined to within one of ten gray levels in any given spectral interval. A multispectral scanner operating in 20 wavelength bands would

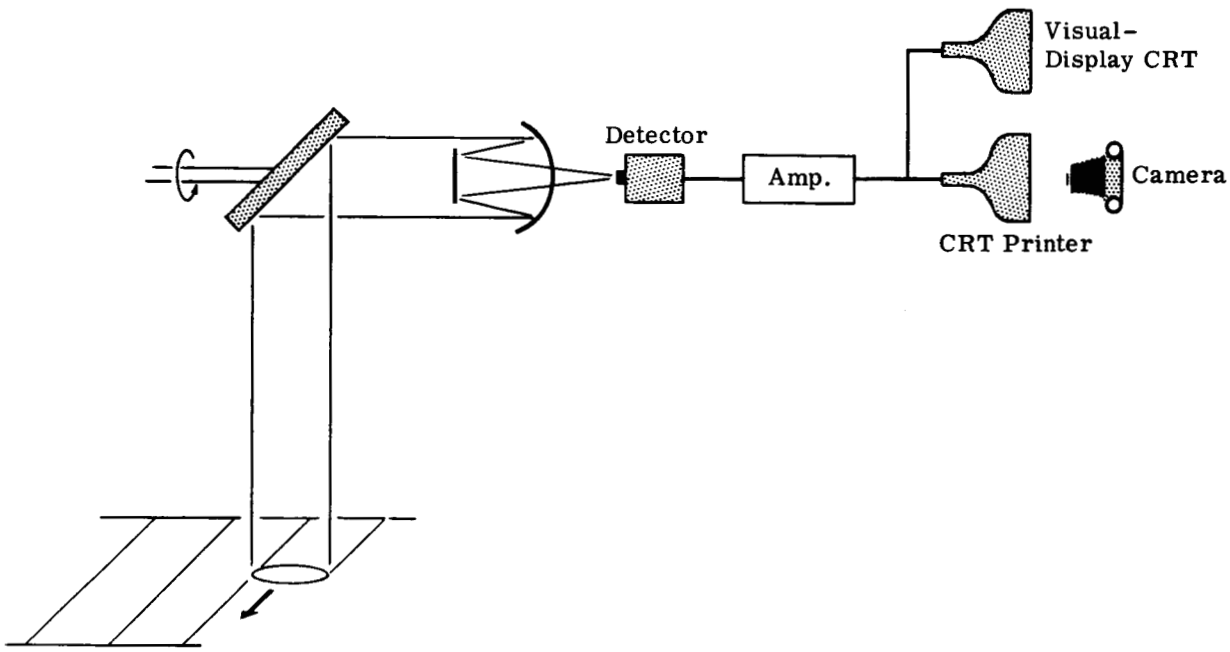

FIGURE 1. SCHEMATIC OF OPTICAL-MECHANICAL SCANNER

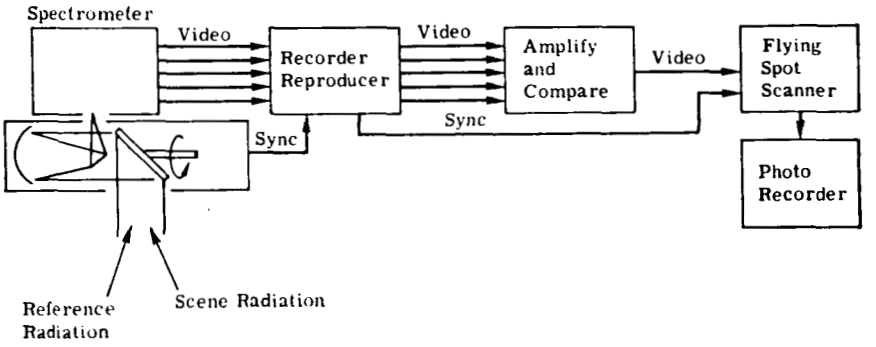

FIGURE 2. SCHEMATIC OF MULTISPECTRAL SCANNER AND DATA PROCESSOR [2]

be capable of distinguishing up to 10^{20} different states. Admittedly, this number of states does not exist in practice: large spectral variations in reflectance and emittance do not occur over narrow spectral intervals in a random manner; variances can occur in a given class of objects; most materials exist as mixtures; and the spectral distribution of the scene illuminance varies. Nonetheless, it is obvious that operation in multiwavelength channels permits one to distinguish between considerably more objects than does single-band operation. As discussed in section 2, the number of wavelength channels of operation is a function of the detector signal-to-noise ratio (SNR) and optical design configuration. Under normal illuminating conditions, the spectral interval of 0.33 to 13.5 μ, where solar reflectance and thermal emittance predominate, can be split into more than 20 bands giving usable signal-to-noise ratios.

To evaluate and demonstrate the potential of SMIS, a 2-phase, 27-month program is required over and above this initial investigative study. Phase I is a 15-month program to build and check out the system. Phase II is a 12-month program to evolve and evaluate signal-processing techniques and to determine the utility of the sensor to various earth-resource applications.

The recommended design of the laboratory model of SMIS, along with rationales and trade-off considerations leading to the performance specifications, is given in section 2. The laboratory model of the system can be considered to be composed of two subsystems: an airborne multispectral data-collecting subsystem and a ground-based signal-analyzing and -processing subsystem.* The design details of the airborne subsystem are, of course, largely dictated by what signal processing and analysis is to be performed by the ground subsystem. The airborne subsystem consists of a simple optical-mechanical scanner with a 6-in.-diameter f/3 collector. The collector images a scene point (3×3 mrad^2) on the entrance slit of a modified Littrow spectrograph. The spectrum from 0.33 to 13.5 μ is dispersed and imaged onto 29 detectors, except for the spectral interval from 5 to 8 μ which is not used because it is heavily attenuated by water vapor. The scanner observes reference calibration sources as well as a sector of terrain $\pm 45^{\circ}$ lateral to the aircraft ground track. The detector signals are amplified and recorded on tape along with pertinent data such as reference levels, gain settings, and synchronous signals.

*Since the laboratory model is used as a research tool to evaluate this new sensing technique and to investigate signal-processing techniques, the signals are recorded in the aircraft and analyzed and processed on the ground. In the final operational model, signal processing may be performed in flight in real time.

At any one instant of time, the simultaneously recorded signals from the multispectral detectors are proportional to the spectral energy emitted or reflected by the source under observation. The ground subsystem is designed to perform two kinds of operations on these signals: (1) select, observe, and format the signals from the sources of interest in order to analyze whether or not terrestrial features of interest have characteristic "spectral signatures" and to determine the optimum detection filter; and (2) playback the multispectral video tapes through a processor using the preferred spectral-pattern-recognition technique, thereby generating a new video signal for pictorial display.

In Phase II, multispectral video data will be collected over areas of interest and under conditions characterized by widely varying environmental parameters such as season, time of day, and meteorological conditions. Spectral signatures of selected targets and backgrounds will be analyzed and optimum recognition techniques will be determined with the aid of a high-speed digital computer. The signal processor in the playback unit will be a versatile analog computer. In association with natural-resources user groups, the resulting imagery will be used to (1) determine the uniqueness of the spectral signature of the feature being sought, (2) determine the effectiveness of this sensing technique for airborne and spaceborne applications, (3) determine desirable display techniques, and (4) provide examples of data from this new sensing system to other possible user groups.

2
PROGRAM DESCRIPTION

The program will be divided into two phases. Phase I is a 15-month program to fabricate and check out the most economical system with which Phase II can be properly implemented. In Phase II, the basic part of the overall program, the hardware and software created in Phase I will be used in a 12-month program of data collection, analysis, and processing to evolve and optimize the data-analysis and -processing methods and then evaluate the overall concept as a tool for use by earth-resource scientists. The theory on which the system depends is introduced in section 2.2. A more formal and mathematical account of this theory is given in appendix I.

During Phase I it will be necessary to design and build an airborne subsystem and a ground subsystem and to develop the software required for their use. The airborne subsystem is a data-collection system with which multi-channel spectral data related to the terrain being overflown can be collected and recorded. The gound subsystem is comprised of a collection of electronic computing and monitoring equipment with which the data recorded by the airborne system can be analyzed or processed (sec. 2.2). The software consists of establishing operational routines for the use of the subsystems and appropriate programs for the use of the general-purpose computers which form an important part of the ground subsystem.

Although the ground subsystem will be assembled primarily from off-the-shelf units, there is no existing hardware suitable for the airborne scanner-spectrometer unit of the airborne subsystem. As the success of the program depends upon data generated with the airborne unit, a preliminary but fairly detailed design study was undertaken to define the airborne unit and its performance requirements. The purpose and operation of this unit are described briefly in section 2.1 and its specifications are detailed in section 2.1.2. An account of the design study and a more detailed description of the resulting design are given in appendix II.

2.1. THE AIRBORNE SUBSYSTEM

The basic concept, which has been explained in section 1 and will be explained in greater detail in sections 2.2 and 2.3, comprises the use of automatic computing equipment to deduce from the spectral content of the optical radiation received from terrain features the nature of these features. The output of an airborne multiband sensory system will be recorded on tape

in the aircraft. The recorded video signals can then be analyzed and processed on the ground with a combination of specialized handling and processing equipment developed for that purpose and large general-purpose computers. The primary requirement that this concept places on the airborne system is, of course, the measurement of the spectrum of that part of the radiant field at the aircraft due to each element of the terrain being overflown. (The size of these elements is selected as a compromise between various factors which will be discussed in section II.1.) These spectra must be available in a form which can readily be transformed into electronic signals suitable for feeding into the computing equipment or, better still, are already in such a form.

Each signal element represents the intensity in one wavelength interval of the radiation coming from one direction which in turn requires two angles for its specifications. Therefore, each signal element must be tagged in some way with these three parameters (wavelength and two angular coordinates). If the information exists or can easily be printed out as an image of the terrain (e.g., a photograph or TV picture), the need for accurate directional information is greatly reduced, as areas of interest can be seen directly on the image readout and thereby marked or gated.

Thus, a series of photographs or TV images of the terrain made simultaneously through different spectral filters will have the sort of information content required. However, such imagery has two serious defects. First, the spectral range is limited to the ultraviolet, visible, and very near infrared. (Infrared vidicons are available but have poor sensitivity.) Second, while the TV videos are already in electronic form and photographs can be turned into electronic form by facsimile scanners, it would be virtually impossible to insure coincidence (registration) of the spectral information. That is, if many photographs (made in different spectral regions) were scanned, it would be extremely difficult to insure that corresponding parts of each photograph are being scanned at the same time.

Both these problems can be avoided if an optical-mechanical scanner is used and if all the radiation of all wavelengths passes through a common path in the scanner through a single field stop* [1] and is then spectrally dispersed onto a matrix of detectors. The dispersion of the radiation leaving the field stop into its several wavelength components could in

*A field stop is the aperture which defines the instantaneous field of view of the optical system. Its image projected backward through the optical system will occur at the ground and will define the area from which radiation is being received at the instant in question.

principle be made in time sequence by means of a scanning spectrometer. This would have to make a complete spectral scan within the time the scanner instantaneous field crosses one resolved element of the terrain. On detailed analysis, this turns out to be quite impracticable from both timing and sensitivity points of view. Alternatively, an array of dichroic beam splitters and filters could be used to insure that only radiation of one wavelength interval reached each detector of a detector matrix, but such an arrangement would have very low optical efficiency. A better scheme is to make the scanner field stop the entrance slit of a spectrograph and place an array of detectors in the focal plane of the spectrograph in such a way that each detector receives some appropriate section of the dispersed spectrum. The feasibility of this scheme has been established in a previous study [9] which also determined the constraints on such a combined scanner-spectrograph. The results of this earlier study have been used as the basis of a preliminary design study for a scanner-spectrograph suitable for the SMIS.

In brief, the airborne subsystem has three principal parts: the scanner-spectrograph assembly, a multichannel tape recorder, and a control console. These are shown schematically in figure 3.

The scanner is an optical-mechanical device which scans the terrain beneath the aircraft in a direction perpendicular to its path. The scan rate is such that the scanned strips either just touch or overlap. Thus, all the terrain in a path whose direction is determined by the ground track of the aircraft is scanned. The width of the path is determined by the scan angle (in this case $\pm 45^{o}$ relative to the nadir) and the aircraft height. The radiation received at any instant coming from the element which the scanner is viewing at that instant is dispersed into 29* relatively narrow wavelength intervals by means of a prism spectrograph. The 29 intervals cover the wavelength range from 0.33 to 13.5 μ as shown in figure 4. The radiation in each of these bands falls onto one of an array of 29 detectors. Two types of photomultipliers (with S-20 and S-1 photocathodes, respectively) and three types of infrared detectors (indium arsenide, indium antimonide, and mercury-doped germanium) are used to obtain optimum performance over the whole wavelength range. The infrared detectors will be mounted in dewars so that they can be maintained at their operating temperatures by filling these dewars with liquified gases. The InAs and InSb detectors will be mounted in one dewar which will be cooled with liquid nitrogen and the Ge:Hg detectors will be in a second dewar and will

*The number of channels is to some extent arbitrary; the spectral resolution used which in turn determines this number is discussed in section II.1.

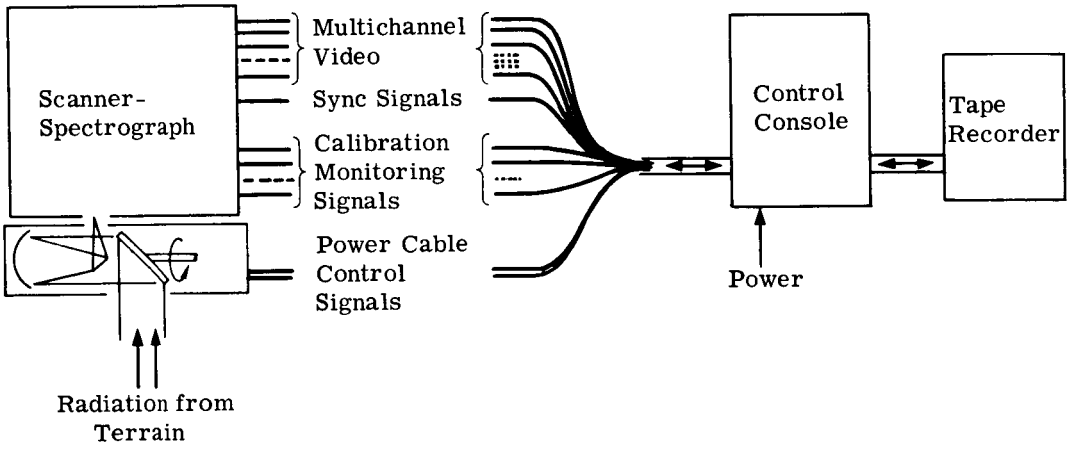

FIGURE 3. SCHEMATIC OF AIRBORNE SUBSYSTEM

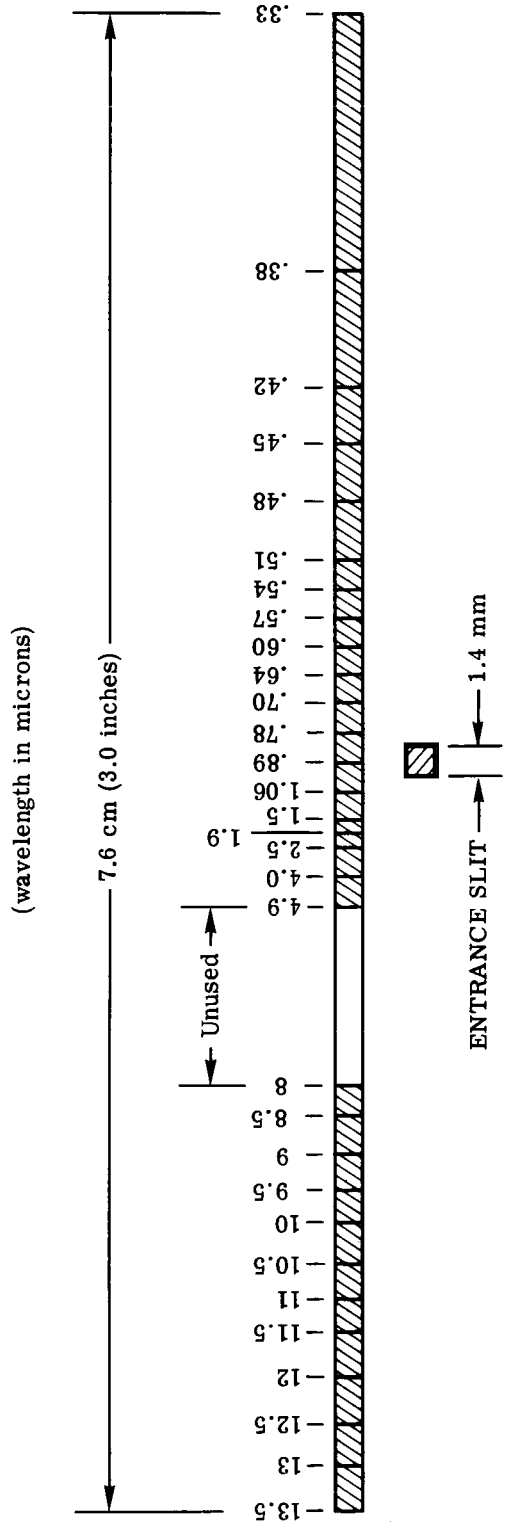

FIGURE 4. SPATIAL DISTRIBUTION OF THE SPECTRUM

be cooled with liquid helium. The output of each detector is amplified to an appropriate level and all, or some convenient selection of, the 29 amplified outputs are recorded simultaneously with a multiplexed, multichannel, wideband tape recorder. Thus, as the scans are performed and as the aircraft moves along its track, video signals are recorded in the various tape channels. Each video signal is proportional to the spectral radiance in one wavelength band of the terrain elements, as these are sequentially and continuously scanned. Image errors resulting from aircraft roll will be corrected by using a roll-error signal from a vertical reference gyro to correct the timing of the scanner synchronization signal. No pitch or yaw correction will be provided, as experience has shown that image distortions caused by pitch and yaw are negligible for normal conditions of flight.

Synchronization, calibration, and other housekeeping signals will also be recorded on the same tape. Operation of the scanner and the tape recorder will be controlled and monitored by two operators using a control console conveniently located in the aircraft.

A detailed description of this subsystem is given in appendix II, together with an account of the various design criteria and possibilities involved and the rationale behind the various choices made. The specifications of the system evolved from this study are given in table I.

2.2. THE GROUND SUBSYSTEM; SIGNAL ANALYSIS AND PROCESSING

2.2.1. INTRODUCTORY DESCRIPTION. A vital part of the SMIS is the signal-analysis and -processing equipment. The signal processor acts as a selective filter and passes only information relating to some chosen item of interest, such as lava flows, concrete highways, asphalt roofs, corn fields, or polluted water. Essentially, the processor may be regarded as an electronic "black box" whose inputs are the various output channels of the multispectral scanner (either direct or tape recorded) and whose output is a strip photograph of the terrain being scanned, with enhancement of some specific objects or materials present on the terrain. An array of dials on the processor would be set in accordance with a previously determined spectral "signature" for the materials to be detected, while another set of dials would be set for suppressing video information on background materials known to be present but not wanted in the output photograph. Thus, the processor would truly act as a filter and pass only video data representing specific terrain objects or materials.

Successful operation of the processor would be dependent upon spectral signature information for the materials or objects present on the scanned terrain which were to be detected. Instrumental in obtaining this signature information would be the signal analyzer. Inputs to the

TABLE I. SPECIFICATIONS FOR THE AIRBORNE SUBSYSTEM

Scanner-Spectrograph Specifications*	Schematic or List of Major Components
1. The Scanner	
Primary-mirror aperture	15-cm diameter (6 in.)
Primary-mirror focal length	45 cm (18 in.)
Primary-mirror figure	18° off-axis paraboloid
Scan mirror	Single face at 45° to spin axis
Scan-mirror rotational axis	Parallel to paraboloid axis
Scan-mirror rotational rate	2000 rpm
Angular width of scanned field	±45°
Field stop (spectrograph entrance slit)	1.4 mm square (0.050 in.)
Instantaneous field determined by field stop	0.003 rad (1/6°)
V/H (maximum)	0.1 rad/sec
2. The Spectrograph	
Dispersing element	30° NaCl prism, back silvered with 20-cm front face
Collimating-mirror aperture	Oval 16 cm high (6 1/4 in.) by 28 cm long (11 in.)
Collimating-mirror figure	Spherical. Radius 75 cm (30 in.)
Pfund-mirror aperture	Oval 14.5 cm high (5 3/4 in.) by 22 cm long (11 in.) with central opening to accommodate entrance and exit beams
Pfund-mirror figure	Flat
Focal-plane radius	37.5 cm (15 in.)
Size of spectrum at focal plane	7.6 cm long × 1.4 mm high
Image slicer	0.33 to 0.38 μ (1 channel). 45° mirror in focal plane
	0.38 to 1.06 μ (12 channels). Fiber-optic bundles
	1.06 to 5.0 μ (5 channels). Infrared fiber-optic bundles with relay lenses
	8.0 to 13.5 μ (11 channels). 45° mirror in front of focal plane
Detectors	0.33 to 0.78 μ (11 channels). S20 photomultiplier tubes
	0.78 to 1.06 μ (2 channels). S1 photomultiplier tubes
	1.06 to 2.5 μ (3 channels). InAs photovoltaic (77°K)
	2.5 to 5.0 μ (2 channels). InSb photoconductive (77°K)
	8.0 to 13.5 μ (11 channels). Ge:Hg photoconductive (4°K)
Cryogenic system	
The infrared detectors will be mounted in dewars and cooled with liquid nitrogen (InAs and InSb detectors) and liquid helium (Ge:Hg detector array)	

TABLE I. SPECIFICATIONS FOR THE AIRBORNE SUBSYSTEM (Continued)

3. Electronics	
Preamplifiers	
0.33 to 1.06 μ	P25Au operational amplifier connected as a follower amplifier with 7.9-μV and 6.0 pA equivalent input noise, 0.02-Hz to 50-kHz bandwidth, gain of 5 and 50 (13 channels)
1.06 to 2.5 μ	2N3089A FET transistor (connected as a source follower and cooled to 77°K) cascaded with an uncooled 2N3117 transistor amplifier. 1.3-μV equivalent input noise. 0.02-Hz to 50-kHz bandwidth, gain of 100 (3 channels)
2.5 to 5.0 μ	Uncooled 2N3117 transistor amplifier 0.91-μV equivalent input noise. 0.02-Hz to 50-kHz bandwidth, gain of 100 (2 channels)
8.0 to 13.5 μ	2N2500 FET transistor (connected as a source follower and uncooled) cascaded with an uncooled 2N311y transistor amplifier. 24-μV equivalent input noise. 0.02-Hz to 50-kHz bandwidth, gain of 100 (11 channels)
Postamplifiers	PP45U operational amplifier connected as a follower amplifier. Gain from 1 to 1000 (29 channels)
Offset circuits	Gain is 1.0 and level is unaffected by amplifier gains (29 channels)
4. Calibration	
0.33 to 0.5 μ	Current-controlled 100-W quartzline lamp (lamp #1) and inside of scanner (zero reference)
0.5 to 1.06 μ	Current-controlled 45-W quartzline lamp (lamp #2) and inside of scanner (zero reference)
1.06 to 2.5 μ	Current-controlled 45-W quartzline lamp (lamp #3) and inside of scanner (zero reference)
2.5 to 13.5 μ	Two temperature controlled blackbody references
0.4 to 2.0 μ	Sunlight directed into scanner
5. Roll correction	Vertical gyroscope signal is used electronically to correct the scanner synchronization signal
6. System sensitivity	See figure 41 in appendix II
7. Recorder	
Type	MINCOM PC500
Number of channels	14 (3 subcarrier FM oscillators used on 11 channels to give 33 channels)
Bandwidth	33 channels 0 to 35 kHz 3 channels 300 Hz to 2 MHz

*The disposition of the major items will be seen in figure 5.

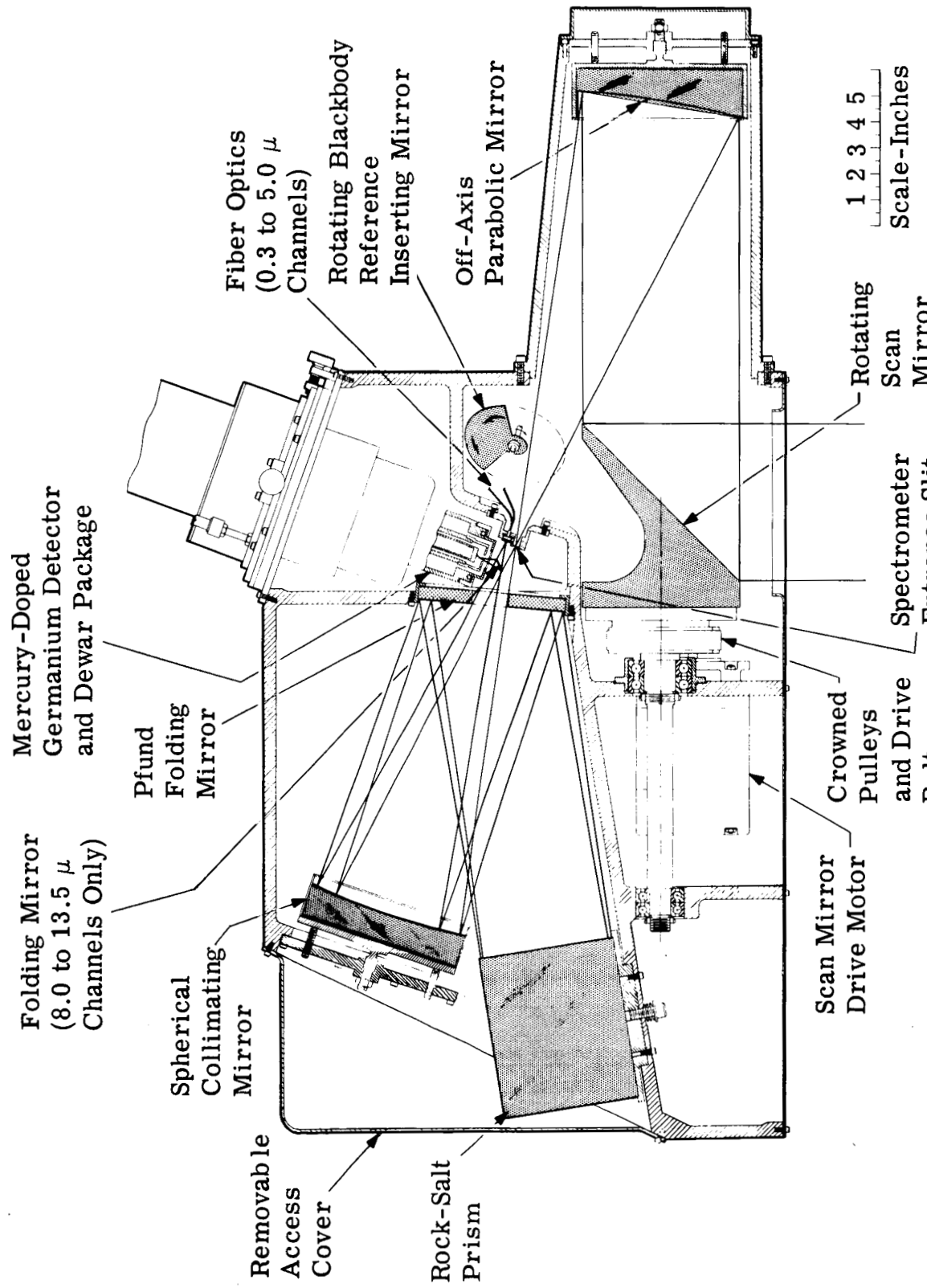

FIGURE 5. THE SCANNER-SPECTROGRAPH

signal analyzer would be output signals of the multispectral scanner for known terrain materials; and the analyzer, operating from this data, would produce a signature representing the material being scanned. Signatures for various materials of interest would be collected and catalogued for later use in setting the dials of the processor.

A block diagram illustrating information flow in the signal-analysis and -processing system is shown in figure 6. In this figure, the signal analyzer is depicted as consisting of two main components, an area selector and a signature computer. When the spectral signature of some known terrain feature, such as a wheat field, is to be determined, a tape recording of multispectral scanner video from the area containing the wheat field to be analyzed is "played back" on the tape recorder to provide multichannel scanner video signals to the signal analyzer. These signals first enter the area selector, where electronically operated switches (gates) are actuated in such a manner as to pass video signals on to the signature computer only at the times when the signals are actually those representing the field to be analyzed. Signals from unwanted fields are eliminated. Thus, the area selector actually selects the portion of the scanned terrain to be analyzed. The edited video from the area selector then passes into the signature computer for subsequent analysis and signature computation. Operating principles and actual mechanization of the signature computer will be discussed below.

After a spectral signature for a field or other terrain feature has been obtained, it may be used to set the processor controls so that the processor will produce an output only when the multichannel scanner video at its input satisfies the requirements specified by the signature used to set the controls. Thus, if the processor controls are set according to a wheat-field signature, the signal processor will produce an output only when the multichannel video at its input represents that of a wheat field. As will be seen in section 2.2.2.2, this spectral curve-fitting approach is not considered to be the optimum signal-processing scheme. The output of the signal processor may be used in two ways. It may be used to produce a picture, showing all scanned terrain areas which have a particular signatures, or it may be electronically integrated and scaled in such a manner as to generate a voltage whose amplitude is proportional to the area of the terrain features having the preset signature. Normally, the signal processor and the signal analyzer would not be used simultaneously.

If the multichannel video is recorded on tape it could be played back into the signal analyzer any number of times searching in turn for any material for which the signature is available.

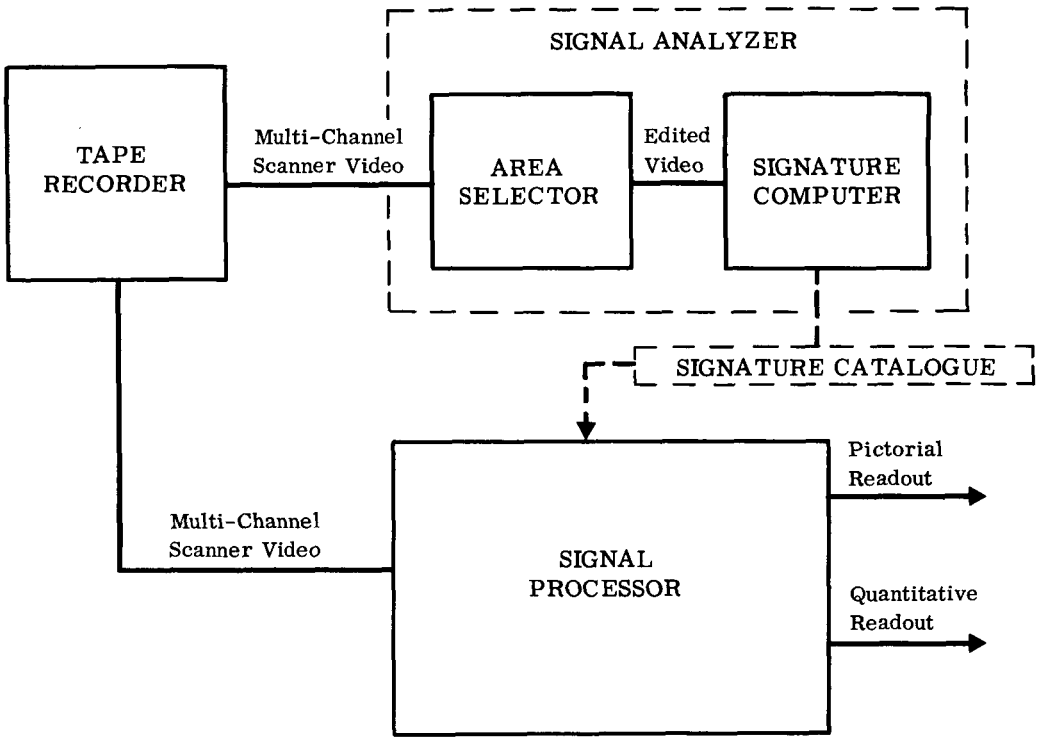

FIGURE 6. INFORMATION FLOW IN THE SIGNAL-ANALYSIS AND -PROCESSING SYSTEM

2.2.2. THE SIGNAL ANALYZER

2.2.2.1. The Area Selector. The area selector is relatively easy to implement if the area to be analyzed is rectangular with its sides parallel to the line of flight of the airborne scanner. For example, a typical strip picture as produced by one of the scanner's video channels might appear as shown in figure 7.

Suppose that the cross-hatched rectangular area labeled A in figure 7 is to be selected by the area selector. If the flight direction is to the right, the left boundary of the field will pass under the scanner at some time t_1, while the right boundary will be passed at a later time t_2. Then during the time interval from t_1 to t_2, the area A is included in the area being scanned. This time interval corresponds to a specific section of the magnetic tape on which the scanner signals are recorded, and the points on the tape corresponding to t_1 and t_2 can readily be found by visually monitoring the tape during playback. Then, if the points t_1 and t_2 are marked on the tape by attaching small adhesive labels on the back at these points, the operator may readily select that section of tape. A more sophisticated approach would be to count scan lines. If the tape format is such that each scan line is individually numbered on an auxiliary tape channel, the times t_1 and t_2 would correspond to specific scan line numbers and the analyzing apparatus could be set to accept only those scan lines whose numbers fell in the interval between the numbers corresponding to t_1 and t_2.

Gating of the portion of each scan line which corresponded to field A could be accomplished by two delay multivibrators and associated apparatus as shown in figure 8.

A synchronizing pulse, recorded on one of the recorder channels, occurs at the start of each scan line. If figure 7 is scanned from top to bottom, the scanner passes the upper boundary of area A at a time interval t_3 from the occurrence of the synchronizing pulse and passes the lower boundary of area A at t_4. The synchronizing pulses from the tape are fed to the two delay multivibrators (fig. 8). The first delay multivibrator emits a pulse at time t_3 and sets the flip-flop, causing it to generate a switching signal which turns on all of the electronic switches to allow the signals from the tape player to pass into the signature computer. The second delay multivibrator emits a pulse at time t_4, and this pulse resets the flip-flop, thus removing the switching signal and cutting off the signals into the signature computer. Thus, the circuit of figure 8 will permit signals to pass from the tape player to the signature computer only during the time interval from t_3 to t_4, which is the time during which area A is scanned.

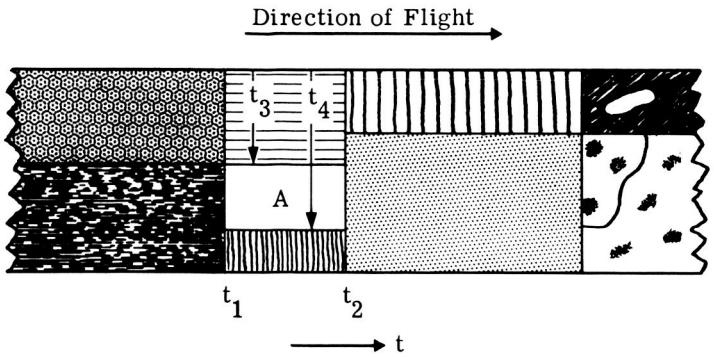

FIGURE 7. EXAMPLE OF AN AREA A TO BE SELECTED FROM A SCANNER AREA

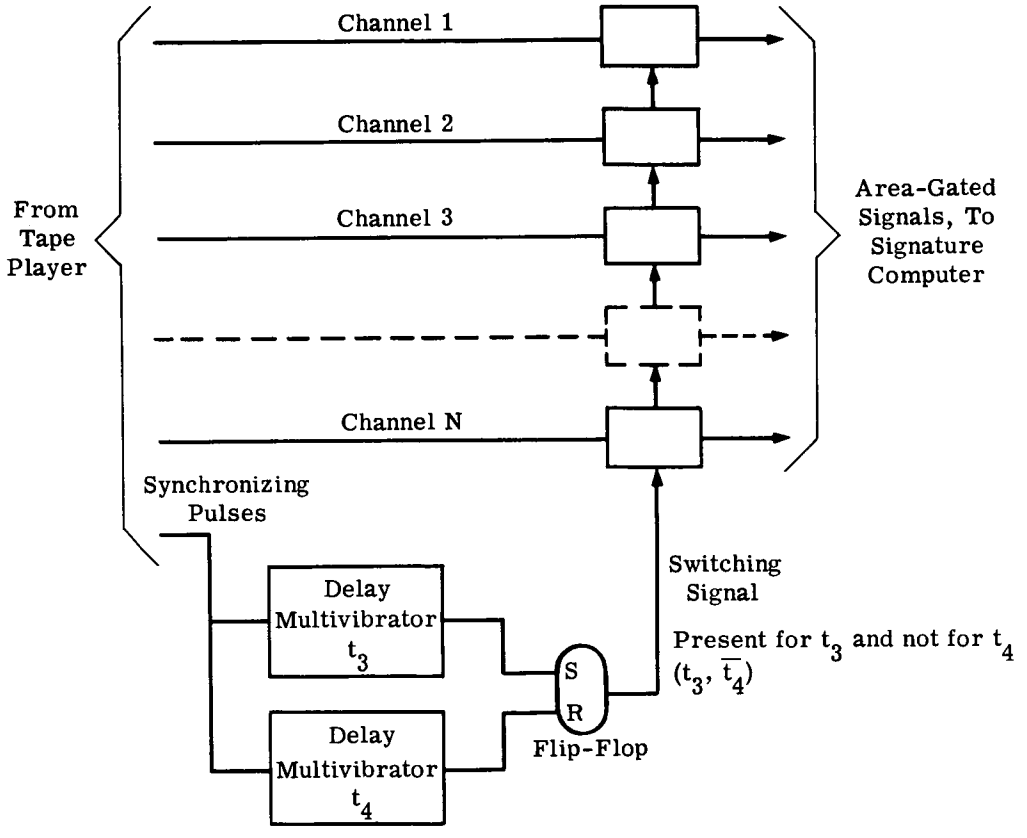

FIGURE 8. CIRCUIT FOR GATING THE PORTION BETWEEN t_3 AND t_4 OF EACH SCAN TIME

If the scanned area which is to be analyzed is not rectangular, the methods just described could be used to select the data from some rectangular area within the area to be analyzed. In most cases, this procedure would yield sufficient data for a satisfactory analysis to be performed.

While the area selector described above is relatively inexpensive and is suitable for large-area targets, the signature of small targets can be extracted only with considerable difficulty. A more versatile system would be a moving window display, one version of which uses a slowly moving tape loop and a high-speed rotating pickup head. This tape-playback system, illustrated in figure 9, permits one to frame and stop any area of interest. From the display of the stationary frame, the multispectral signals from any area can be selected by gates defined by time delays or a light pencil.

2.2.2.2. Analysis Methods

2.2.2.2.1. Nature of Multispectral Data. Before considering methods of analysis, it is better to discuss the nature of the data obtained from the multispectral scanner. Each output channel of the scanner produces an analog voltage whose magnitude is proportional to the intensity of radiation received by the detector which is driving that channel. The scanner is so arranged that each of its detectors responds to a different wavelength range for received radiation. Thus, at any instant of time the voltages present on the scanner's output channels should represent points on the spectral curve for the material being scanned at that instant (fig. 10). Assuming that the curve shown in figure 10 is the spectral curve for the resolution element being scanned at some moment and that the scanning is being performed by a 10-channel scanner, with channel 1 covering a wavelength range of λ_0 to λ_1, channel 2 covering λ_1 to λ_2, etc., each channel output, as indicated by the correspondingly numbered dots, should be proportional to the average height of the curve within the wavelength range covered by that channel. If we had a CRT (cathode-ray-tube) display consisting of 10 dots evenly spaced horizontally, and with the vertical displacement of each dot corresponding to the output voltage of a separate scanner channel, the result would be a dynamic display of the spectral curve of the radiation from the terrain element being scanned. Suppose that the display is being driven from tape-recorded multispectral scanner data and that the tape recorder is operating very slowly so that all fluctuations on the curve can be easily observed. The shape of the curve, as indicated by the dot positions, would be continuously changing as the scanning aperture passes over the varied terrain being scanned. Certainly, the curve could be expected to undergo considerable change in shape as the scanner passes from one material to another, but it would

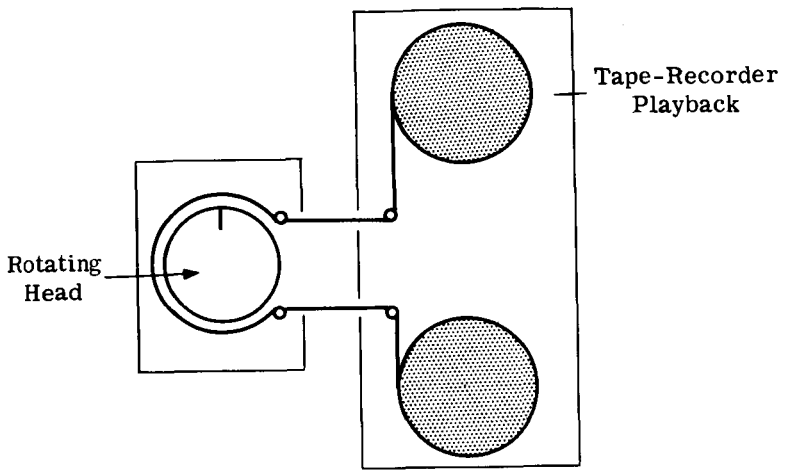

FIGURE 9. SCHEMATIC FOR MOVING-WINDOW DISPLAY

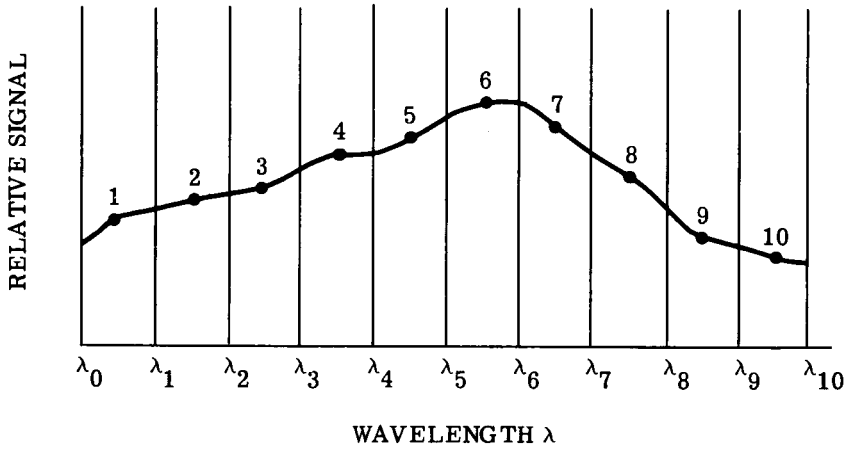

FIGURE 10. SPECTRAL CURVE

also fluctuate considerably while the scanner was covering the same type of material. The problem in analysis for signatures is that of finding some way of mathematically describing and cataloguing the various spectral curves in such a manner that all curves representing the same basic type of earth feature, e.g., a corn field, would fit into one category while curves resulting from different terrain types would fall into different categories. Fluctuations in the curve resulting from changes in temperature, lighting, atmospheric transmission, scanner altitude, and many other factors must be accounted for in such a manner that the signature will not be dependent upon these parameters but only on the nature of the material being scanned.

2.2.2.2.2. Curve-Fitting Approaches. A first approach to the problem of analysis of scanner data for signatures might be one of curve fitting. It seems likely that changes in illumination intensity, atmospheric transmission, and height of the scanner above the terrain will not change the basic shape of a spectral curve for a given material but would only tend to raise or lower the level of the entire curve. Of course, one end of the curve would probably be raised or lowered more than the other, but the fundamental shape of the curve would remain unchanged, and a trained observer, watching a CRT display of the scanner output such as that described above could conceivably recognize the pattern or shape of the curve and so identify various materials. The problem is one of pattern recognition, and any automatic analyzer must be implemented in such a manner that it recognizes and describes the basic shape of the curve.

A simplified first approach to describing the curve shape might be to designate whether the slope of the curve is positive or negative between the various adjacent channels. In figure 10, for example, the slope between points 1 and 2 is positive, as is that between points 2 and 3, 3 and 4, 4 and 5, and 5 and 6. Starting at point 6, however the remaining slopes are negative. If a 1 is used to designate a positive slope and a 0 is used for a negative slope, the curve could be designated by a 9-digit binary number obtained by listing the sequence of the positive and negative slopes. Thus, for figure 10, this number would be 111110000. Clearly, however, there could be many different curves, probably corresponding to different materials, with their first five slopes positive and the remaining slopes negative, so the signature number so obtained would not correspond to only one material. A more sophisticated approach to describing the curve would be to designate the magnitude of each slope. Since these magnitudes would vary with intensity of illumination and other factors not related to the type of material being scanned, it would actually be necessary to designate an acceptable range of magnitudes for each slope for a given material.

Still another possibility would be to first normalize the curve so that some channel, say channel 5, always had the same output magnitude. Thus, all normalized spectral curves would have identical amplitudes for point 5. Then, for each material, the mean amplitudes and permissible deviations from the mean amplitudes for all of the other points on the spectral curve could be specified.

If any of the curve-identification schemes just discussed are found to be satisfactory, it will be a simple matter to implement the processor so that it will pass data only when the spectral curve fulfills any of these specific identification criteria.

2.2.2.2.3. Statistical Analysis. A method of analysis which appears to make full use of all properties of the spectral curves which have been discussed previously as well as all other possibly significant properties uses a statistical approach. A derivation and description of the method is given in more detail in appendix I, so it will only be described very briefly here.

First, the output signals of the n detector channels of the multispectral scanner are defined as the n orthogonal components of an n-dimensional vector. The entire spectral curve, as shown in figure 10, then becomes a single vector in n-dimensional vector space. The spectral curves obtained from many samples of a single terrain feature under various conditions become sample vectors describing a multivariate statistical distribution (in the n-dimensional vector space) which is characteristic of the material being scanned. This distribution may be measured and specified in terms of means and variances of the vector components (scanner-channel outputs) and covariances between the various components. Of course, higher order moments of the distribution could also be computed, but at present it is felt that this is unnecessary. Therefore, an $n \times n$ matrix whose elements are the variances and covariances of the statistical distribution of the spectral vector for a given material may be regarded as the spectral signature for that material. The means must also be specified, as these determine the coordinates of the centroid of the distribution in the n-dimensional space. Then, using the spectral signature of some target material which is to be detected and some signatures of various background materials which are known to be present in the terrain being scanned, we can construct a mechanization of a processor unit which is optimal in the sense that for a given probability of target detection, the probability of false alarm detection of unwanted background material is minimized. The processor implementation will be discussed in more detail in section 2.2.3.3.

2.2.2.3. Analyzer Implementation. Of the various analysis methods discussed in the preceding section, the statistical analysis approach is the most comprehensive. In fact, any of the other methods, except possibly that of visual recognition of spectral curves, may be regarded as a subset of the statistical approach. Therefore, it is recommended that the analyzer be designed to compute statistical signatures.

Although the means, variances, and covariances may be computed with analog equipment, it would be necessary to use a digital computer for the additional steps such as inverting and transforming the matrix (see app. I). Since there is no real-time requirement on analyzer operation, it seems advisable to digitize the information from the scanner channels and perform all analyzer computations digitally.

For most efficient operation, the multichannel data tape could be played back at slow speed and fed through the area selector to an A/D (analog-to-digital) converter, which could then feed a digital computer directly. Since a sufficiently capable digital computer is not available for use in close proximity to the other equipment, however, it will probably be necessary to produce a second analog tape in which the data are sampled and serialized, and then use this tape driving an A/D converter, to produce the spectral information in digital form. The digital output of the A/D converter would be digitally recorded in a format suitable for use as a direct input to a digital computer.

Equipment for serializing and converting the data so that they may be digitally recorded has been developed in the Infrared and Optical Sensor Laboratory of the Willow Run Laboratories for a 14-channel system, so it should be relatively easy to design and construct apparatus for a 28-channel system.

A necessary part of the analyzer would be some means of monitoring the tape to permit setting the area selector and starting and stopping the tape at the correct places to choose the area which is to be analyzed. A C-scan oscilloscope, giving a picture like a slow-sweep television receiver, would probably be suitable for this.

In addition, a CRT display which presented the spectral curve in the manner illustrated by figure 10 would be a useful accessory device. In addition to giving research personnel considerable insight into the nature of the spectrum of the material being scanned, it would also be useful in troubleshooting.

Finally, some type of photorecording apparatus, capable of translating the scanner video into a photograph, should be available for making pictorial records of the scanned area chosen to be analyzed. In summary, the analyzer equipment would consist of

(1) An analog tape playback
(2) An area selector (analog)
(3) A data sampler and serializer (analog)
(4) An A/D converter
(5) A digital tape recorder
(6) A digital computer
(7) A C-scan monitor
(8) A spectral curve CRT display
(9) Photographic recording equipment

Items 4, 5, and 6 are available for project use and thus would not require procurement for this project.

2.2.3. THE PROCESSOR

2.2.3.1. Dependence of the Processor upon the Analyzer. The design of the processor is heavily dependent upon the method chosen for data analysis, since the signatures resulting from this analysis are used for setting up the processor. The statistical approach recommended in section 2.2 would require a more elaborate processor than those which would result from the other analysis methods discussed. At this time, it is not known how detailed a signature description must be in order to be usable. Obviously it is desirable to simplify the processor as much as possible without impairing its effectiveness, but the possibility of simplification can be determined only be experimental procedures. Therefore, the complete processor which is needed for use with statistical descriptions of signals should be implemented, and it may be simplified later if experimental results indicate that simplifications are warranted.

2.2.3.2. Equipment Considerations. The processor accepts multispectral data in analog form, operates on all channels simultaneously, and produces an analog video signal which is used for producing a picture. Since inputs and outputs are analog, and since the processor must operate on a number of channels simultaneously, it appears evident that the processor should be analog rather than digitally oriented. Also, since the proposed method of analysis and processing requires experimental testing, the processor should be made from general-purpose laboratory-type analog computing equipment, so that the actual equipment setup can be readily modified as required. If modern wideband analog equipment is used, the processor should be able to operate in real time without any deterioration of performance over that obtained from slow-time operation.

2.2.3.3. Processor Circuitry and Equipment Requirements. The processor implementation will be considered in terms of the circuitry necessary to make use of the signatures obtained by statistical analysis, as discussed in section 2.2.2.2 and in appendix I. If signatures in the form of variance-covariance matrices for a number of materials have been obtained, the processor can be set up to accept signals representing one specific material while specifically rejecting signals from other background materials. As explained in appendix I, if the distributions of the n-dimensional vectors representing the target and background materials are Gaussian the likelihood ratio equation to be used in the processor is

$$\frac{p_T\sqrt{\left|\theta_T^{ij}\right|}\exp -\frac{1}{2}\left[\sum_{i=1}^{N}\sum_{j=1}^{N}\left(u_i - u_i^T\right)\theta_T^{ij}\left(u_j - u_j^T\right)\right]}{\sum_{k=1}^{M}p_k\sqrt{\left|\theta_k^{ij}\right|}\exp -\frac{1}{2}\left[\sum_{i=1}^{N}\sum_{j=1}^{N}\left(u - u_i^k\right)\theta_k^{ij}\left(u_j - u_j^k\right)\right]} \geq c \qquad (1)$$

where c is a constant which determines the probability of detection

θ^{ij} are the elements of the inverse of the variance-covariance matrix for the target material

θ_k^{ij} are the elements of the inverse of the variance-covariance matrix for background material k

u_i, u_j are the signals from the ith and jth channels of the scanner

u_i^T, u_j^T are the means of the ith and jth channels when the target is being scanned

u_i^k, u_j^k are the means of the ith and jth channels when material k is being scanned

p_k is the estimated percentage of k material in the area being scanned

N is the number of scanner channels

M is the number of background materials considered

Analog mechanization of equation 1 requires an unreasonably large number of multipliers. As shown in section I.3, because of the nature of the variance-covariance matrices, it is possible to rewrite equation 1 in a form which involves squaring function generators rather than multipliers:

$$\frac{P_T \sqrt{\left|\theta_T^{ij}\right|} \exp\left[-\sum_{i=1}^{N}\left(y_i^T\right)^2\right]}{\sum_{k=1}^{M} p_k \sqrt{\left|\theta_k^{ij}\right|} \exp\left[-\sum_{i=1}^{N}\left(y_i^k\right)^2\right]} \geqq c \tag{2}$$

where

$$y_i^T = \sum_{j=i}^{N} b_{ij}^T \left(u_i - u_i^T\right) \qquad i = 1, \ldots, N \tag{3}$$

and

$$y_i^k = \sum_{j=i}^{N} b_{ij}^k \left(u_i - u_i^k\right) \qquad i = 1, \ldots, N \tag{4}$$

The coefficients b_{ij}^T and b_{ij}^k are constants which may be computed digitally from the elements θ_T^{ij} and θ_k^{ij}. The determinants $\left|\theta_T^{ij}\right|$ and $\left|\theta_k^{ij}\right|$ are also constants.

Analog computation of an exponential of the form

$$e^{-\sum_{i=1}^{N}\left(y_i^T\right)^2}$$

starting with the u_i's for N channels is a straightforward process and may be accomplished by the circuit shown in figure 11. The signals $[u_1, u_2, \ldots, u_n]$ from the scanner enter at the left as shown. First the terms $u_i - u_i^T$ are formed and these terms are linearly combined to form the y_i^T's at the outputs of the summing amplifiers which are approximately horizontally centered in the figure. Note that both $+\left(u_i - u_i^T\right)$ and $-\left(u_i - u_i^T\right)$ must be formed in each case because the coefficients b_{ij} may be either positive or negative. Each y_i^T is then squared, the squares are added in a summing amplifier, and the voltage representing the sum of the $\left(y_i^T\right)^2$ terms drives an exponential function generator to produce

$$e^{-\sum_{i=1}^{N}\left(y_i^T\right)^2}$$

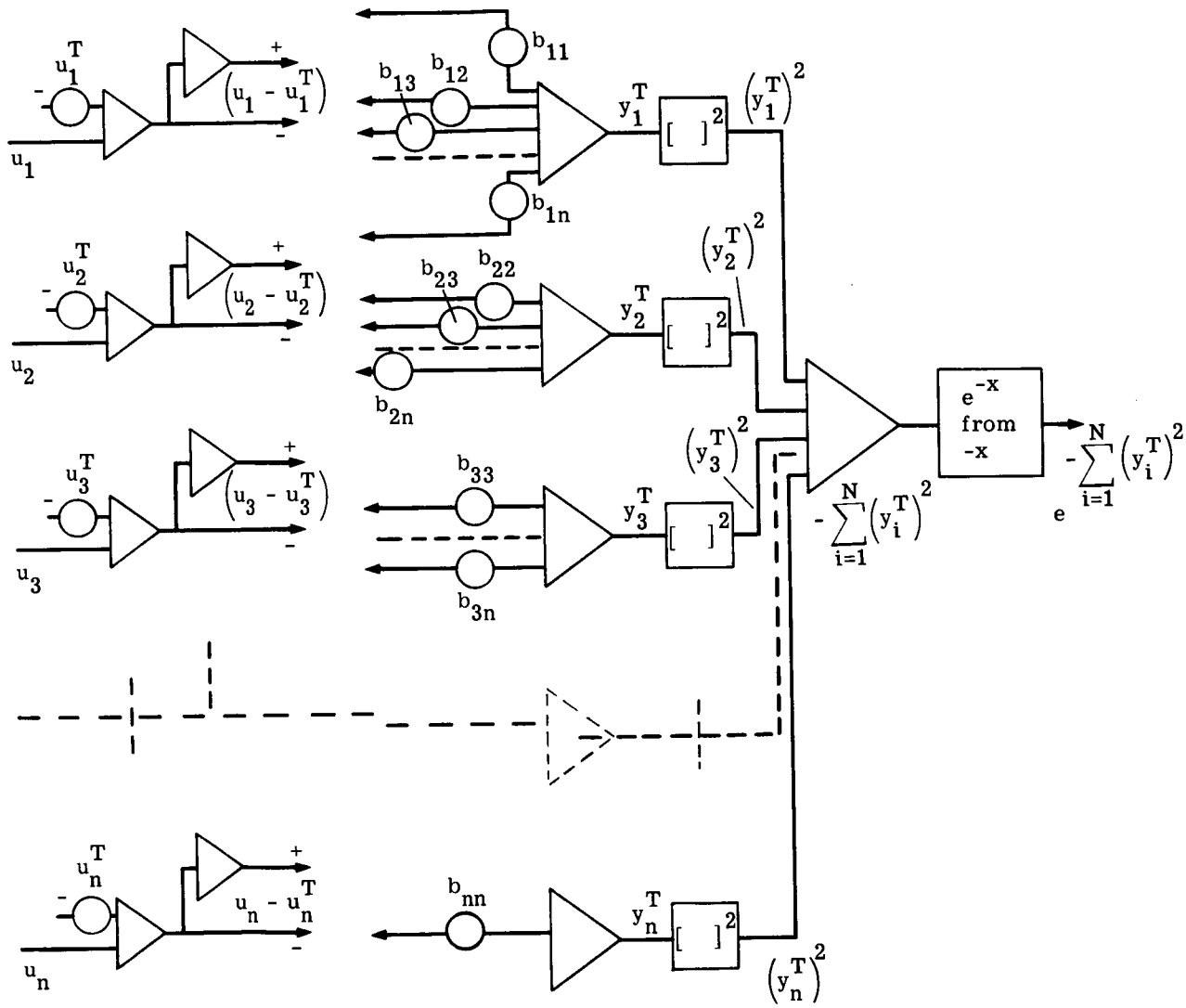

FIGURE 11. ANALOG COMPUTER CIRCUIT FOR GENERATING $e^{-\Sigma y}$

Equipment requirements can be determined from figure 11. From inspection, it is apparent that the circuit requires 3N + 1 summing amplifiers, N squarers, and one exponential function generator. Formation of all N of the $\left(u_i - u_i^T\right)$ terms requires N coefficient potentiometers. Formation of the y_1^T term requires N coefficient potentiometers. The y_2^T term requires N - 1 potentiometers, the y_3^T term, N - 2, and so on, with the y_N term requiring only one. Total potentiometer requirements for generating all N of the y_i^T terms is therefore $1 + 2 + 3 + \ldots + N$ or $\frac{N(N+1)}{2}$, and including the N potentiometers for the $\left(u_i - u_i^T\right)$ terms brings the total for the circuit to $N + \frac{N(N+1)}{2}$ potentiometers. In summary, then, the analog computing equipment requirements for the circuit of figure 11 are

1	exponential function generator
N	squaring function generators
3N + 1	operational amplifiers
$N + \frac{N(N+1)}{2}$	coefficient potentiometers

A circuit similar to that of figure 11 is required for each of the denominator terms of equation 2 as well as for the numerator, thus making a total of M + 1 circuits of this type if M background materials are to be specifically rejected. Figure 12 shows a block diagram of the entire analog setup for mechanizing equation 2. It amounts to a block diagram of the processor. Each block at the left side represents a circuit like that of figure 11. There are M + 1 of these. The one labeled $e_T^{-\Sigma}$ generates the numerator of equation 2 while each of the blocks labeled $e_i^{-\Sigma}$ (where i = 1, 2, . . . , M) generates one of the denominator terms. The numerator and each denominator term are multiplied by their coefficients as specified by equation 2 and the numerator is divided by the weighted sum of the denominator terms to form the quotient B/A, corresponding to the left side of equation 2. The comparator then produces an output voltage whenever $B/A \geq c$, and this output may then be used as an input to the pictorial and quantitative readout devices.

Including the equipment requirements previously determined for each of the $e^{-\Sigma}$ circuits, the total analog equipment requirements for the processor are

M + 1	exponential function generators
(M + 1)(N)	squaring function generators
(M + 1)(3N + 1) + 1	operational amplifiers
$(M + 1)\left(N + \frac{N(N+1)}{2}\right) + M + 2$	coefficient potentiometers
1	divider
1	comparator

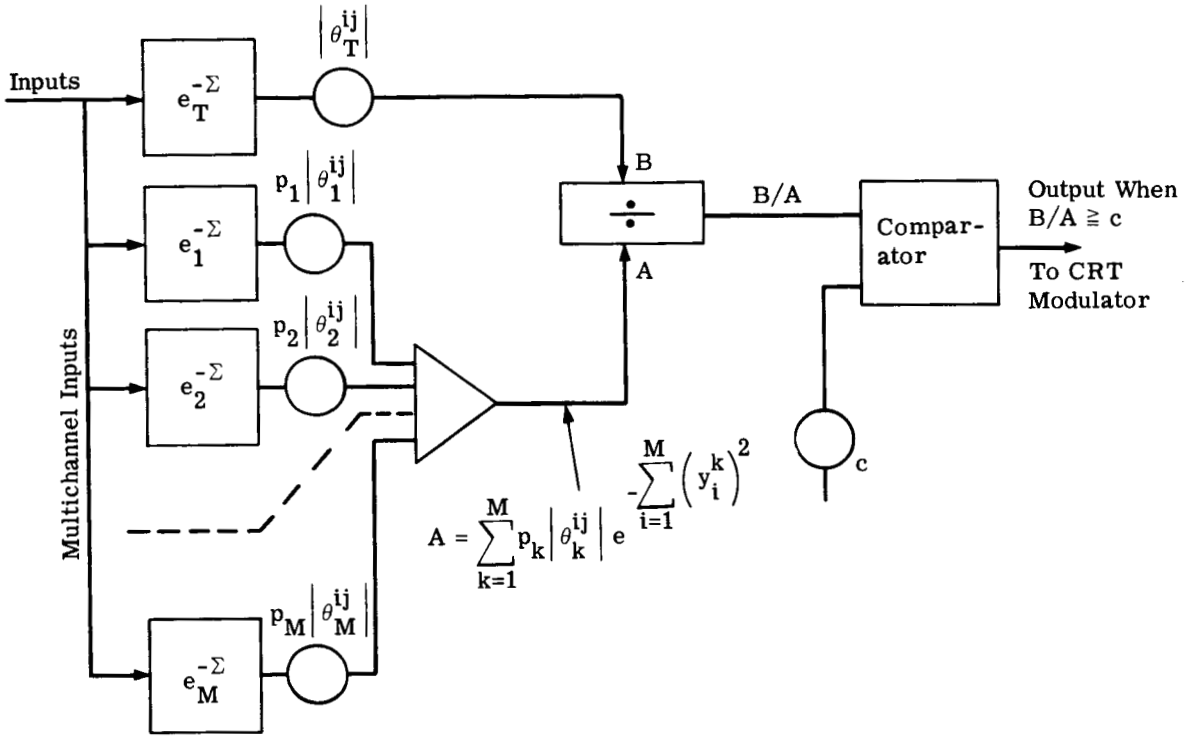

FIGURE 12. BLOCK DIAGRAM OF THE PROCESSOR

where N is the number of channels and M is the number of background materials considered. The equipment requirements can be quite large. For example, for M = 10 and N = 28, the requirements would be

11 exponential function generators
308 squaring function generators
936 operational amplifiers
4478 coefficient potentiometers
1 divider
1 comparator

Clearly, the requirements for potentiometers, operational amplifiers, and squaring function generators are excessive, so either M or N or both should be reduced. The analysis studies in Phase II will point to the required values of M and N for effective detection and discrimination.

2.2.3.4. Processor-Output Presentation. The output signal from the processor may be a constant whenever the scanner is scanning target material and zero otherwise. Some of the output displays and presentations for which it may be used are discussed in the following sections.

2.2.3.4.1. Photorecording. The processor output signal may be mixed with video from one of the scanner channels to produce a video signal in which target areas are enhanced, or it may be used alone as a video signal to produce a picture showing the areas covered by the target material. In either case, some type of photorecording equipment is needed. It is believed that a cathode-ray tube would be superior to a glow-tube with mechanical scanning for producing the image, and a cathode-ray tube with a fiber-optics face which could be placed in contact with the recording photographic medium would be superior to a conventional CRT with a lens for projecting its image onto the recording medium. Consequently, it is recommended that the photorecording setup employ a CRT with a fiber-optics face and a film transport mechanism which keeps the film in contact with the CRT face. The photorecording apparatus should be capable of using fast-developing as well as conventional photographic materials.

2.2.3.4.2. Live Displays. If several hundred scan lines were recorded on a short length of tape and this length of tape were repetitively scanned at a high rate, the resulting signal could be used to generate a television type of picture on a large CRT screen. Such a device

would be quite useful for examining processed as well as unprocessed video and would save much time in equipment setup and testing. Methods of producing a live display of this type will be discussed in more detail in section 2.2.4.

2.2.3.4.3. Quantifiers. Another use of the processor output would be the determination of the quantity of target material scanned. This could be easily accomplished by feeding the processor output signal into an analog integrator. The integrator output, then, would be directly proportional to the amount of target material scanned.

2.2.4. TAPE RECORDING. The tape-recording and playback equipment forms the link between the scanner and the analyzer or the processor in the SMIS. It also provides a means for permanent storage of scanner output data in a form which may be played back for further analysis at any convenient time. It is important, therefore, that the tape-recording and playback systems be capable of handling the multispectral data without introducing any significant noise or distortion.

2.2.4.1. Tape-Recorder Specifications

Bandwidth. The recorder should have sufficient bandwidth to prevent blurring of fine details in the picture, but excessive bandwidth would produce excessive noise and would be needlessly more expensive. A convenient formula, based on experimental observations, which relates rise time and bandwidth in amplifiers is as follows [10]:

$$\text{rise time} = \frac{0.35 \text{ to } 0.45}{B} \text{ sec} \tag{5}$$

where B is the bandwidth in cycles per second and the rise time is the time required for the output to go from 10% to 90% of its final value when an input voltage is suddenly applied to the amplifier. Assuming that the tape record-reproduce system behaves as an amplifier would, and using the larger numerator constant in the equation, the bandwidth would be given by

$$B = \frac{0.45}{\text{rise time}}$$

It is now necessary to determine the rise time for the scanner. If the scanner rotates at 2000 rpm, the number of milliradians of angle scanned per second is given by:

$$\text{scan rate} = \frac{2000}{60}(1000)(2\pi) = 209{,}440/\text{sec}$$

and the time to scan 1 m is $(209,440)^{-1}$ or 4.77 μsec. If this is set equal to the rise time, the required bandwidth would be

$$B = \frac{0.45}{4.77 \times 10^{-6}} = 94 \times 10^{3} \text{ Hz}$$

If the rise time corresponded to the time required to scan 2 mrad, the required recorder bandwidth would be reduced to one-half of 94 kHz or 47 kHz. A curve showing bandwidth requirements versus milliradians of scan for the rise time is plotted in figure 13.

Since the scanner resolution is 3 mrad, it seems reasonable to use this value of scan angle for one rise time. Doing this results in a bandwidth requirement of 31 kHz. Thus, a specification of a 35-kHz bandwidth for the tape-recording system would provide some margin with respect to the 31-kHz figure.

Number of Channels. The multispectral scanner has 29 output channels, so a capability of recording at least 29 data channels plus other information such as scan line number, ambient illumination, and scanner altitude is required. Each data channel should have a flat frequency response from dc to 35 kHz.

Output Linearity and Accuracy. Since the correct operation of the analyzer and the processor depends heavily upon the accuracy of the input data, the error tolerance for the recording system should be as low as possible. Maximum errors in linearity and accuracy on the order of 1% would be acceptable, but better figures than this would be desirable.

Wow, Flutter, and Speed Accuracy. Since wow and flutter directly contribute to noise on the recorded data and the calibration accuracy is dependent upon the accuracy of the speed of the tape transport, it is essential that the tape-recording and reproduce mechanisms employ electronic speed-compensation systems to reduce wow, flutter, and speed variations to a minimum.

2.2.4.2. Choice of Tape Recorder. Instrumentation tape recorders having 29 or more channels, each with a frequency response to 35 kHz, are not standard commercially available items. However, it is entirely feasible to use a standard wideband 14-channel recorder and multiplex two or three data channels on each of the tape-recorder channels. The simplest scheme for recording three data channels on a single tape-recorder channel would involve the use of three voltage-controlled oscillators, each with a different average frequency. Each of the three data channels to be multiplexed would frequency modulate one of the oscillators, and the signals from the three oscillators would be electronically added and recorded on one tape-

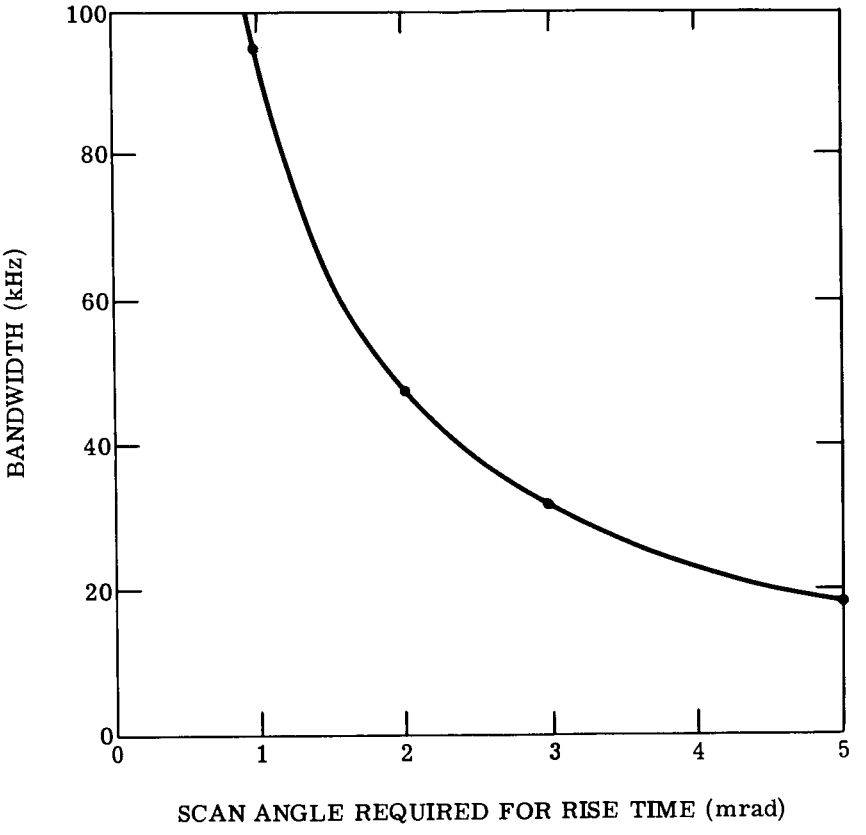

FIGURE 13. BANDWIDTH REQUIREMENTS AS A FUNCTION OF SCAN ANGLE OCCUPIED BY RISE TIME

recorder channel. When the channel is played back, the three recorded frequencies could be separated by filters, and each applied to a demodulator unit to recover the original data signal. Equipment for performing operations of this type is commercially available.

It would be possible to use a wideband single-channel video-type recorder and multiplex all 29 data channels on this single recorder channel, but the crosstalk problems would be greater and there could be troubles with synchronization. It is recommended, therefore, that a 14-channel instrumentation recorder with multiplexing of signals on the individual channels be used.

2.2.4.3. Recording Format. The tape-recording format which will eventually be used cannot be specified in detail at this time. The equipment will be quite flexible, however, so that the format may be changed easily whenever a change is desirable. A possible use of the 14 tape-recorder channels would be as listed in table II.

Table II lists a 3-scanner channel multiplex on each of 11 recorder channels, thus giving a recording capability of 33 channels. Since the scanner has only 29, the four extra are available as spares in case of malfunction of one or more of the assigned channels.

Tape-recorder channel 12 would be a direct-record channel and would be used for recording oral comments and notes during the flight.

Tape-recorder channel 13 would be used for recording the scanning-line number (for use in the area selector), the altitude of the scanner, ambient illumination, temperature, and other miscellaneous data.

Since the recorder would have a bandwidth of about 2 MHz for direct record, it would be feasible to record a standard television video signal on one of the channels. It is recommended that the vehicle carrying the scanner be fitted with an inexpensive vidicon-type television camera, oriented to cover the area being scanned. The signal from the camera would be direct recorded on channel 14. Then, when the tape is being played back, a standard TV monitor connected to the output of channel 14 would show the area being covered. An index line could be placed on the monitor to indicate the part of the scene being scanned at any instant by the multispectral scanner. This would be of considerable help in monitoring the tape playback, identifying particular scenes, finding desired data on the tape, etc.

2.2.4.4. Moving-Window Display. In addition to other tape-recording equipment, a repetitive playback device using a tape loop and a high-speed moving head for producing a stationary-

TABLE II. SUGGESTED CHANNEL ASSIGNMENTS FOR THE TAPE-RECORDING SYSTEM

Tape-Recorder Channel	Use
1	3 Scanner Channels (Multiplex)
2	3 Scanner Channels (Multiplex)
3	3 Scanner Channels (Multiplex)
4	3 Scanner Channels (Multiplex)
5	3 Scanner Channels (Multiplex)
6	3 Scanner Channels (Multiplex)
7	3 Scanner Channels (Multiplex)
8	3 Scanner Channels (Multiplex)
9	3 Scanner Channels (Multiplex)
10	3 Scanner Channels (Multiplex)
11	3 Scanner Channels (Multiplex)
12	Direct record, voice comments
13	Scanning line count, altitude, ambient light, temperature, and other data
14	Television picture of area being scanned

or moving-window display would be useful in area selection and in monitoring. A device of this type is described in section 2.2.2.1 and illustrated by figure 9. This unit is also commercially available and will be listed in the recommended ground equipment.

2.3. PHASE II—SIGNAL-PROCESSING STUDY AND SYSTEM EVALUATION

This phase of the development program follows the fabrication and functional checkout of the laboratory model of SMIS. Multispectral video data will be collected over two or three areas of interest under a variety of environmental conditions (weather, time of day, and season). Each area will be thoroughly documented as to its contents and condition at the time of overflight and simultaneous aerial photography in black and white, infrared, color, and infrared camouflage-detection film will be generated. The photography will be used as a reference with which to evaluate the potential of SMIS.

The spectral signals from calibration sources, targets, and backgrounds will be extracted from the taped video data. These will be used to produce quantitative spectra of the radiance of selected scene points. These spectra of identified and classified objects together with a record of the factors which may seriously affect them (such as illuminating conditions, sun angle, observation angle, ground conditions, season, growth state, etc.) will be used in the analysis performed with a digital computer. The analysis will determine the signal-processing procedure which will minimize false-alarm counts from a model background for a given detection probability of a material.

The optimal signal-processing technique is not known at this time and determination of the signal-processing requirements is to be one of the major outputs of the Phase II effort. Included in this analysis will be the determination of the signature variance introduced by operational and environmental parameters, such as view angle, sun angle, cloud cover, season, and geographical location. From these data the degree of compensation or correction for variations in these parameters can be assessed. In principle, many of these corrections can be made automatically, although some may require auxiliary measurements by the multispectral scanner, e.g. observation of the solar spectral irradiance at the time of the flight. While the detailed signal-processing requirements are not known, it is fairly certain that the statistical analysis approach (or some variation thereof) as discussed in section 2.2.2.2 and appendix I will be preferred.

Once the signatures of features of interest are acquired, the multispectral video tapes will then be played back through the processor and the processed image will be evaluated in the

following manner. Working with user scientists, the capability of SMIS in at least two modes of operation will be analyzed:

(1) The ability of SMIS to identify outright a selected object or class of objects with a given probability of detection and within an acceptable error or false count. Such detection would be useful for such applications as land-use classification and agricultural surveys.

(2) The improvement in interpretation of images generated by SMIS as compared with conventional imagery such as photography. Interpreters of conventional imagery rely heavily on shape, texture, tone, and environment. The tones in imagery from SMIS can be just a graphic presentation of processed information or video from a given channel with processed data superimposed. Further, the processed signal can vary from binary (yes, no) to continuous tone where brightness represents the probability of identification. The optimum display technique for maximizing the interpretability of SMIS imagery is not known and must be evolved by working closely with the user-interpreters. The ultimate question which the user-interpreter must answer, of course, is "does SMIS expedite identification or bring out information that would be lost by other sensors?"

3
PROGRAM SCHEDULE

3.1. PHASE I

Schedules for the airborne subsystem and the ground subsystem of Phase I are given in figures 14 and 15, respectively. The need for a 15-month program is determined by the time needed to detail the design of the scanner-spectrometer and its associated electronics, to breadboard the latter, and to provide adequate time for check out and retrofit. While it is not anticipated that the optical-mechanical system will need to be reworked after initial assembly, it is to be expected that some changes will have to be made in the low-level and other circuitry to obtain optimum performance both on the bench and after installation in the aircraft.

A delivery time of five or six months is expected for the detector arrays and some of the optical components, but this will not affect the envisaged program. The ground subsystem could be completed in less time, but its schedule has been stretched to be compatible with the airborne-subsystem schedule.

3.2. PHASE II

A year's program is proposed for Phase II (fig. 16). This allows measurements to be made over a complete seasonal cycle, but, more important, it is regarded as the least time in which the personnel engaged in data analysis and processing could both obtain a deep understanding of the overall system and optimize their techniques.

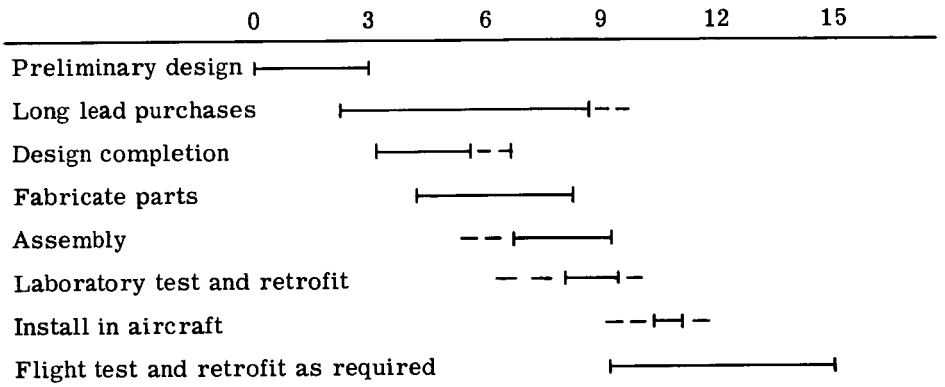

FIGURE 14. SCHEDULE FOR PHASE I: THE AIRBORNE SUBSYSTEM

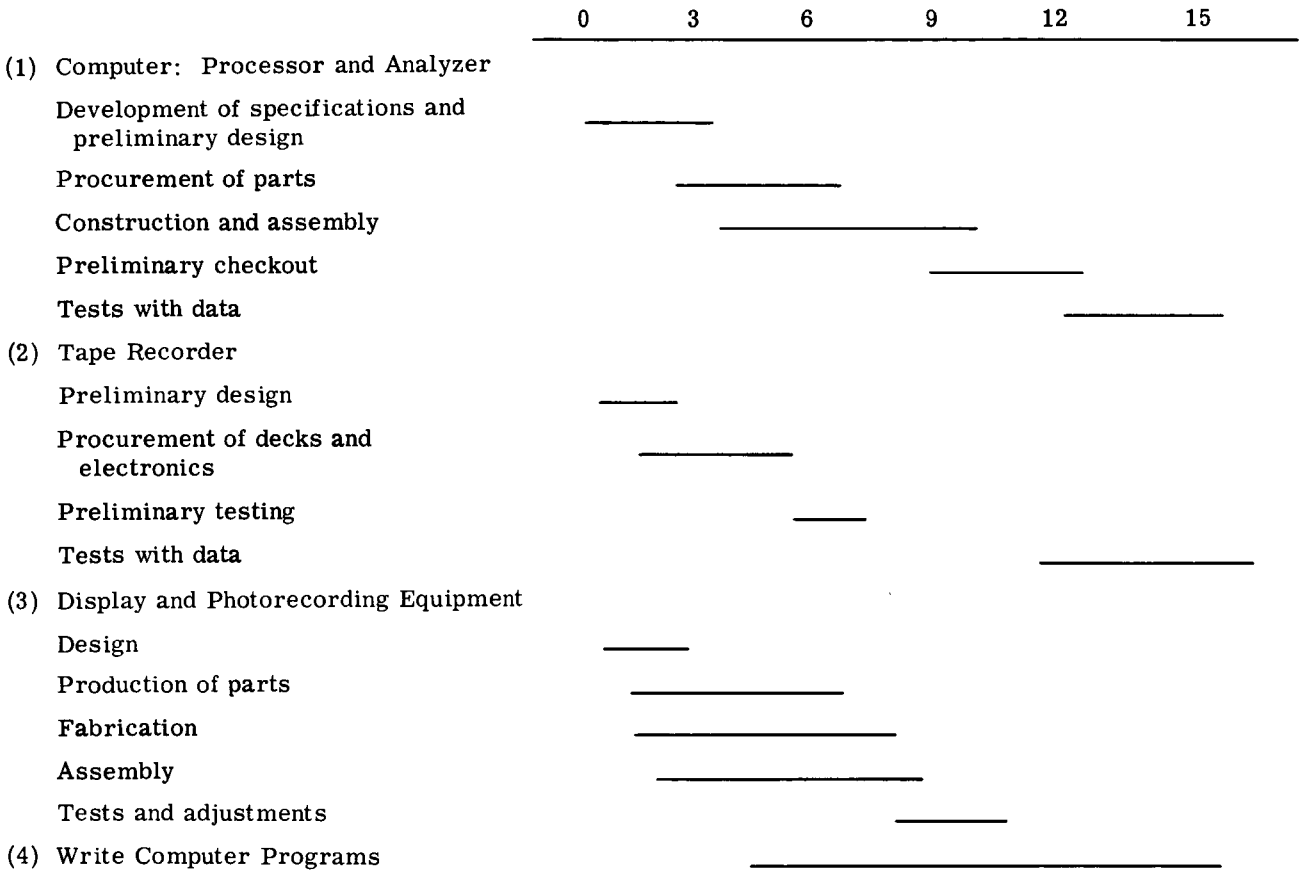

FIGURE 15. SCHEDULE FOR PHASE I: THE GROUND SUBSYSTEM

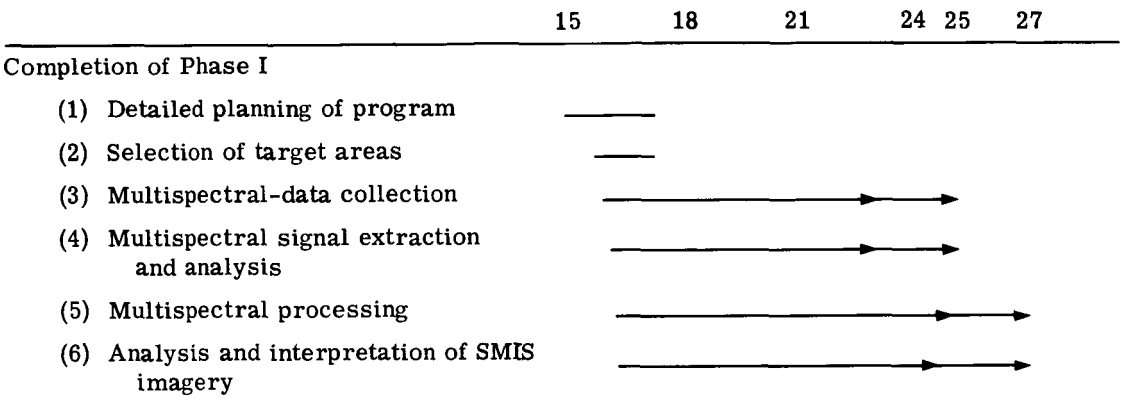

FIGURE 16. SCHEDULE FOR PHASE II: SMIS EVALUATION

4
PROGRAM COSTS

The estimated costs for Phase I and Phase II are $710,000 and $337,000, respectively. A breakdown of these costs is given in tables III and IV. The labor costs are based upon its being built by the Willow Run Laboratories. As far as possible, current list prices were used as the cost of the purchased items. For the optical components, prices were estimated using the costs of recent purchases of comparable items. For the infrared detector arrays and the NaCl prism, budgetary estimates were obtained from Santa Barbara Research Center and Harshaw Chemical Company, respectively. It is anticipated that two tape recorders and the drum storage will be provided as Government-furnished equipment (GFE). For completeness, costs for these items are included in table III, but have been excluded from the total and subtotal costs.

TABLE III. COST BREAKDOWN FOR PHASE I

	Scanner-Spectrograph	Airborne Console	Airborne Recorder	Test Flights	Analyzer	Processor
Labor and associated costs	$127,000	$71,000	$6,000	$20,000	$46,000	$56,000
Travel and Reports	4,000	2,000	1,000		3,000	3,000
Purchase Parts Aircraft Costs	120,000	23,000		11,000	57,000	160,000
Total	251,000	96,000	7,000	31,000	106,000	219,000
GFE Parts			55,000		15,000	97,000

Major Purchased Parts

(1) Scanner-Spectrograph		
1 detector array (Ge:Hg) mounted in dewar		$35,000
1 detector array (InSb) mounted in dewar		15,000
1 NaCl prism		2,200
1 beryllium scan mirror		7,000
(2) Analyzer		
1 preprocessor electronics		27,000
1 data serializer		15,000
1 tape recorder (Ampex 7-channel FR 1300)		12,000
(3) Processor		
350 drift stablized operational amplifier @$153		53,500
960 coefficient potentiometers @$16.23		15,500
60 squaring function generators @$300		18,000
1 digital voltmeter		3,500
(4) Recommended tape recorders (GFE)		
1 ground tape recorder		
1 Mincom PC-500 mechanism with 14 record heads, 14 playback heads, 14 direct-record, and 14 direct-reproduce channels		$40,333
3 DCS Model GOV-3 voltage-controlled oscillators @$305		915
3 DCS Model GOV-3/F frequency units @$100		300
1 DCS Model GSA-1 mixer-driver		305
33 DCS Model GFD-8 FM demodulators @$1000		33,000
66 DCS Model GFD-8/TU tuning units @$125		8,250
66 DCS Model GFD-8/TU low-pass filters @$150		9,900
5 DCS Model GMA-3 module assemblies @$950		4,750
	Total	$97,753
1 airborne tape recorder		
1 Mincom PC-500 mechanism with 14 record heads, 14 playback heads, 14 direct-record, and 2 selectable direct-reproduce channels		$30,474
33 Data Control Systems Model GOV-3 voltage-controlled oscillators @$305		10,065
33 DCS Model GOV-3/F frequency units @$100		3,300
11 DCS Model GSA-1 mixer-drivers @$305		3,355
3 DCS Model GFD-8 FM demodulators @$1000		3,000
3 DCS Model GFD-8/TU tuning units @$125		375
3 DCS Model GFD-8/TU low-pass filters @$150		450
4 DCS Model GMA-3 module assemblies @$950		3,800
	Total	$54,819

TABLE IV. COST BREAKDOWN FOR PHASE II

	Data-Gathering Flight Program	Data Analysis and Processing
Labor	$ 94,000	$134,000
Aircraft Costs and Materials	95,000	
General-Purpose Computer		2,000
Travel and Reports	6,000	6,000
Totals	195,000	142,000

Total Cost of Phase II: $337,000

Appendix I
THEORY OF STATISTICAL SPECTRAL DISCRIMINATION

I.1. DISCRIMINATION PROCESSOR

The methods used to design an optimal signal processor are those of statistical decision theory. These methods when applied to a problem such as spectral discrimination are called pattern-recognition techniques. They are usually developed in abstract mathematical terms, with little or no reference to the equipment intended to implement the discrimination process, and then translated into equipment specifications.

To illustrate this discussion, we shall consider a discrete representation of the spectral distribution and limit ourselves to two spectral samples. Everything said will apply to more spectral samples and continuous spectral distributions. Let u_1 be the power observed in the first spectral region and u_2 the power observed in the second. The random variation in the observed spectra forms a scatter diagram such as figure 17. To find the proportion of the spectral observations that lie in any region A, we seek a multivariate density $f(\bar{u})$ which defines the probability of an observation occurring in region A by

$$\text{probability } \{\text{observed spectrum lies in A}\} = \int \ldots \int f(\bar{u})\, d\bar{u} \tag{6}$$

Since the observed spectrum from an object varies randomly, we must abandon the notion of an object spectrum and consider regions or sets of spectra to decide what object is present. This decision rule is a partition of the set of all possible observed spectra into disjoint regions. If the observed spectrum lies in region A, we decide that the object present is the one we have chosen to associate with A. Figure 18 illustrates such a decision partition.

The decision rule specifies a partition into sets, and the probability distribution specifies the probability of these sets. These two notions provide a basis for characterizing and evaluating proposed spectral discrimination schemes, and, more important, they provide a basis for the design of discrimination schemes.

Evaluation of Spectral-Discrimination Schemes. A spectral filter may be the detector spectral response and/or a special material designed to yield the desired response. The output from a spectral filter has the form

$$f_1 u_1 + f_2 u_2 = y \tag{7}$$

where f_i is the percent of spectral transmission

and $0 \leqq f_1, f_2 \leqq 1$

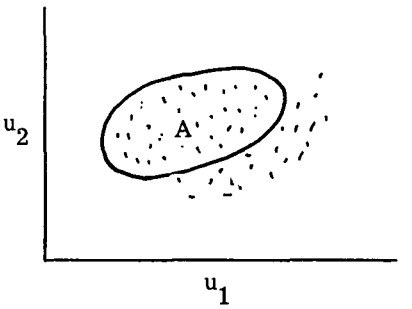

FIGURE 17. DISTRIBUTION OF OBSERVED SPECTRA

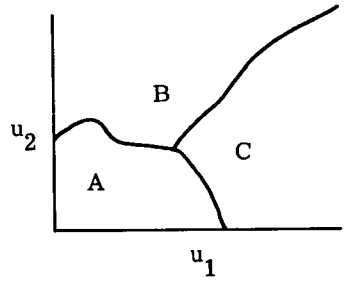

FIGURE 18. DECISION PARTITION

in the first or second spectral band. A target is present if y exceeds a threshold T. The target and noise regions are shown in figure 19. Figure 19 illustrates an important characteristic of any spectral filter. The discrimination regions are separated by lines whose slopes are invariably negative. If both the target and noise spectrum distributions have concentrations that are oriented positively (fig. 20), clearly no line with negative slope will separate target from background as well as will a line with positive slope.

This example indicates the importance of the orientation of the concentration of the spectral distribution. The correlation,

$$\rho_{12} = \text{cor}\,(u_1, u_2) = \frac{\text{avg}\,(u_1 - \bar{u}_1)(u_2 - \bar{u}_2)}{\sqrt{\text{avg}\,(u_1 - \bar{u}_1)^2\ \text{avg}\,(u_2 - \bar{u}_2)^2}} \tag{8}$$

between two spectral bands is such a measure. In general, if u_1 is greater than its average $\bar{u}_1$ implies that u_2 is greater than its average $\bar{u}_2$, and conversely, the concentration is at least approximately positively oriented. If both target and noise distributions have positive correlations, any spectral filter, even the optimum, discriminates inadequately. The correlation statistic is useful in evaluating a discrimination scheme.

Another proposed discrimination scheme takes the difference between two spectral channels

$$y = |u_1 - u_2| \tag{9}$$

The spectral bands are usually chosen so that the average background signal in both channels is the same. If $y > T$, a target is present; otherwise background is present. Figure 21 illustrates the decision regions. If the correlations of both background and target are negative as in figure 22, this discrimination scheme will not work as a filter.

In the two-dimensional infrarimetry technique, the quantities r_i, defined as

$$r_i = \frac{u_i}{u_1 + u_2} \tag{10}$$

are computed. Since r_2 depends linearly upon r_1, the decision depends upon the value of the r_i's. A target is present if $0 \leq r_1 \leq a$.

In general, the discrimination regions defined by the infrarimetry scheme (fig. 23) are cones with vertexes at the origin. The scheme recognizes only that the observed spectrum lies on some line through the origin, not where on the line. As in the difference scheme, the infrarimetry scheme will not discriminate adequately if the spectral distributions of both target and background are negatively correlated.

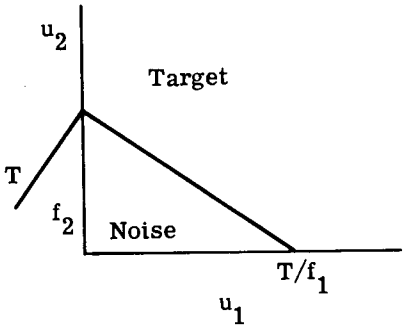

FIGURE 19. REGIONS SPECIFIED BY SPECTRAL FILTER

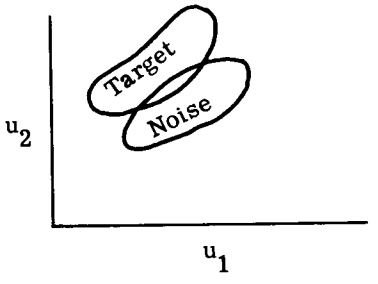

FIGURE 20. OBSERVED SPECTRA WITH POSITIVE CORRELATIONS

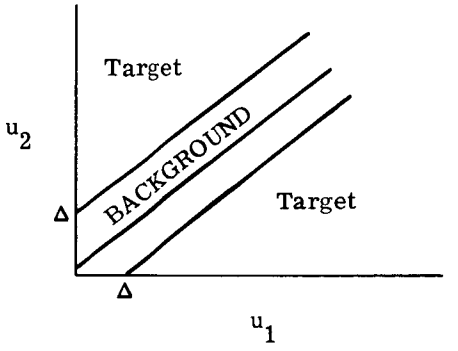

FIGURE 21. SPECTRAL DECISION REGIONS: SPECTRAL DIFFERENCES

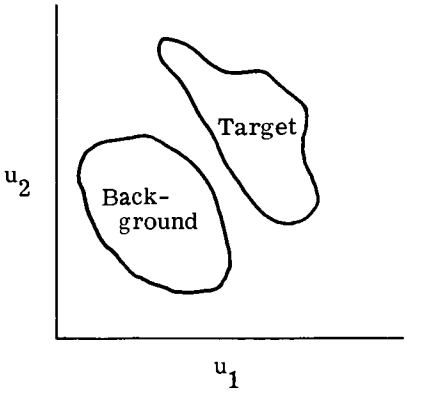

FIGURE 22. OBSERVED SPECTRA WITH NEGATIVE CORRELATION

The three schemes considered are similar in that the boundary between decision regions is a straight line. However, if the distributions of target and background have concentrations similar to those shown in figure 24, the "kidney" concentration, then no line will adequately partition the spectra observations. Thus, we have shown how failure to consider statistical aspects in the design of a spectral-discrimination scheme can lead to failure of the scheme.

Design Problem. To illustrate the statistical approach to the design of spectral-discrimination schemes, we consider the spectral matching problem. Suppose we have a spectrum $(u_1, \ldots, u_N) = \vec{u}$ that defines a target A. We observe a spectrum $u_1^0, \ldots, u_N^0 = \vec{u}^0$. Is the observed spectrum close enough to u to justify stating that the object is A? To define "close," we consider the Euclidean distance

$$d(\vec{u}, \vec{u}_0) = \sqrt{\sum \left(u_i - u_i^0\right)^2} \tag{11}$$

The observed spectrum $\vec{u}^0$ is the target A if $d(\vec{u}, \vec{u}_0)$ is less than some constant c. With equation 11 as the distance, the decision region is a circle (fig. 25). If $\vec{u}^0$ lies in the circle, target A is present.

If one spectral channel, number one, is noisier than the other, the concentration of the distribution might appear as in figure 26. Consequently, the probability of a deviation from u^0 as large or larger than c_1 in the first channel might be the same as the probability of a deviation in the second channel as large or larger than c_2. The dispersion in a channel may be measured by its variance. The larger the variance, the less we want to weight that coordinate of the distance. Let us weight each coordinate with the reciprocal of its variance. The new distance is then

$$d^1(\vec{u}, \vec{u}^0) = \sqrt{\sum \frac{\left(u_i - u_i^0\right)^2}{\sigma_{u_i}^2}} \tag{12}$$

The region $d^1(u, u^0) \leqq c$ is an ellipse with axes of length $c\sigma_{u_1}$ and $c\sigma_{u_2}$ (fig. 26). If the observed value $\vec{u}^0$ lies in the ellipse it is "close" to u and we have a target.

Our concentrations may have orientations, i.e., the ellipse's axes, ρ_{ij} (eq. 8). Consider the array of numbers $\{\rho_{ij}\}$. Let $\{\rho^{ij}\}$ be the elements of the reciprocal matrix. A new distance is then defined as

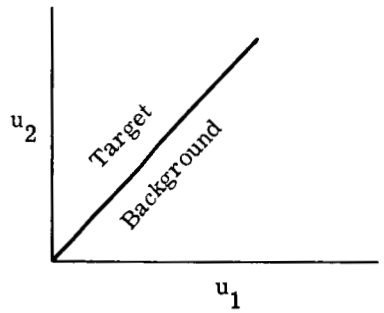

FIGURE 23. DISCRIMINATION REGIONS: INFRARIMETRY SCHEME

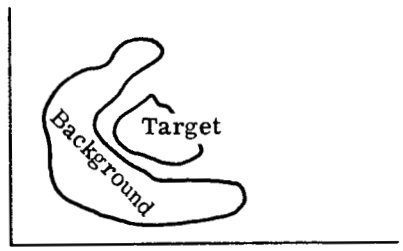

FIGURE 24. BACKGROUND DISTRIBUTIONS

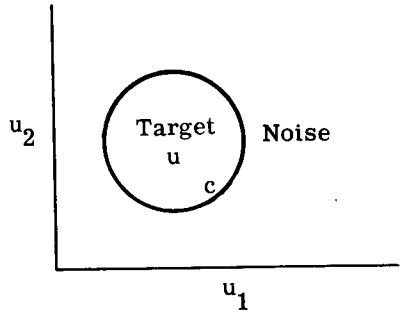

FIGURE 25. DISTANCE BETWEEN SPECTRA

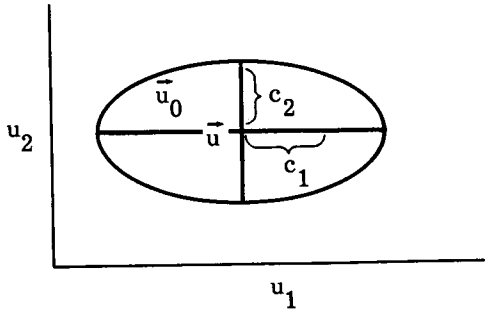

FIGURE 26. CONCENTRATION OF DISTRIBUTION

$$d^2(\vec{u}, \vec{u}^0) = \sqrt{\sum_i \sum_j (u_i - u_i^0)\rho^{ij}(u_j - u_j^0)} \tag{13}$$

This is a distance in a coordinate system with oblique axes. As an example, suppose $\rho_{12} = \rho_{21} = 1/2$ and $\sigma_1 = \sigma_2 = 1$.

$$\{\rho_{ij}\} = \begin{bmatrix} 1 & 1/2 \\ 1/2 & 1 \end{bmatrix}$$

then

$$\{\rho^{ij}\} = \begin{bmatrix} 4/3 & -2/3 \\ -2/3 & 4/3 \end{bmatrix}$$

Equation 13 becomes

$$d^2(\vec{u}, \vec{u}^0) = \sqrt{\frac{4}{3}\left[(u_1 - u_1^0)^2 - (u_1 - u_1^0)(u_2 - u_2^0) + (u_2 - u_2^0)^2\right]}$$

The major axis of this ellipse (fig. 27) is in the direction (1, 1).

Closeness as defined above is essentially a characteristic of the target's spectral distribution and its variation. The distance defined in equation 13 is specified by the first and second moment statistics of the target's probability distribution. Section I.2 outlines a very general method for designing spectral-discrimination schemes.

I.2. OPTIMAL STATISTICAL SPECTRAL DISCRIMINATION

We shall now introduce a notion of optimality for a spectral-discrimination scheme and a general rule for the design of optimal spectral-discrimination schemes. This rule takes into account all of the statistical problems raised so far. Suppose we want our discrimination techniques to have a probability P of target detection. A scheme is optimal if the probability of a false alarm for that system is smaller than the false-alarm probability for any other system. Any spectral discrimination scheme can be represented as a partition of the observable spectrum space. Our design problem reduces formally to the selection of a target-detection region A with the properties:

(1) The probability of an observed spectrum from a target falling in A is P.

(2) Among all detection regions R, the region A should have the smallest probability of an observed background spectrum falling in A (probability {$\vec{u}$ is in A given background spectrum}

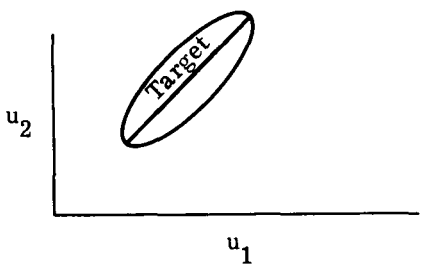

FIGURE 27. ORIENTED ELLIPSE OF CONCENTRATION

< probability {u is in R given background spectrum}). The solution to this problem is well known in mathematical statistics. Let A be the set of observed spectra $(u_1, \ldots, u_N)$ that satisfy the inequality

$$\frac{f_T(u_1, \ldots, u_N)}{f_B(u_1, \ldots, u_N)} \geqq c \tag{14}$$

where $f_T(u_1, \ldots, u_N)$ and $f_B(u_1, \ldots, u_N)$ are the probability densities of the signals representing the target and background, respectively. The constant c is the solution to the equation

$$\text{probability} \left\{ \frac{f_T(\vec{u})}{f_B(\vec{u})} \geqq c \text{ given a target present} \right\} = P \tag{15}$$

The ratio in equation 15 is known as the likelihood ratio. As Birdsall and Peterson point out [11], this ratio is central in the theory of signal detectability. In fact, the optimization of many apparently different criteria leads to the likelihood ratio. Equation 15 satisfies condition 1. We shall now show that the region A defined by (14) and (15) satisfies condition 2.

Consider any other discrimination scheme and its target-detection region R. Let A-R be the set of points in A but not in R and, conversely, R-A the set of points in R but not in A. From (14) we have the inequalities

$$\begin{aligned} \int_{R-A} f_T(\vec{u})\, d\vec{u} &\leqq c \int_{R-A} f_B(\vec{u})\, d\vec{u} \\ \int_{A-R} f_T(\vec{u})\, d\vec{u} &\geqq c \int_{A-R} f_B(\vec{u})\, d\vec{u} \end{aligned} \tag{16}$$

But since the region R has a probability of target detection P, we have

$$\int_{A-R} f_T(\vec{u})\, d\vec{u} = \int_{R-A} f_T(\vec{u})\, d\vec{u} \tag{17}$$

Using (17) in (16), we obtain

$$\int_{R-A} f_B(\vec{u})\, d\vec{u} \geqq \int_{A-R} f_B(\vec{u})\, d\vec{u} \tag{18}$$

If we add the points common to both A and R, we have

$$\int_{R} f_B(\vec{u})\, d\vec{u} \geqq \int_{A} f_B(\vec{u})\, d\vec{u} \tag{19}$$

which is precisely condition 2. The spectral discrimination defined by (14) and (15) is an optimal scheme using the criteria of conditions 1 and 2.

The implementation of the spectral-discrimination scheme specified by (14) can be seen in figure 28. The schemes discussed in section 3, with the exception of the spectral filters, all require some computational manipulation of the detected signals. This computation is generally done electronically. Spectral filter schemes use the filter and detector as a computer, an attractive feature of their implementation. One can see clearly that the design of an optimal system requires knowledge of the statistical properties of both the target and the background. Lack of knowledge rather than the theory is the limiting factor.

More may be required of a spectral-discrimination scheme than the simple indication of the presence or absence of a target. In many instances we want to decide which of many objects is present on the basis of the observed spectrum $\vec{u}$. The likelihood-ratio test discussed above partitions the sample space $\vec{u}$ into two regions. A classification scheme partitions the space into many regions (see fig. 18). We may represent this multiple partition by a function $D(\vec{u})$ defined as

$$D(\vec{u}) = i \quad i = 1, \ldots, n \tag{20}$$

if $\vec{u}$ lies in the region specifying the ith target

The likelihood-ratio test assumes n = 2 and essentially finds an optimal partition function or decision function $D(\vec{u})$. We shall now construct an optimal decision function $D(\vec{u})$. Additional data are required to achieve a satisfactory solution. First, we must have some a priori estimates of the probability p_i that an object will occur in the scene. This is not as difficult as it at first sounds. We generally have a fairly good estimate of the proportion of a scene occupied by a certain object. Let p_i be the a priori probability that an object i will be present in a scene. There is generally some cost associated with classifying the jth object as being the ith object. Let the cost of classifying the jth object i be $C(i|j)$. Given a spectral observation $\vec{u}$ the conditional probability of the j population is given by Bayes theorem,

$$p(j|\vec{u}) = \frac{p_j f_j(\vec{u})}{\sum_{i=1}^{n} p_i f_i(\vec{u})} \tag{21}$$

where $f_i(\vec{u})$ is the probability density of $\vec{u}$ given that the observation comes from the ith population. If we classify an observation $\vec{u}_0$ as coming from the ith object, the average cost incurred is given by

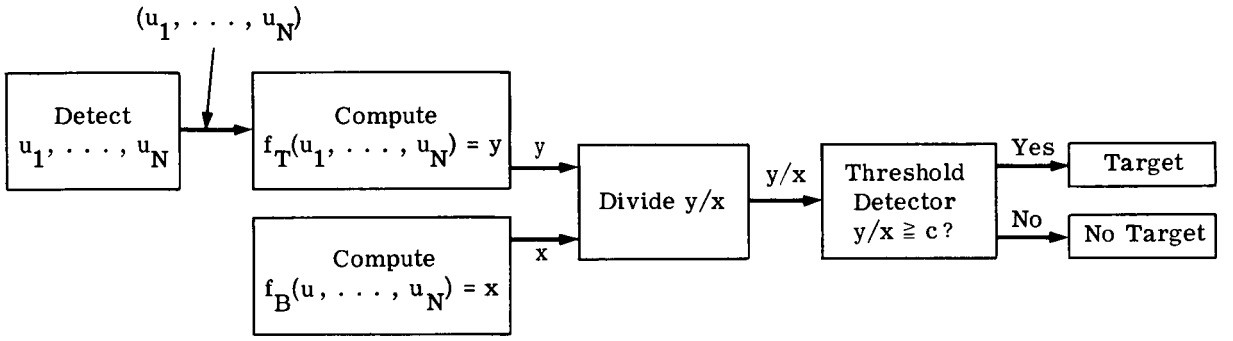

FIGURE 28. BLOCK DIAGRAM OF LIKELIHOOD-RATIO SCHEME

$$\text{average cost } (\vec{u}_0 \text{ comes from i}) = \sum_{\substack{j=1 \\ j\neq 1}}^{n} \frac{p_j f_j(\vec{u})}{\sum_{i+1}^{n} p_i f_i(\vec{u})} C(i|j) \tag{22}$$

We now want to choose i so that the cost equation 22 is minimized. The decision function $D(\vec{u})$ which minimizes the cost of a misclassification is given by

$$D(u) = i \text{ when } \sum_{\substack{j=1 \\ j\neq 1}}^{n} p_j f_j(\vec{u}) C(i|j) \leqq \sum_{\substack{j=1 \\ j\neq 1}}^{n} p_j f_j(\vec{u}) C(k|j) \tag{23}$$

$$\text{for all } k = 1, \ldots, n$$

The function $D(\vec{u})$ defines a partition of the space into n regions. Let us now consider a situation closely related to the binary decision space of the likelihood-ratio model. The target is object 1 and the objects in the background are $2, \ldots, N$. The costs of calling a target any background object are equal. The costs of calling any background object the target are equal. The costs of calling one background object another background object are zero. The cost situation is summarized in equation 24:

$$\begin{aligned} C(i|1) &= a \qquad i = 2, \ldots, n \\ C(1|j) &= b \qquad j = 2, \ldots, n \\ C(i|j) &= 0 \quad i, j = 2, \ldots, n \end{aligned} \tag{24}$$

From equation 23 we obtain for the target region the specification

$$D(\vec{u}) = 1 \text{ when } b \sum_{j=2}^{n} p_j f_j(\vec{u}) \leqq a p_1 f_1(\vec{u}) \tag{25}$$

Equivalently, a target is present when

$$\frac{f_1(u)}{\sum_{j=2}^{n} p_j f_j(\vec{u})} \geqq \frac{b}{a p_1} \tag{26}$$

This is, of course, the likelihood ratio of equation 14, where the background is composed of many objects. In most practical cases, the background does, in fact, consist of a number of distinct objects. A more detailed discussion of this theory is found in reference [12].

Let us partially specify the target and background distributions and derive the optimal system. Suppose both $f_T(u_1, \ldots, u_N)$ and $f_B(u_1, \ldots, u_N)$ are Gaussian with means $\left(u_1^T, \ldots, u_N^T\right)$, $\left(u_1^B, \ldots, u_N^B\right)$ and variance-covariance matrix $\left\{\theta_{ij}^B\right\}$. Ignoring constants, we find the densities to be

$$f_T(\bar{u}) = \exp -\sum_i \sum_j \theta_T^{ij}\left(u_i - u_i^T\right)\left(u_j - u_j^T\right)$$
$$f_B(u) = \exp -\sum_i \sum_j \theta_B^{ij}\left(u_i - u_i^B\right)\left(u_j - u_j^B\right) \tag{27}$$

where θ_B^{ij} and θ_T^{ij} are elements of the inverse of the background and target variance-covariance matrices. Inserting equation 27 into the likelihood ratio and taking the log of the ratio, we obtain equation 28 for the target-detection-region specification:

$$\sum_i \sum_j \theta_B^{ij}\left(u_i - u_i^B\right)\left(u_j - u_j^B\right) - 0_T^{ij}\left(u_i - u_i^T\right)\left(u_j - u_j^T\right) \geqq c \tag{28}$$

If the output as computed in (28) exceeds the threshold c, the spectral-discrimination system will indicate a target detection. Figure 29 illustrates the type of partition that might arise in a likelihood-ratio scheme. The analog computing circuitry to implement (28) requires adders, subtracters, and multipliers. The complexity of this circuitry depends upon the constants θ_B^{ij}, θ_T^{ij}, u_i^B, and u_i^T, or, in short, upon the complexity of the statistics of both background and target.

While individual background objects may be said to be Gaussian, the background consists of multiple objects. The probability that a given resolution element is an object is the proportion of the scene occupied by the object. Let p_i be this proportion. The discrimination scheme developed generally in equation 26 specifies the spectral processor. Equation 29 is the mathematical specification of the spectral-processing hardware.

$$\text{A target is present if } \frac{p_T\sqrt{\left|\theta_T^{ij}\right|}\ \exp -\frac{1}{2}\left[\sum_{i=1}^{N}\sum_{j=1}^{N}\left(u_i - u_i^T\right)\theta_T^{ij}\left(u_j - u_j^T\right)\right]}{\sum_{k=1}^{M} p_k\sqrt{\left|\theta_k^{ij}\right|}\ \exp -\frac{1}{2}\left[\sum_{i=1}^{N}\sum_{j=1}^{N}\left(u_i - u_i^k\right)\theta_k^{ij}\left(u_j - u_j^k\right)\right]} \geqq c \tag{29}$$

The parameters u_j^k, θ_k^{ij} specify the target and background statistics. The resolution element is said to be a target when the spectrum $(u_1, \ldots, u_N)$ satisfies equation 29.

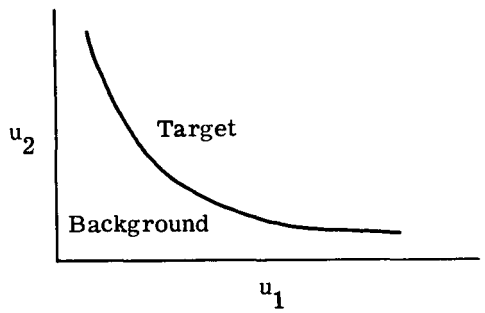

FIGURE 29. LIKELIHOOD-RATIO DISCRIMINATION REGIONS

I.3. SIMPLIFICATION OF THE MATHEMATICAL OPERATIONS FOR OPTIMAL SPECTRAL DISCRIMINATION

The likelihood-ratio method for spectral discrimination, assuming multivariate Gaussian distribution and multiple background objects, is as follows. Assume N channels and M background objects. The likelihood-ratio test says that the observation $(u_1, \ldots, u_N)$ for a resolution element is a target if

$$\frac{p_T\sqrt{\left|\theta_T^{ij}\right|}\exp -\frac{1}{2}\left[\sum_{i=1}^{N}\sum_{j=1}^{N}\left(u_i - u_i^T\right)\theta_T^{ij}\left(u_j - u_j^T\right)\right]}{\sum_{k=1}^{M} p_k\sqrt{\left|\theta_k^{ij}\right|}\exp -\frac{1}{2}\left[\sum_{i=1}^{N}\sum_{j=1}^{N}\left(u_i - u_i^k\right)\theta_k^{ij}\left(u_j - u_j^k\right)\right]} \gtrless c \tag{30}$$

The numbers u_i^T, u_i^k, θ_T^{ij}, θ_k^{ij}, p_T, and p_k, where i, j = 1, . . . , N and k = 1, . . . , M, are constants. The major computational problem arises in computing the exponents such as

$$\sum_{i=1}^{N}\sum_{j=1}^{N}\left(u_i - u_i^T\right)\theta_T^{ij}\left(u_j - u_j^T\right) \tag{31}$$

Now, since $\theta_T^{ij} = \theta_T^{ji}$, we have $\frac{N(N+1)}{2}$ multiplications of the form $u_i u_j$. Since u_i and u_j are variables, multipliers must be used (not fixed potentiometers as may be used for multiplying by a constant such as θ_T^{ij}). Each exponent in the denominator of equation 30 has the form

$$\sum_{i=1}^{N}\sum_{j=1}^{N}\left(u_i - u_i^k\right)\theta_k^{ij}\left(u_j - u_j^k\right) \quad k = (1, \ldots, M) \tag{32}$$

which is similar to (31). Consequently, we have $\frac{(M+1)N(N+1)}{2}$ multiplications to be performed. These must be done simultaneously because of time requirements for the processor. Suppose, for example, that N = 28 and M = 1; then the number of multipliers is 812. This number of multipliers with 35-kHz bandwidth is prohibitive.

Since squaring an instantaneous voltage is simpler than multiplying two instantaneous voltages, we shall manipulate (31) and (32) to this end. The constants θ_T^{ij} and θ_k^{ij} are always chosen so that for all values of $(u_1, \ldots, u_N)$ both (31) and (32) are equal to zero if and only if $(u_1, \ldots, u_N) = \left(u_1^T, \ldots, u_N^T\right)$ and are otherwise greater than zero. Consequently, (31) and (32) are positive definite quadratic forms. Under these circumstances we may compute both (31) and (32) using squaring and addition operations only. Expression 31 may be written as

$$\sum_{i=1}^{N}\sum_{j=1}^{N}\left(u_i - u_i^T\right)\theta_T^{ij}\left(u_j - u_j^T\right) = \sum_{i=1}^{N} y_i^2 \tag{33}$$

The y_i's are defined as

$$\begin{aligned} y_1 &= b_{11}\left(u_1 - u_1^T\right) + b_{12}\left(u_2 - u_2^T\right) + \ldots + b_{1N}\left(u_N - u_N^T\right) \\ y_2 &= b_{22}\left(u_2 - u_2^T\right) + \ldots + b_{2N}\left(u_N - u_N^T\right) \\ &\vdots \\ y_N &= b_{NN}\left(u_N - u_N^T\right) \end{aligned} \tag{34}$$

or

$$y_i = \sum_{j=i}^{N} b_{ij}\left(u_j - u_j^T\right) \qquad i = (1, \ldots, N) \tag{35}$$

Expression 32 may be computed in a similar manner. Note that the coefficients b_{ij} will differ when we compute (31) or (32) and will also depend upon the value of k in expression 32. Thus, the computation of the exponents for (30) involves only addition and squaring of varying voltages. The number of squaring operations required is (M + 1)N. For the example in which M = 1 and N = 28, a total of only 56 squaring function generators is required, as compared with the 812 multipliers needed to compute (30) in its original form.

Appendix II
THE AIRBORNE SUBSYSTEM

The purpose of this appendix is to supplement the very brief description of the hardware given in section 2 and to justify the selection of the chosen design. The material in this section is also used as a basis for the relevant parts of the schedule and cost analysis of sections 3 and 4, respectively.

Much thought and trial and error were involved in the evolution of the design of the scanner-spectrograph. The various compromises involved are indicated in the discussion. While the system may at first appear complex, it is in fact much simpler and more compact than any alternative system. That it was found to be practical to cover this very wide wavelength range from 0.33 to 13.5 μ in a satisfactory manner with a single dispersing system is remarkable. This possibility is to some extent fortuitous, not so much in that the useful transmission region of a NaCl prism covers this range, but in that the dispersion curve of NaCl is adequately matched to the needs of the system. The dispersion of NaCl is very poor between 2 and 5 μ, but there is also a minimum in the radiance spectrum of terrestrial targets in this region; better dispersion in this wavelength region would, in fact, have been impracticable from an SNR point of view. In the longer visible and near-infrared regions and in the 8- to 14-μ region, the dispersion is adequate. In the shorter visible and near-ultraviolet regions, the dispersion is greater than needed, but this has no deleterious effects as it would have in the infrared where it is desirable to minimize detector area to obtain optimum performance. For the non-dark noise-limited conditions of use which apply here, the performance of a photomultiplier is essentially independent of the area of its photocathode.

The development of the design of the electronic aspects of the system was relatively straightforward as was the selection of an appropriate airborne tape recorder.

Methods used to predict the performance of the subsystem are discussed in section II.8.

II.1. GEOMETRICAL PARAMETERS

As was shown in an earlier study [9], the sensitivity of a multispectral scanning radiometer of the type described can be calculated once a number of system parameters have been fixed. It was also shown that there are relations between many of the parameters so that not

all of these may be fixed independently. These parametric equations and relationships are reproduced in section II.8 and are then used to deduce the performance of the proposed system. This section discusses the selection of the primary parameters and the consequences of these selections.

(V/H). The V/H (velocity-to-height) ratio occurs in several places in the parametric relationships. It can, to some extent, be controlled by the experimenter. However, as the correct rotational rate of the scan mirror and the optimum electronic bandwidth of the amplifier-recorder chains are dependent on V/H, the overall design depends upon the maximum value which V/H will be allowed to assume. In earth-orbital operation V/H will not be greater than 0.025, which is equivalent to a relatively low performance aircraft flying at lower altitudes. High-speed aircraft at low altitudes may, however, have V/H two orders of magnitude greater, e.g. 600 mph at 350 ft. If the vehicle exceeds the design value of V/H, there will be underlap, that is, there will be gaps between the ground strips scanned during each revolution of the scan mirror. This is usually undesirable, as important features may be missed. On the other hand, if the vehicle V/H is smaller than that of the scanner, there will be overlap. In this case, a wider than optimum electronic bandwidth must be used. However, it can be shown that by proper processing of the data there need be no loss in performance. High V/H necessitates high scan-mirror rotational rates which in turn lead to engineering difficulties. Furthermore, wide electronic bandwidths are required which make it difficult to utilize theoretical detector performance. The designer, therefore, prefers to design for a low V/H. We have chosen a design V/H = 0.1 rad/sec as a compromise between the various factors discussed. In combination with the chosen β of 0.003, this gives a scan-mirror rotational rate of 2000 rpm which is quite reasonable, and an electronic bandwidth of 35 kHz which is also acceptable. It also allows the medium performance aircraft in which the scanner will be used to fly low enough to give a ground resolution of about 5 ft, e.g., V = 140 fps at H = 1400 ft, without incurring underlap.

β. Closely associated with V/H in the parametric relationships is the instantaneous field of view β. Ground resolution is better if β is made relatively small, but the system performance (SNR) is proportional to β^2 and most design problems are eased if β is relatively large. The value chosen, $\beta = 0.003$ is in fact dictated by the design chosen for the spectrograph as discussed in section II.2.2. The fact that $\beta = 0.003$ is an acceptable compromise between the SNR and spatial-resolution requirements is, on the other hand, the principal reason for accepting the single dispersing system recommended.

$\Delta\lambda$. The overall wavelength range of operation chosen is from 0.33 to 13.5 μ. This is the total range over which appreciable atmospheric transmission occurs in the optical region of the

electromagnetic spectrum. It is thus the most ambitious choice available for inspection of the earth's surface by a remote optical sensor. Thus, it will be possible to study relationships between widely separated spectral regions which had not previously been explored.

$\delta\lambda$. The spectral resolution $\delta\lambda$ is one of the most basic parameters. Ideally, it would be set by the nature of the target and background spectra to be differentiated. It should be made fine enough that the required interpretations can be made without ambiguity, but no finer, as this will merely lead to degraded SNR performance and greater hardware complexity because of the larger number of signal channels involved. There is evidence that much spectral differentiation of terrain features of agricultural and geological interest can be carried out using a resolving power ($\Delta\lambda/\delta\lambda$) of 20 in both the visible and the 10-μ regions. The recommended design achieves this resolution in the yellow region of the visible and over the 8- to 13.5-μ region. The resolution in the intervening regions of the infrared is much poorer (cf., fig. 32). This was accepted on the grounds that a more complicated overall system involving some sort of beam division and a second spectrograph would have been required to provide better spectral resolution in this region. Also, no specific requirements of higher spectral resolution in this region were known and its use would have degraded the SNR, which is relatively low in this region of the spectrum.

D_1. The diameter of the entrance aperture D_1 has been set at 15 cm (6 in.). The SNR performance is directly proportional to D_1. The size chosen is believed to be convenient and not too cumbersome for this type of instrument.

D_2. Using parameters described later (sec. II.8) together with values of $(d\theta/d\lambda)$ for a 30^o back-silvered NaCl prism, we find that the prism aperture D_2 must be 12.5 cm (5 in.). A ray trace of such a prism in the optical arrangement suggested shows that the hypotenuse face of the prism must be 8 in. long. This is a rather large prism but well within the state of the art for this material.

II.2. OPTICAL LAYOUT

A ray trace of the optical system is given in figure 30. The complexity of this diagram is a result of the number of folding mirrors used to avoid off-axis effects and to minimize obscuration. Otherwise, the system is very simple, consisting of the scanning mirror, two concave mirrors, and the prism.

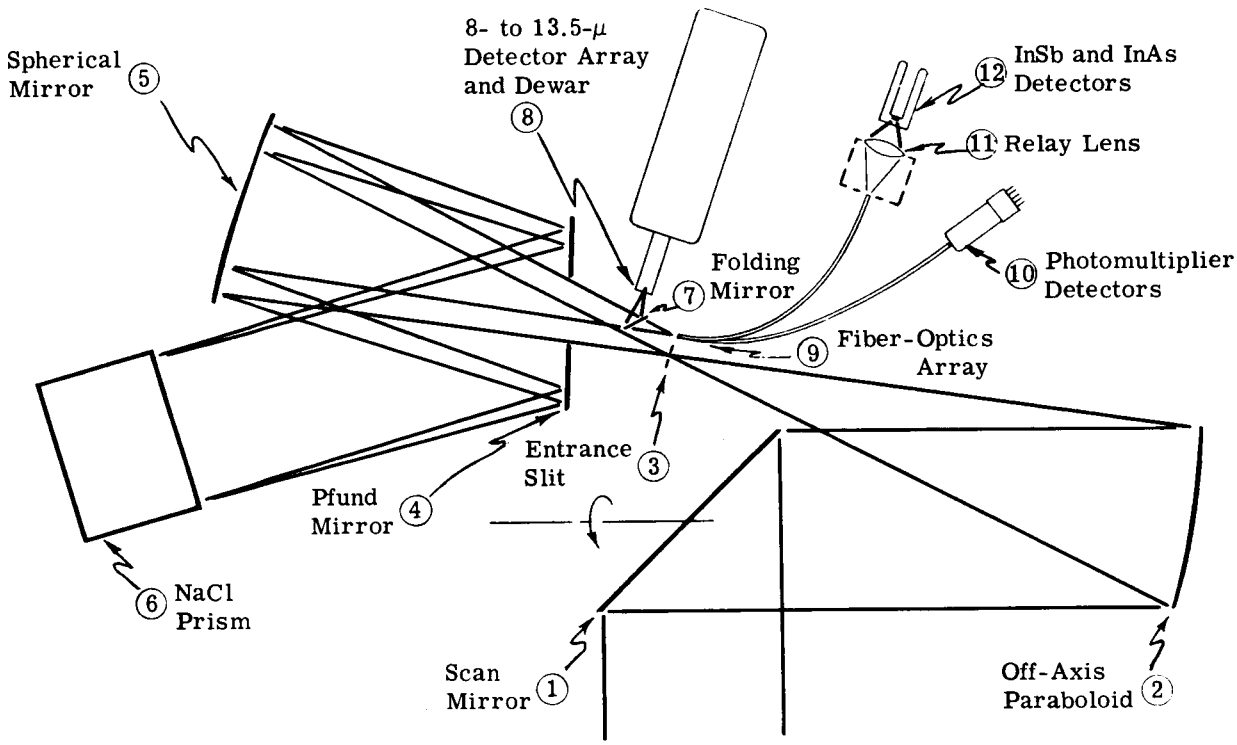

FIGURE 30. SCHEMATIC OF OPTICAL LAYOUT (SIDE VIEW)

The 1.4-mm-diameter aperture (3) forms both the entrance slit of the spectrograph and the field stop of the spatial scanning system. The latter consists of the 45° scanning mirror (1) which rotates about the axis indicated, the 6-in.-diameter f/3 off-axis paraboloid (2).

The radiation entering the spectrograph through the aperture is collimated by the spherical mirror (5) and falls on the plane mirror (4). This mirror has a slot cut in its center, as shown, to accomodate the entering and exiting beams of the spectrograph. This Pfund mirror (4) is angled as shown to reflect the collimated beam onto the face of the 30°, back-silvered, NaCl prism (6). The apex of this prism is parallel to the plane of the drawing so that the diverging fan of spectrally dispersed rays returned by the prism toward the Pfund mirror (4) lie in a plane normal to the plane of the diagram. This fan of collimated rays falls on the Pfund mirror which then reflects it back onto the collimating mirror (5). The collimating mirror then focuses the resolved spectrum onto a focal surface just above the entrance aperture.

The operation of the spectrograph is better illustrated in the ray diagram given in figure 31. This diagram has been drawn as though the large folding mirror is not used so that the geometrical relationship can be seen more clearly. (The position of the folding mirror is marked AA and when inserted its effect will be to fold that part of the diagram consisting of the prism and the parallel beams between it and the line AA about this line. Because of the slot in the middle of the folding mirror, the rays converging in the focal plane are not folded.) This diagram also shows that the center of curvature of the collimating mirror lies at the point of convergence of the axes of the dispersed parallel beams leaving the prism. Thus each of these beams is symmetrically distributed about a radius of the spherical mirror and off-axis aberrations are eliminated (as in a Schmidt camera). Note also that the entrance aperture is positioned slightly below the plane of figure 31 so that the focused spectrum lies slightly above this plane. This is necessary to obtain clearance between the entrance apertures and the focused spectrum.

Transferring the radiation from the focal plane of the spectrograph to the various detectors is one of the most critical parts of the overall design. Figure 32 diagrams the spreading of the spectrum along the focal plane. As explained in textbooks on experimental spectroscopy, the attainable wavelength resolution is fixed by the size of the monochromatic image of the entrance slit at the exit slit. The size of this image is indicated in the diagram, as is the recommended breakup of the spectrum. It will be seen that throughout much of the visible and near infrared spectra the attainable spectral resolution is used.

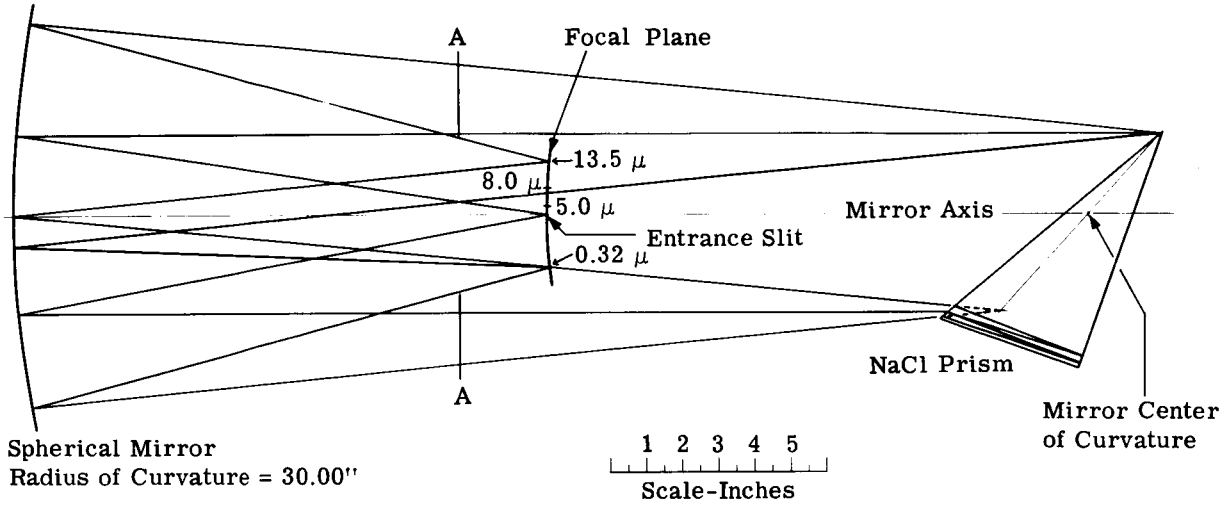

FIGURE 31. SPECTROGRAPH RAY DIAGRAM (UNFOLDED)

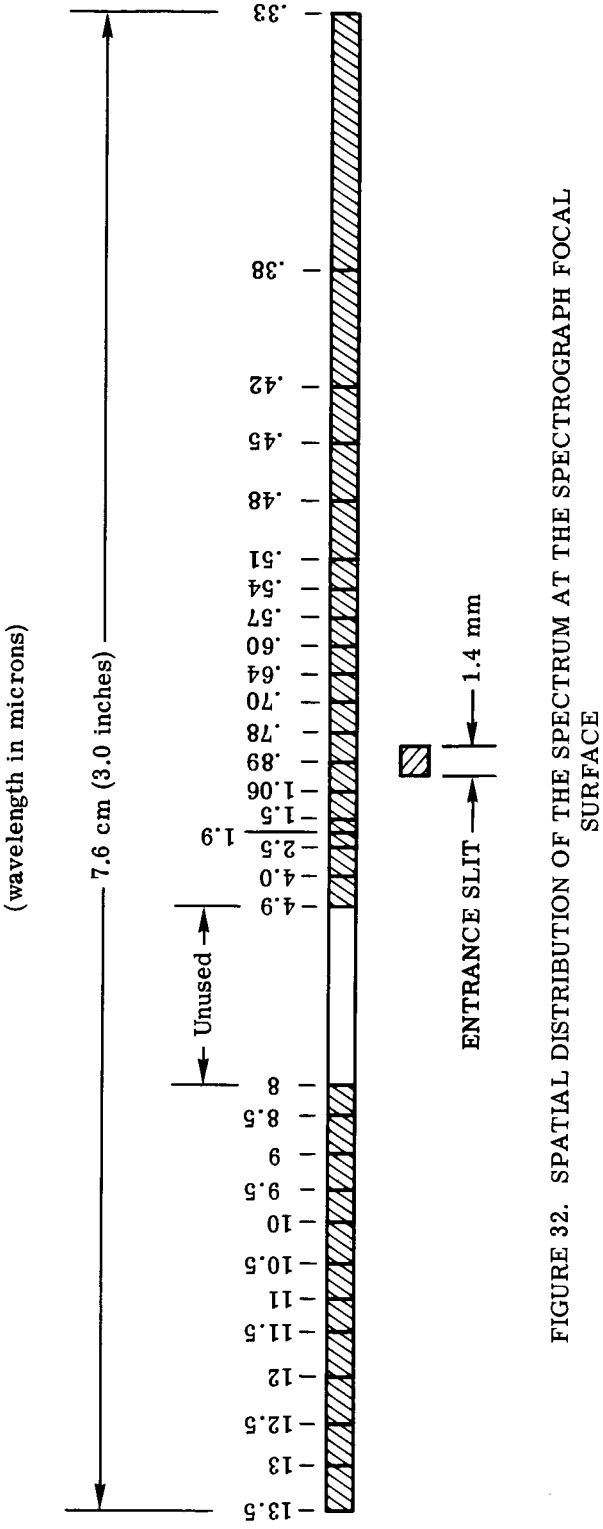

FIGURE 32. SPATIAL DISTRIBUTION OF THE SPECTRUM AT THE SPECTROGRAPH FOCAL SURFACE

II.2.1. DETECTOR ARRAYS AND RELAY OPTICAL SYSTEM. Over the 0.33- to 5-μ region a fiber-optics image disector is used to transfer the energy from the focal plane to a matrix of detectors; photomultipliers are used for the 0.33- to 1-μ region, InAs detectors for the 1- to 2.5-μ region, and InSb for the 2.5- to 5-μ region. For the InAs and InSb channels, the radiation leaving the free ends of the fiber bundles must refocused onto the individual detector elements because these elements must be kept as small as possible and must also be mounted inside evacuated enclosures (dewars) so that they can be cooled to the temperature of liquid nitrogen in order to obtain maximum sensitivity. No reimaging is necessary for the photomultiplier channels, as these are relatively large area detectors and it is sufficient to point the free ends of the fiber bundles at the detectors with the ends of the former close to the windows of the latter.

Satisfactory fiber optics for the longer infrared wavelengths are not available, and the mercury-doped detectors used for these wavelengths must be formed into an array and put directly into the focal plane. A 45° mirror is used in front of this detector array to provide clearance between the liquid-helium dewar flask in which the array must be mounted and the fiber-optics image slicer. The suggested layout simplifies the design of the helium dewar as the detectors face directly down and therefore can be located in a snout projecting from the bottom of the dewar. Experience has shown that such an end-window arrangement is much more satisfactory than the use of a side window.

II.2.2. THE OPTICAL DESIGN. This section indicates the design alternatives and the rationale of the choices made. It should be pointed out that it is not possible at the present time to set down firm requirements based on user needs for the basic parameters of the system. The two most fundamental parameters are spatial and the spectral resolution. High resolution is generally desirable for analytical purposes, but too-high resolution will lead to reduced signal-to-noise ratio and will compound the processing problem. Crop spectra in the 0.5- to 0.8-μ region with a resolution of about 0.03 to 0.04 μ can be used to demonstrate a good deal of valuable information on crop type and condition. Also, Lyon [8] and others have shown that valuable mineralogical information is contained in infrared spectra of rocks in the 10-μ region if a spectral resolution of 0.5 μ or better is used. Use of the SNR equations shows that excellent SNR performance can be obtained with these spectral resolutions if spatial resolutions of 1.5 and 6 mrad are used for the visible and 10-μ wavelength regions, respectively. It is highly desirable, from the data processing point of view, to have the data coincident both spatially and spectrally. To insure this, it is necessary to use a single field stop (spectrograph entrance slit) for all wavelengths. If, for example, a double-ended scanner is used with spectrographs

coupled to each end, it is virtually impossible to insure that the two ends have coincident instantaneous fields of view, because very fine tolerances are required on the angles between the two scan mirrors and the axis of rotation. It should also be pointed out here that temporally scanning single-detector spectrometers cannot be considered because such devices cannot be made with sufficiently fast scan times, nor would they have comparable sensitivity to the detector-array spectrographs considered here. Taking all this into account, 3 mrad was selected as a compromise for the spatial resolution for all wavelengths. In an earlier study [9], an SiO prism was considered for the shorter wavelengths and a grating for the 10-μ region. To cover the whole region from 0.33 to 13.5 μ would necessitate the use of a third spectrograph to cover the intermediate region (2.5 to 5 μ). It would then be necessary to use two dichroics or other beamsplitting devices to divide the radiation from the common field stop between the three spectrographs. A system of this sort would have the advantage that the various detector types necessary to cover the large wavelength range could be separated easily. While such a system would undoubtedly be practical, detailed examination shows that it would be both complicated and cumbersome. However, with the compromise spatial resolution of 3 mrad, it becomes possible to cover the whole wavelength range and meet the required spectral resolution at 0.6 and 10 μ using a large sodium chloride prism. If such a prism is used in a Czerney-Turner spectrograph, it is necessary to use a large focal ratio (f-number) to keep the off-axis aberrations sufficiently small. This in turn makes the scanner-spectrograph rather large. A common method of avoiding off-axis aberrations is to use a stop at the center of the curvature of a spherical mirror as in a Schmidt camera. An optical layout illustrating a concentric layout of this kind is illustrated in figure 31. As drawn the layout is impracticable because of the obstruction caused by the detector array. However, when used with a Pfund folding mirror with a central hole to pass the entrance and exit beams as shown in figure 33, it becomes quite practical. In this way, it is possible to use an f-number of about 3 which makes possible the compact system shown in figure 33. The use of an off-axis paraboloid in the scanner was introduced originally to avoid obscurations, but it also leads to a more compact overall system then would the more conventional Cassegrainian or Newtonian systems. The use of a simple 45° scan mirror spinning about an axis which passes through its midpoint has the advantage over most alternatives that the whole mirror is in use throughout the scan so that modulation resulting from mirror defects cannot occur.

The method of slicing the imaged spectrum at the focal surface of the spectrograph and relaying its slices to individual detectors is described in section II.2.1. The use of fiber optics in this manner for the visible and near-infrared spectra has been used and proven highly satis-

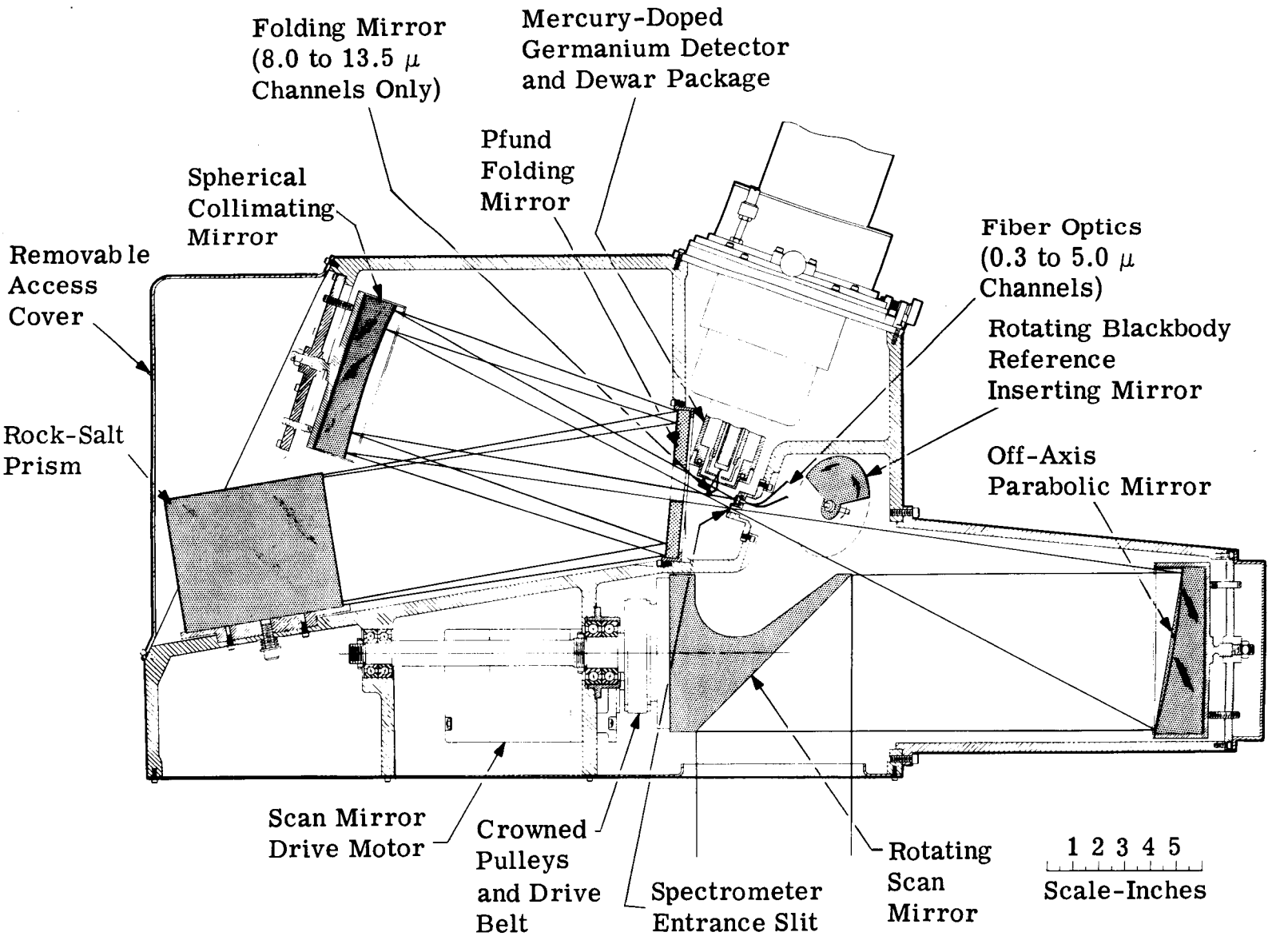

FIGURE 33. THE SCANNER-SPECTROGRAPH

factory in a previous program and is discussed in section II.5.1.4. Unfortunately, satisfactory fiber optics for the 8- to 13.5-μ region are not available, and the best 2.5- to 5-μ fibers have somewhat poorer performance than the optical glass fibers used at shorter wavelength. The atmospheric absorption band from 5 to 8 μ creates a gap for which no detectors need be provided. Thus this spectral region may be blocked, which makes permissible the use of a folding mirror in front of the 8- to 13.5-μ region of the focal surface. Thus the spectrum can be focused directly onto the Ge:Hg detector array used for this spectral region.

As there is no such gap on the short-wavelength side of the 2.5- to 5-μ region, the use of a folding mirror in front of the focal plane would lead to unacceptable vignetting and difficult mechanical clearance problems. The shortest possible infrared fiber bundles would have effective transmissions of 20% to 25% compared with about 60% for conventional fiber bundles in the visible region. This would be just acceptable, though the possibility of using a folding mirror at the focal plane should be investigated further as a means of improving the efficience of this part of the system. Whether a fiber-optics slicer or a mirror slicer is used, it will be necessary to use a relay lens to match InAs and InSb detectors to the spectrum. The performance of these detectors is inversely proportional to their size and only by using relay lenses can they be kept to the optimum size.

The selection of detectors for the various spectral regions is indicated in table I (sec. 2.1). The most sensitive detectors (for the conditions of use envisaged) were chosen in each case.

A final word should be said about the 1- to 5-μ region. The spectral power density from sunlight terrestrial scenes is relatively weak in this region, so high spectral resolution is undesirable from an SNR point of view. With the NaCl prism system it is possible to resolve the 1- to 1.5-μ, the 3- to 4.1-μ, and the 4.5- to 5-μ atmospheric windows. The 1.5- to 1.8-μ and the 1.0- to 2.5-μ bands, however, would not be resolved, so individual narrowband filters will be used over detectors to separate these two bands to complete the partial resolution provided by the spectrograph.

II.3. THE CALIBRATION SYSTEM

To produce absolute results which can be compared with spectra obtained at other times or in other ways, it is necessary to provide a continuous calibration of the scanner-spectrograph. This is done by introducing sources of known spectral intensity into the optical path of the scanner during the dead time between scan lines. For the channels operating at wavelengths below 4 μ these sources are a set of quartz-iodine-tungsten lamps of various wattages. The lamps are placed beside the scan mirror and are baffled in such a way that radiation from each

lamp is reflected into the beam in turn during the dead time of the scanning sequence. The wattage and geometry of the lamps are arranged so that the signal levels they create bracket the range of interest. (A calibration system of this type is already in use in an airborne scanner at the Willow Run Laboratories.) For the thermal infrared channels ($\lambda > 4\ \mu$), lamps are not satisfactory, and cooler but larger blackbody sources must be used. For convenience, these are introduced by the mirror chopper which is illustrated in figure 33 just in front of the entrance slit of the spectrograph. Two small blackbodies whose temperatures will be controlled by thermoelectric heater/coolers will be focused in turn into the entrance slit of the reflecting blades of the chopper by means of a convex mirror of appropriate focal length. The phasing of the mirror chopper and the angles of its blades are set so that the radiation from these two reference sources are introduced into the spectrograph beam at appropriate times. The temperatures of the two sources are controlled to bracket the temperatures of the scene being overflown at the time of each flight.

A solar illumination level reference will also be provided by using a relatively long fiber-optics relay bundle. One end of this relay bundle will be connected to an optical receiver mounted on the top of the aircraft fuselage. The other end of the bundle will terminate at the scanner case at such a position that the radiation leaving it strikes the scan mirror and enters the spectrograph at an appropriate time during each revolution.

II.4. CRYOGENIC SYSTEM

The detectors used to cover the infrared region at wavelengths longer than 1.06 μ must be cooled to 77°K or below in order to obtain the necessary sensitivity and response time. While the performance and reliability of the various thermodynamic refrigeration systems have improved, we feel that for a laboratory model of an airborne system of the size and usage involved, a liquid storage system will prove more satisfactory and more reliable. Liquid nitrogen would be used for the InAs and InSb detectors and liquid helium for the Ge:Hg detectors. The latter can be operated satisfactorily at higher temperatures using liquid neon or hydrogen, but the former is more expensive than helium and the latter considered unsafe for airborne use, so alternative coolants are not considered. The use of liquid helium has a further advantage, in that it is possible to use a low-resistance type of doped germanium which is unsatisfactory at the higher temperatures of liquid hydrogen or liquid neon because of double time constant effects.

Supplies of liquid nitrogen and helium present no logistic problem within the United States, where this program would be conducted. If later it becomes necessary to use the airborne

subsystem in locations at which supply of these liquids was impossible then closed-cycle cryostats should be incorporated in the subsystem.

The detectors will be mounted in dewars by the detector manufacturers. These dewars will be integrated with the spectrograph system. In order to provide long hold times, they will be filled during flight from larger storage dewars carried in the aircraft. Such liquid transfer operations during flight are carried out regularly by Willow Run Laboratory personnel and present no problems.

II.5. MECHANICAL INTEGRATION AND ALIGNMENT

While mechanically configuring this instrument, the chief criteria have been that its main use will be that of a research tool. Versatility and ease of access, handling, and modification have been fundamental considerations. Weight and bulk have biased the design only secondarily. Aside from the primary experimental function of the instrument—of gathering and processing multispectral data—no other elaboration on new state-of-the-art work has been sought or desired. This is to say that, as far as is possible, all auxiliary equipment such as cryogenic coolers, bearings, motors, etc., involve conventional techniques only.

II.5.1. THE OPTICAL-MECHANICAL ASSEMBLY. The optical layout of the instrument was illustrated in figure 30. Figure 33 shows the same optics now mounted and enclosed in a mechanical structure, a cross section of which is shown. Basically, the structure is an aluminum casting to which are attached either internally or as appendages the numerous optical components. Because of the complex angular relationships existing between the various optical elements, it was felt that these relationships could best be achieved and maintained by using an annealed casting for the basic structure. The fabrication process will be to rough cast the structure, anneal it, and subsequently machine the mounting seats or surfaces thereon.

It now becomes convenient to discuss the instrument in terms of three subassemblies: the scanner unit, the spectrometer unit, and the detector systems.

II.5.1.1. The Scanner Unit. The scanner consists of a 45° single-face scan mirror cantilevered out from its support bearings. The mirror itself will be of aluminum or possibly beryllium. The flat polishing of either of these materials and the deposition of a mirror surface thereon is a known process which is accomplished without difficulty. The back side of the mirror is relieved to partially facilitate balancing. When removing this material, the remain-

ing material will need to be proportioned such that no flexure occurs. At a rotational speed as low as 2000 rpm the problem of maintaining mirror rigidity appears to be quite minimal.

The truncated mirror itself is to be bolted to a flanged one-piece stainless-steel shaft. Integral to this shaft is a crowned drive pulley. The shaft is supported by two pairs of preloaded, close-tolerance bearings. The duplex bearing pair on the right is fixed in its hanger while the pair on the left is free to move axially in its housing. This mounting arrangement has great rigidity, eliminating axial and radial play as well as skewing motion. Such precautions are necessary to insure that the scan mirror will always be viewing at right angles to the forward motion of the aircraft.

For smooth operation it is imperative that the scan shaft be well balanced dynamically. Because the unit is intended to operate at only one speed, a high degree of balance ought to be possible in spite of the inherently unsymmetrical shape of the scan mirror. Final balancing is to be accomplished with the scan shaft and mirror mounted in their bearings and supported by the hangers provided in the casting. A high degree of balance ultimately results in smoother operation, better optical resolution, and elimination of microphonic noise pickup in the detectors.

The power unit selected for driving the scan mirror is a 400-cycle hysteresis synchronous motor operating at a speed of 4000 rpm. This seemed a logical choice for several reasons: (1) 400-cycle power is commonly available aboard aircraft; (2) such a motor provides good speed regulation dependent upon the aircraft electrical inverter which itself may be closely controlled; and (3) an ac motor as contrasted to a dc motor emanates much less radio and line noise. This latter consideration is of great concern when working with low output signal level infrared detectors.

Power transmission from the motor occurs through a flat mylar belt running over two crowned pulleys which provide a speed reduction of 2:1. A mylar belt was chosen again because of the smooth, vibrationless performance which it can be expected to provide.

The other optical element in the scanner subsystem is an off-axis paraboloid. This collector mirror is restrained by a kinematic mount allowing for a 3-degree-of-freedom adjustment such that incident radiation is redirected and focused upon the entrance slit of the spectrometer system. The unit is contained in a cylinder which is bolted and pinned to the main casting. Removal of this cylinder allows for convenient access to the spectrometer entrance slit—a feature particularly desirable during laboratory testing and alignment of the spectrometer system.

II.5.1.2. The Spectrometer. The spectrometer has already been described in some detail and it is the intent of this section to amplify only on the physical mounting of the various optical elements. The entrance slit of this spectrometer is located immediately adjacent to an array of fiber-optic bundles. Each of these bundles might be considered as an exit slit of the spectrometer. Figuratively speaking, then, the entrance and exit slits of this spectrometer are located side by side in a common machined assembly. This unit is then bolted into a seat fabricated for it in the main casting. Similarly, the Pfund folding mirror is fixed in its seat immediately behind the slit. A small folding mirror is located in this region and serves to intercept and redirect the 8- to 13.5-μ energy of the spectrally dispersed exiting beam.

The remaining two optical elements of the spectrometer (i.e., the spherical mirror and the prism) are provided with positioning adjustments such that an overall alignment of the spectrometer may be affected. The spherical mirror is supported by a mount of kinematic design providing 3 degrees of freedom. Its manipulation allows for properly directing and focusing the entering and exiting beams of the spectrometer. The prism is mounted on a table which may be rotated such that the spectrum of the exiting beam may be properly centered.

Because the salt prism is slightly hygroscopic, it must be maintained at a slightly elevated temperature. This serves to preclude condensation on the prism. A resistance heater of approximately 100-W capacity with some simple form of thermostatic control is to be mounted directly below the prism support table.

Associated with the spectrometer is a small chopper mirror located immediately ahead of the entrance slit. Its function is to direct a thermal calibration signal to the spectrometer. Rotation of this chopper is synchronized with the scan mirror through a flexible drive shaft linked directly to the scan-mirror shaft. (For the sake of clarity this drive connection has not been shown in fig. 33.) Implementation of system calibration was discussed in section II.3.

II.5. The Detectors. The detectors are the most critical part of the instrument. Considerable equipment must be integrated into a small package. Essentially, the detectors or their associated fiber optics constitute the exit slit of the spectrometer. They need to be precisely positioned and in the case of the infrared fiber optics the lengths need be minimized to avoid undue energy attenuation.

For the spectral channels falling in the 0.32- to 5.0-μ region fiber optics are to be used, thus decentralizing these detectors and avoiding an impossibly compact array of detectors. In figure 33 the location of these fibers relative to the spectrometer is indicated. They are shown

mounted in a dovetail slide such that their wavelength position in the dispersed radiation may be varied. Also shown in figure 33 is the 8.0- to 13.5-μ detector array and its associated liquid-helium cooling dewar. Because satisfactory fiber optics for this wavelength region have not yet been developed, it has not been possible to utilize fibers, and the positioning of the detectors immediately at the focal plane has been necessitated. The dewar is held in an adjustable mount providing for linear adjustments along its three orthogonal axes.

The optical fibers for the 1.0- to 5.0-μ infrared channels will be made of arsenic trisulfide. Glass fibers will be utilized in the 0.4- to 1.0-μ region, and a quartz light pipe will suffice for the single ultraviolet channel. Of these, the arsenic trisulfide fibers exhibit an exceedingly large attenuation per unit of length, thus implying that the detectors for these wavelength bands must be located closest to the spectrometer focal plane. These fibers will be between 2 and 4 in. long, a tolerable length in terms of signal loss. Figure 34 shows the detector end of one of these infrared transmitting fibers. These fibers transfer the spectrum to a position where it can be conveniently reimaged with a relay lens onto a cooled detector array mounted in a vacuum dewar. Reimaging with a relay lens is required because: (1) the cooled detector cannot be brought in contact with the end of the fiber bundles and (2) the detector sensitivity is inversely proportional to the detector area and the radiation emerging from the fibers should be imaged onto the detector into as small an area as possible.

As is indicated, the fiber terminus is fixed relative to the field lens, but the two are adjustable as a unit such that focusing upon the detector flake may be affected. Five detectors will utilize this configuration.

The remaining detectors for the wavelength bands below 1.0 μ are all to be photomultipliers. A generalized configuration for these detectors is shown in figure 35. Because the sensitive area of the photomultiplier is of gross size, it is necessary only that the fiber end be directed at the face plate. These fibers will be 6 to 8 in. long, allowing for much more latitude in placement of the photomultipliers. Approximately 13 spectral channels will utilize photomultiplier detectors.

II.5.1.4. Comparison with the Willow Run Laboratories 12-Channel System. Willow Run Laboratories has previously built and operated a spectrometer detector system which utilized photomultiplier sensors in conjunction with glass fiber optics. This existing system operates only in the 0.4- to 1.0-μ region. Its concept is not unlike that of a portion of the system now being proposed. Several views of the existing spectrometer detector are shown in figures 36 and 37. Figure 38 shows the fiber-optic assembly prior to its incorporation into that system.

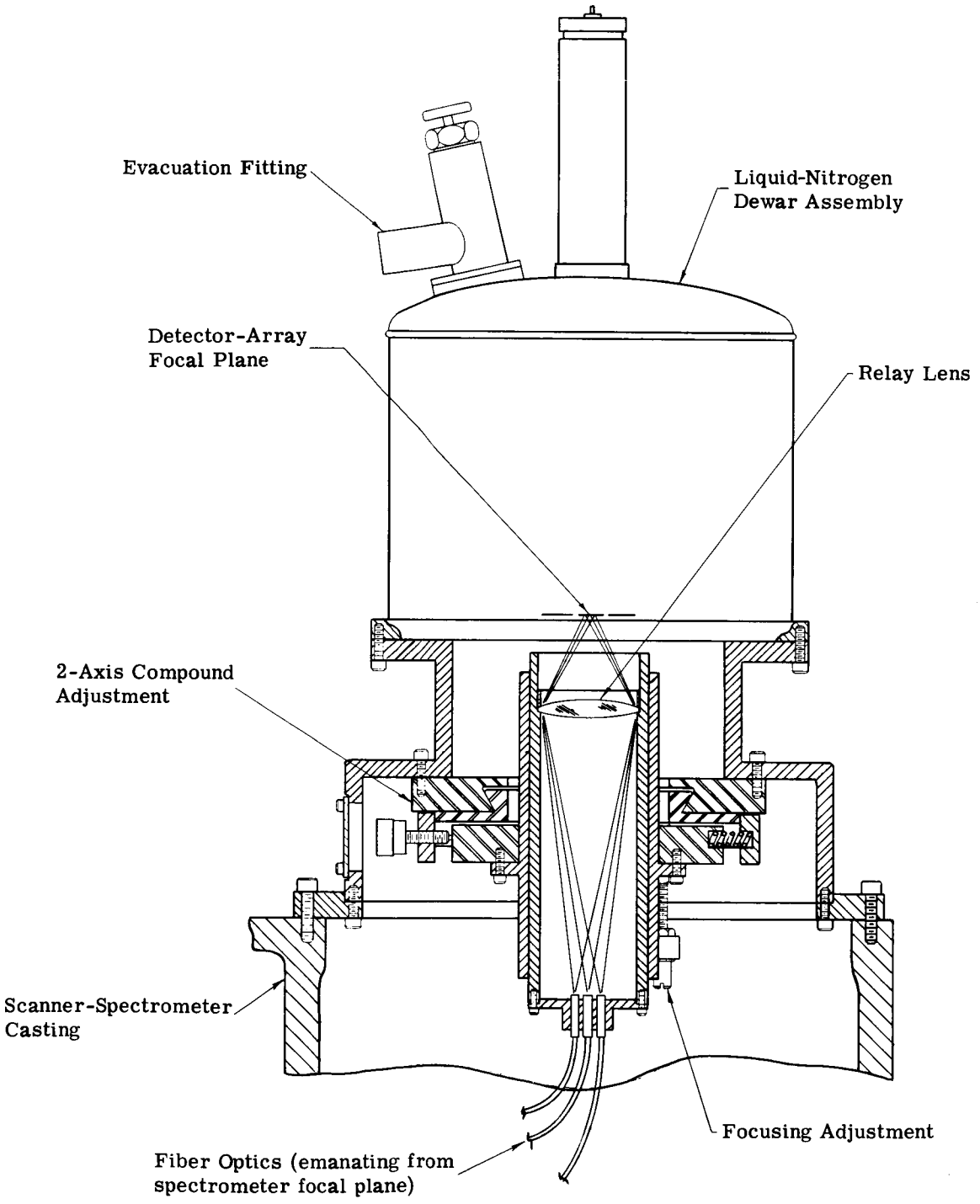

FIGURE 34. TYPICAL CONFIGURATION OF INFRARED DETECTORS (1.0 to 5.0 μ)

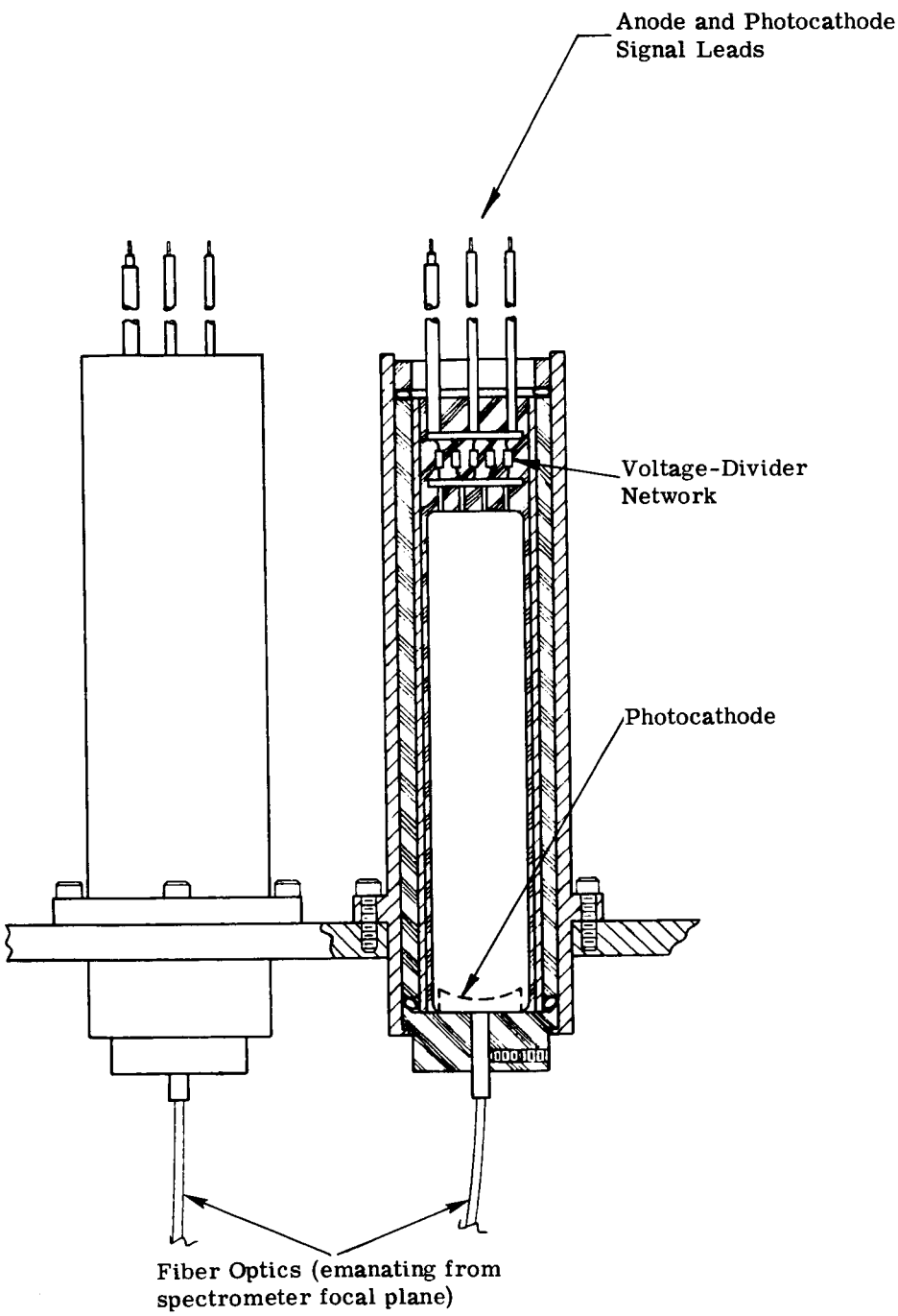

FIGURE 35. TYPICAL CONFIGURATION OF PHOTOMULTIPLIER DETECTORS (0.32 to 1.0 μ)

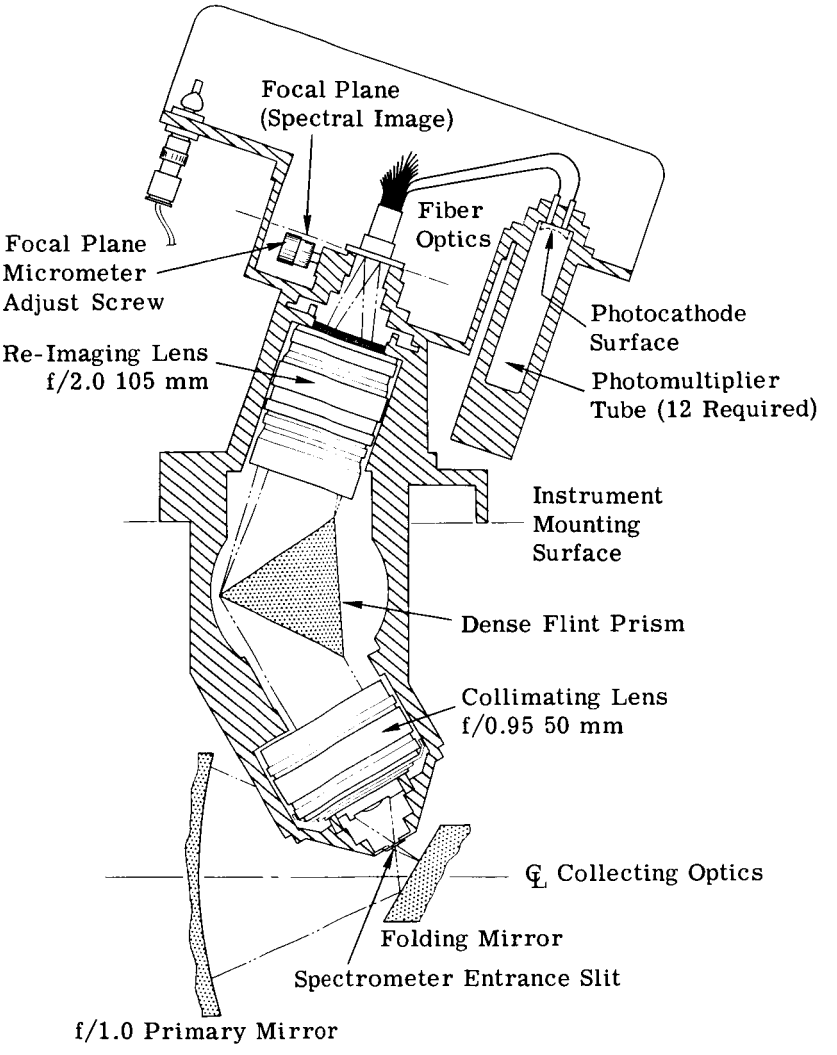

12-CHANNEL SPECTROMETER
(0.4 μ To 1.0 μ)

FIGURE 36. CONCEPTUAL SECTIONED VIEW OF EXISTING SPECTROMETER DETECTOR SYSTEM

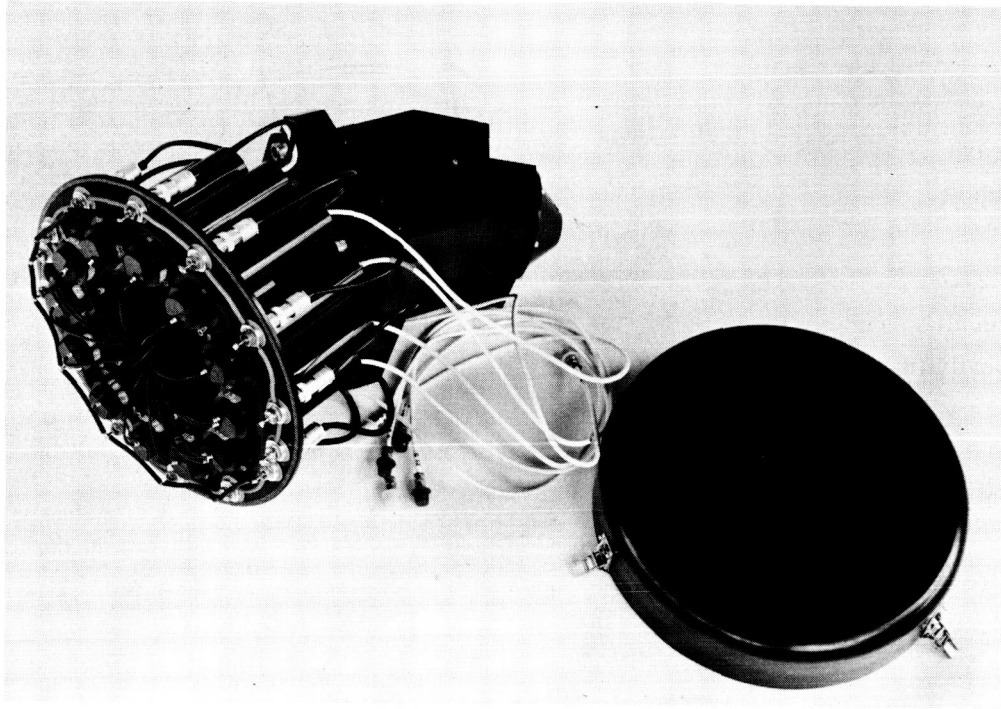

FIGURE 37. EXISTING SPECTROMETER DETECTOR SYSTEM WITH ACCESS COVER REMOVED

FIGURE 38. FIBER OPTICS OF EXISTING SPECTROMETER DETECTOR SYSTEM

This spectrometer as of this writing has been operated continuously for four months on a relatively heavy flying schedule. Strip-map quality from the system has been as good as has ever been achieved with any single-element infrared detector.

II.5.2. OPTICAL-MECHANICAL ALIGNMENT. In section II.5.1 many allusions were made to system alignment and the adjustments provided therefore. Figure 39 and table V serve to categorically list these numerous adjustments. In the table the linear adjustments along the x, y, and z axes are tabulated as are the angular motions of yaw and pitch. Suffice it to say that the freedom provided by these various adjustments will be adequate for full and complete alignment of the instrument system.

II.6. AIRBORNE ELECTRONICS

II.6.1. AIRBORNE DISPLAY AND CONTROLS. An airborne operator task list is shown in table VI. The controls are about equally divided between two consoles, each the responsibility of one operator. A Tektronic 545 scope with a four-channel preamplifier is provided for each operator to view four "A scans" simultaneously. Any four signal channels can be selected out of either the postamplifiers, offset circuit, or tape recorder. Another scope preamplifier is provided which allows the operator to view an A scan of any preamplifier output. Other functions are listed in table VI.

II.6.2. AIRBORNE SIGNAL AMPLIFIERS. Figure 40 is a block diagram showing the four types of signal channels. Several important features such as single point grounding, clipping, dc restoration, and modular construction are planned to give good performance and easy maintainability.

Each detector-preamplifier combination has a single point grounding at the detector. This has been done to minimize ground loops, resulting in less power frequencies and power fluctuations in the signal channels. Each detector-preamplifier combination is powered with a battery. The charge condition of the batteries can be checked by switching in a load and voltmeter across each battery during a preflight check. The postamplifier and the tape recorder have a common signal grounding which is separate from the detector ground and power ground. Much consideration has been given to grounding, since this problem limits the present scanner sensitivities rather than the amplifier, or more desirably, the detector, noise.

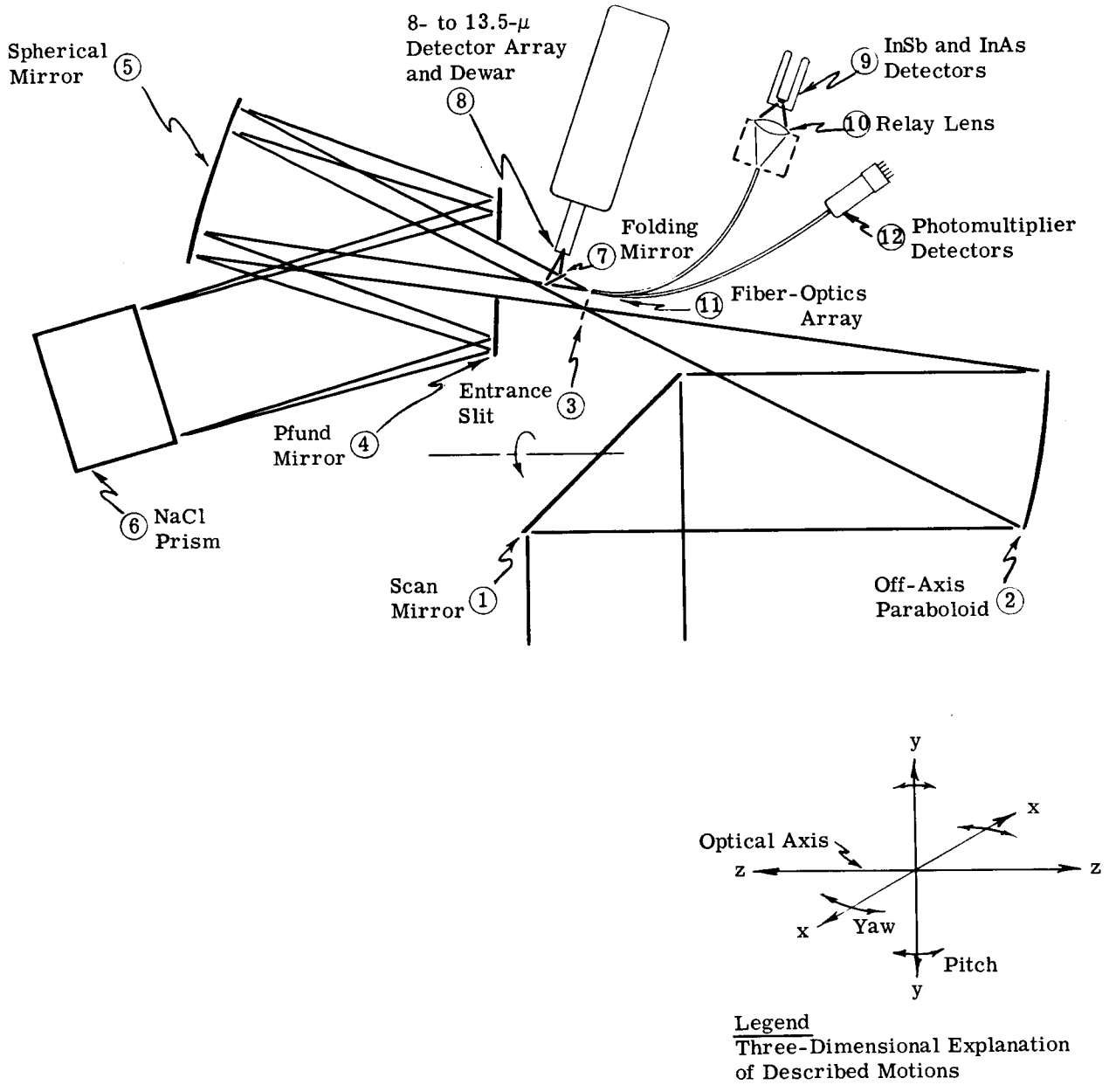

FIGURE 39. OPTICAL ADJUSTMENTS

TABLE V. OPTICAL ADJUSTMENTS

Element	Adjustment					Notes
	Linear Motion			Rotary Motion		
	x	y	z	Yaw	Pitch	
Scan mirror 1.†						Rotary scan motion only
Off-axis paraboloid 2.			✓	✓	✓	
Entrance slit 3.						Fixed position—not adjustable
Pfund mirror 4.						Fixed position—not adjustable
Spherical mirror 5.			✓	✓	✓	
Rock-salt prism 6.				✓		
Folding mirror 7.						Fixed position—not adjustable
8- to 13.5-μ detector array and dewar 8.	✓	✓	✓			
InSb and InAs detectors 9.*						Fixed position—not adjustable
Detector relay lens 10.*	✓	✓	✓			
Fiber-optics array 11.	✓					
Photomultiplier detectors 12.						Fixed position—not adjustable

† Numbers refer to figure 39.

*See figure 34 for more detail.

TABLE VI. AIRBORNE-CONSOLE FUNCTIONS

Operator A 0.33- to 2.5-μ Console	Operator B 2.5- to 13.5-μ Console
Controls	Controls
Lamp #1 current	Blackbody #1 temperature
Lamp #2 current	Blackbody #2 temperature
Preamplifier gain	Lamp #3 current
Postamplifier gain	Postamplifier gain
Offset	Offset
Intercommunication level	
Tape recorder (start-stop)	
Scanner power	
Gyro (cage-uncage)	
Window (open-close)	
Monitor	Monitor
Alert and ready indicator	All He on N_2 levels
	Alert and ready indicator

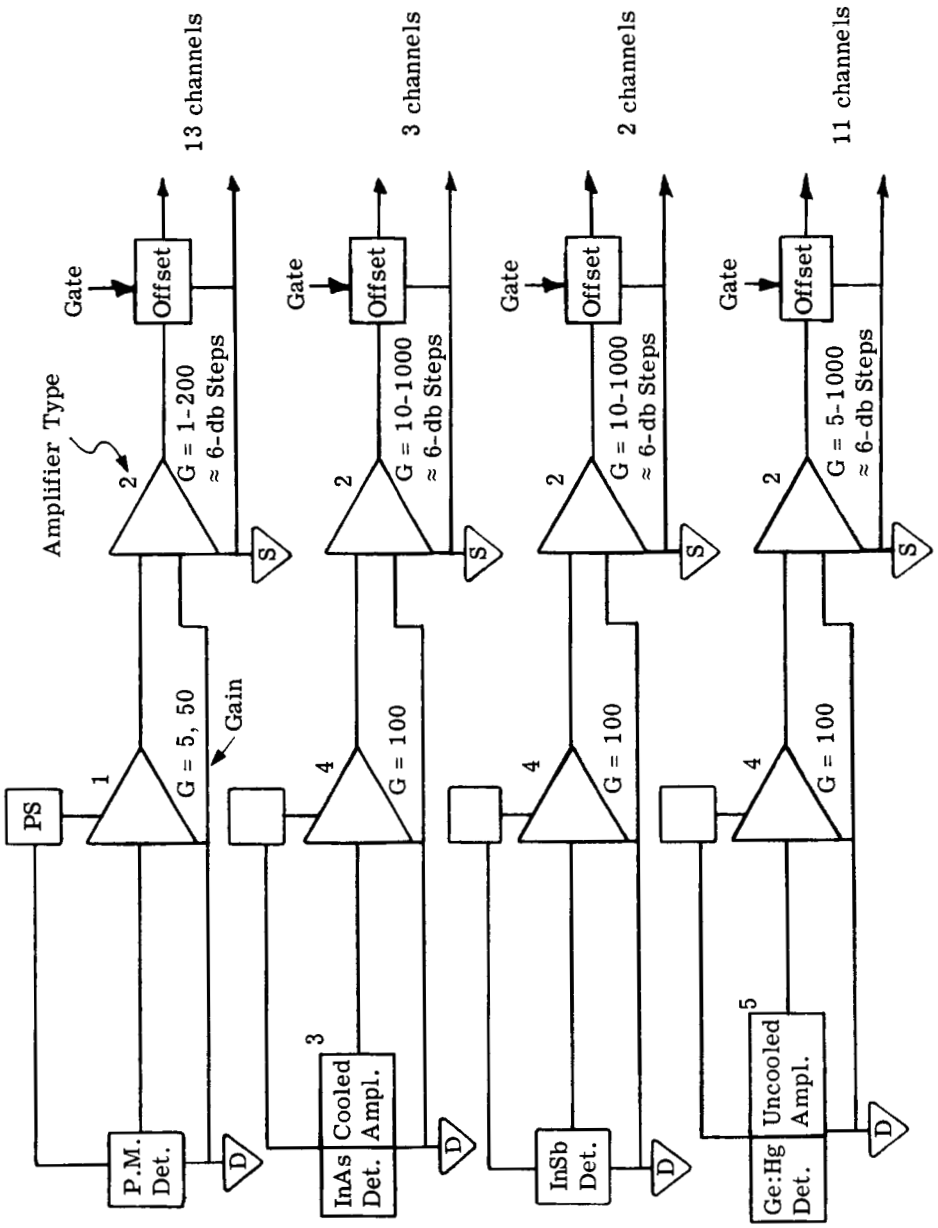

FIGURE 40. AIRBORNE SIGNAL AMPLIFIERS

Hard limiting (clipping) will be incorporated into the postamplifiers to preclude overdriving the tape recorder. Hard rather than soft limiting is used to give the operator and data analyzer a good indication of limiting when it occurs.

To eliminate dc drift, ac coupling is used, but the coupling frequency is low enough to allow less than 1% signal droop during a scan.

An offset capability is incorporated after each postamplifier which is independent of channel gain and which automatically adjusts one reference voltage (zero radiation voltage in reflective channels and one blackbody voltage in the thermal channels) to a stable level.

The preamplifiers and postamplifiers are modules which are interchangeable and replaceable during a flight.

The 13 photomulitplier channels utilize a Philbrick P25AU operational amplifier (OA) as a preamplifier (type 1 of fig. 40). This is possible because, first, this OA has a noise figure less than 1 db (adds less than 13% to the noise voltage over an uncooled ideal amplifier) and second, because the electron multiplier inside the photomultiplier is really the preamplifier.

The three InAs detectors require the use of a cooled source follower (such as a 2N3089A transistor cooled to liquid-nitrogen temperature) located either in the detector dewar or within several inches of the dewar (type 3 of fig. 40). The resulting output signal should be followed by a good low-noise uncooled preamplifier (such as a 2N3117 transistor) (type 4 of fig. 40).

The two InSb detectors do not require the use of cooled preamplifiers, but the use of low-noise transistors such as the 2N3117 is indicated.

The 11 Ge:Hg detectors require the use of an uncooled source follower (such as a 2N2500 transistor) located within several inches of the dewar as the InAs detectors (type 5 of fig. 40). This amplifier should be followed by a preamplifier (such as a 2N3117 transistor).

The mentioned requirements for source-follower amplifiers and preamplifiers are based on near detector noise-limited channels. The postamplifiers each utilize a Philbrick P45AU operational amplifier (type 2 of fig. 40) which can provide a gain of up to 1000. Step gain settings separated by about 6 db are planned over the anticipated range required. We chose dc restoration or automatic offset adjustment, first to reduce the offset drift caused by ac coupling and second to reference each resolution element's voltage radiance to a fixed voltage rather than a voltage corresponding to the average scene radiance as would result from ac coupling.

II.6.3. ROLL CORRECTION. The roll-correction sensor is a vertical gyroscope which will provide a dc signal proportional to the aircraft roll angle. This signal is compared to a ramp voltage that was initiated by the uncorrected sync pulse. When the ramp voltage equals the gyro voltage the roll-corrected sync pulse is generated. This technique is conventional and a detailed explanation of the implementation is not deemed necessary.

II.6.4. AIRBORNE POWER. Almost all power required for the airborne equipment is 400 Hz. This will be derived from two 2.5-kVA (400-Hz) inverter driven from the 28-V bus. The 28-V 200-A generators are driven directly from the aircraft engines. This amount of power allows for some power growth and should therefore be adequate.

II.7. THE AIRBORNE TAPE RECORDER

Performance specifications for the airborne tape recorder should be comparable with those listed for the ground-based tape recorder in section 2.2.4.1. In addition, the unit should be reasonably small and lightweight, with a capability of operating satisfactorily from electrical power available in the aircraft.

The MINCOM Model PC 500 recorder manufactured by the MINCOM Division of the 3M Company appears to be the most satisfactory unit for this purpose. This unit may be operated from either 60-Hz or 400-Hz power at 115 V ac. It may be obtained with a direct-record bandwidth of 2-MHz, and with 14 channel record and reproduce heads for 1-in. tape. Each of the first 11 of the record heads would be connected to a record amplifier which was being driven by three voltage-controlled oscillators, with each oscillator having a different average frequency. This would permit multiplexing three data channels on each of the first 11 heads, thus providing capacity for the 29 scanner channels plus 4 spares. The remaining three record channels would be equipped with direct-record electronics, and would be used as described in section 2.2.4.3 to record voice comments, miscellaneous data, and possibly a television signal picturing the area being scanned.

Some method of monitoring the data recorded on the tape is needed to guarantee that all record channels are operating properly. It would not be necessary to provide a full complement of reproduce electronics for the airborne recorder, however, as a switch could be used to switch one set of electronics from one playback head to the next. Thus, the playback electronics for the airborne recorder would consist of direct reproduce electronics which could be switched between playback heads 12, 13, and 14 and a set of three FM reproduce channels

with three separate center frequencies, driven by a preamplifier whose inputs could be switched to any of the remaining playback heads. The recorded scanner signals could be monitored at one of the consoles.

II.8. SCANNER-SPECTROGRAPH PERFORMANCE PREDICTION

Basic parametric relationships for a scanner-spectrograph system of the kind described in this appendix have been developed by Braithwaite [9]. For ease of reference the most important of these relations are reproduced below. Further work now in process at Willow Run Laboratories has made it possible to express the sensitivity in terms of noise-equivalent reflectance difference or noise-equivalent temperature difference. These equations, the derivation of which will be published soon, are also given below.

Braithwaite's equations

$$\dot{\alpha} = \frac{2\pi(V/H)}{n\beta}$$

$$\tau = \frac{n\beta^2}{2\pi(V/H)}$$

$$\delta\lambda = \frac{D_1\beta}{D_2(d\theta/d\lambda)}$$

$$d_2 = \beta D_1 F_2$$

$$d'' = m\beta D_1 F_d$$

$$L = M\beta D_1 F_2$$

$$\Delta f = \frac{\pi(V/H)}{\beta^2 n}$$

$$(SNR)_{D\lambda} = \frac{N_\lambda \delta\lambda'}{4}\sqrt{\frac{\pi n}{m^p}}\cdot\frac{D_1 D^*\beta^2}{F_d\sqrt{V/H}}(o.e. \times s.e.)$$

$$(SNR)_{S\lambda} = 4.2 \times 10^8 D_1\beta^2\Delta\rho_\lambda\sqrt{\frac{nR_c H_\lambda \delta\lambda(o.e.)}{\rho_\lambda(V/H)}}(s.e.)$$

New equations

$$(NE\Delta\rho)_{D\lambda} = \frac{4FD\sqrt{\pi(V/H)}}{H_\lambda \delta\lambda\beta^2 D_1 D^*_\lambda(o.e.)}$$

$$(NE\Delta T)_I = \frac{4Fd\sqrt{(V/H)/\pi}}{\epsilon_\lambda N_\lambda \delta\lambda \beta^2 D_1 D_\lambda^*(o.e.)}(c_2/\lambda T^2)^{-1}$$

$$\left(\frac{NE\Delta\epsilon}{\epsilon}\right)_{D\lambda} = \frac{c_2}{\lambda T^2}(NE\Delta T)$$

$$(NE\Delta\rho)_{s\lambda} = \frac{2.41 \times 10^{-7}}{\beta^2 D_1} \frac{(V/H)}{H_\lambda \delta\lambda R_c(o.e.)}$$

where

D_1 = scanner telescope aperture

D_2 = aperture of dispersing element

D^* = specific detectivity of solid-state detectors

d'' = width of one detector

d_2 = width of exit slit

$d\theta/d\lambda$ = angular dispersion of dispersing element

F_2 = f-number of spectrograph telescope

F_d = f-number of beam at the detector

H = vehicle altitude

H_λ = irradiance at target

M = number of spectral channels

$m = \delta\lambda'/\delta\lambda$

N_λ = target radiance

n = number of faces of scan-mirror assembly

o.e. = optical efficiency

p = 2 if field lenses are used but 1 if they are not

R_c = cathode radiant sensitivity of photoemissive detector

$(SNR)_{D\lambda}$ = spectral signal-to-noise ratio when noise level is independent of signal level

$(SNR)_{S\lambda}$ = spectral signal-to-noise when signal-dependent shot noise predominates

s.e. = signal efficiency

V = vehicle velocity

$\dot{\alpha}$ = rotational rate of scan mirror

β = instantaneous angular field of view of scanner

Δf = electronic noise bandwidth

$\Delta\rho_\lambda$ = reflectance variation

$\delta\lambda$ = instrument-limited resolved wavelength interval

$\delta\lambda'$ = resolved wavelength interval used

λ = wavelength (as a subscript it denotes "spectral")

ρ_λ = target spectral reflectance (generally a function of angle of view and angle of illumination)

τ = dwell time

c_2 = the second constant in Plank's equation

T = surface temperature

$(NE\Delta\rho)_{D\lambda}$ = noise-equivalent spectral-reflectance difference (noise independent of signal level)

$(NE\Delta T)_I$ = noise-equivalent temperature difference (noise independent of signal level)

$(NE\Delta\epsilon)_{D\lambda}$ = noise-equivalent spectral-emittance difference (noise independent of signal level)

$(NE\Delta\rho)_{s\lambda}$ = noise-equivalent spectral-reflectance difference when signal-dependent shot noise predominates (i.e., photomultiplier tubes)

The $NE\Delta\rho$ is the change in ρ between two resolved ground elements which will give rise to a signal equal in magnitude to the rms value of the total noise from all sources (i.e., system noise, photon noise, etc).

The computed spectral performance characteristics for the system are plotted in figure 41. To obtain these results, values for the system parameters enumerated in table I of section 2.1 have been inserted in the appropriate equation together with other parameters whose selection is discussed below.

(1) The solar spectral irradiance (H_λ) is given in figure 42. (2) The cathode radiant responsivities (R_c) of two photomultipliers are shown in figure 43. These cells were selected for their high responsivities over the wavelength regions of interest. (3) The detectivities of several infrared detectors are plotted in figure 44. Again, these cells were selected on the basis of their wavelength (and temperature-dependent characteristics). (4) Figure 45 shows the spectral resolution of the system from which the $\delta\lambda$'s have been deduced. Only the points marked have significance. The curves are shown only to indicate trends. (5) No estimate of atmospheric-transmission effects has been included. Such effects will be slight except in those channels whose wavelength range includes atmospheric absorption bands. For those channels for which atmospheric absorption is not negligible, the most likely source of error in the

curves lies in the difficulty of estimating the optical efficiency and preamplifier noise figures (cf. table VII). While the reflection efficiency of each mirror can be predicted fairly accurately, when a large number of mirrors are used the overall uncertainty is compounded. Fiber-optics transmissions are also somewhat uncertain, particularly from the 3- to 4-μ and 4- to 5-μ channels for which As_2S_3 fibers may have to be used. However, conservative estimates have been used for these efficiencies and the performance curves given should be representative or slightly pessimistic compared to what will be achieved in practice.

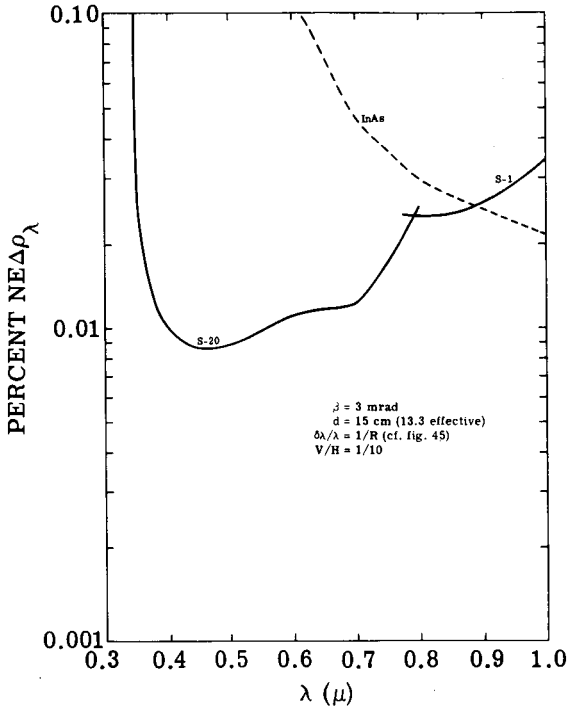

(a) 0.35 to 1 μ

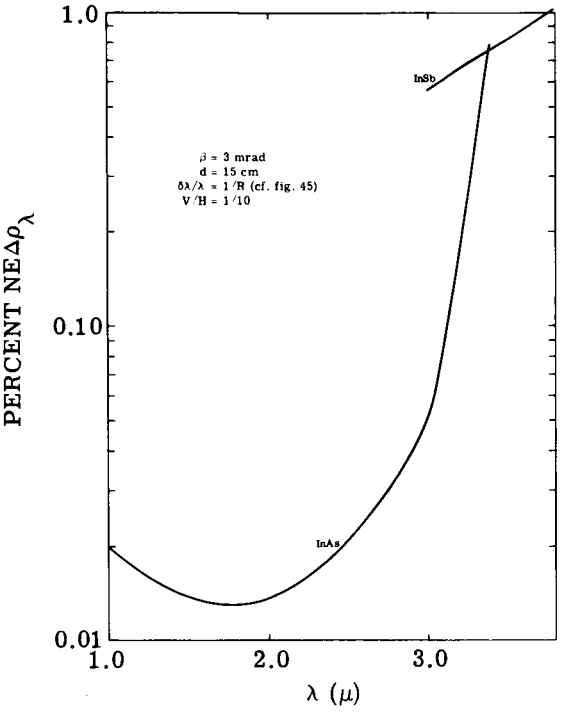

(b) 1 to 3.4 μ

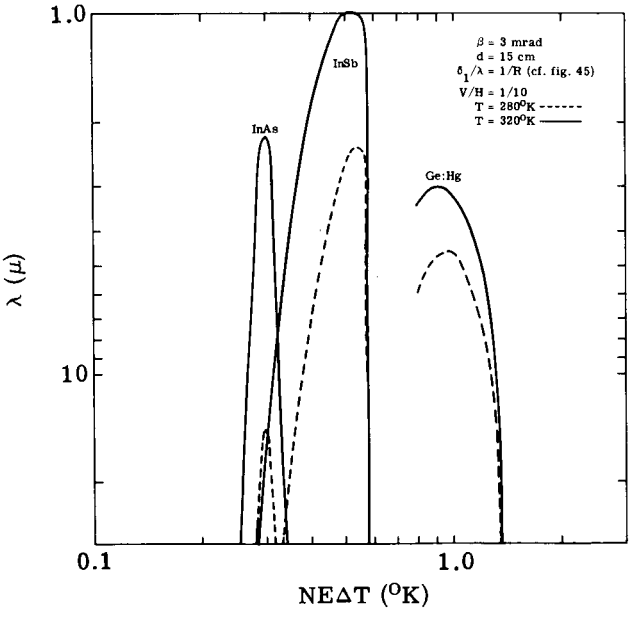

(c) 2.5 to 15 μ

FIGURE 41. COMPUTED SYSTEM PERFORMANCE

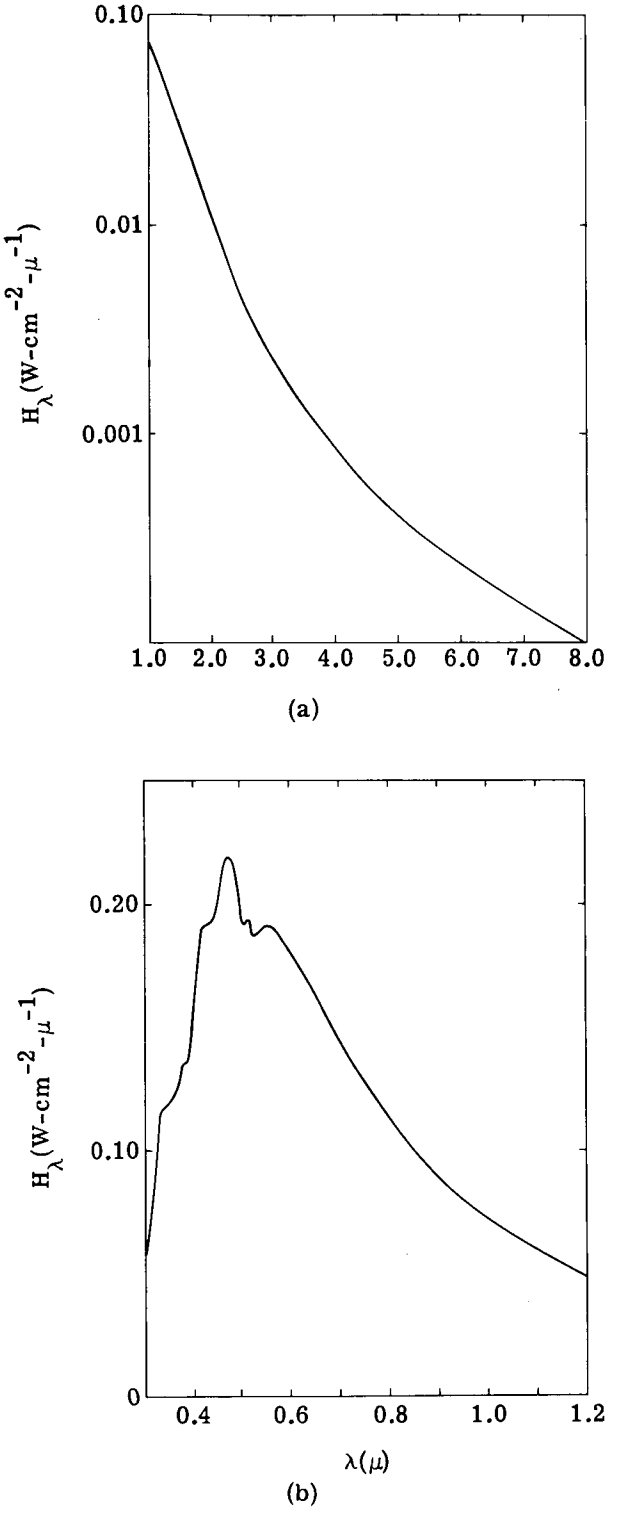

FIGURE 42. SOLAR SPECTRAL IRRADIANCE (ABOVE ATMOSPHERE)

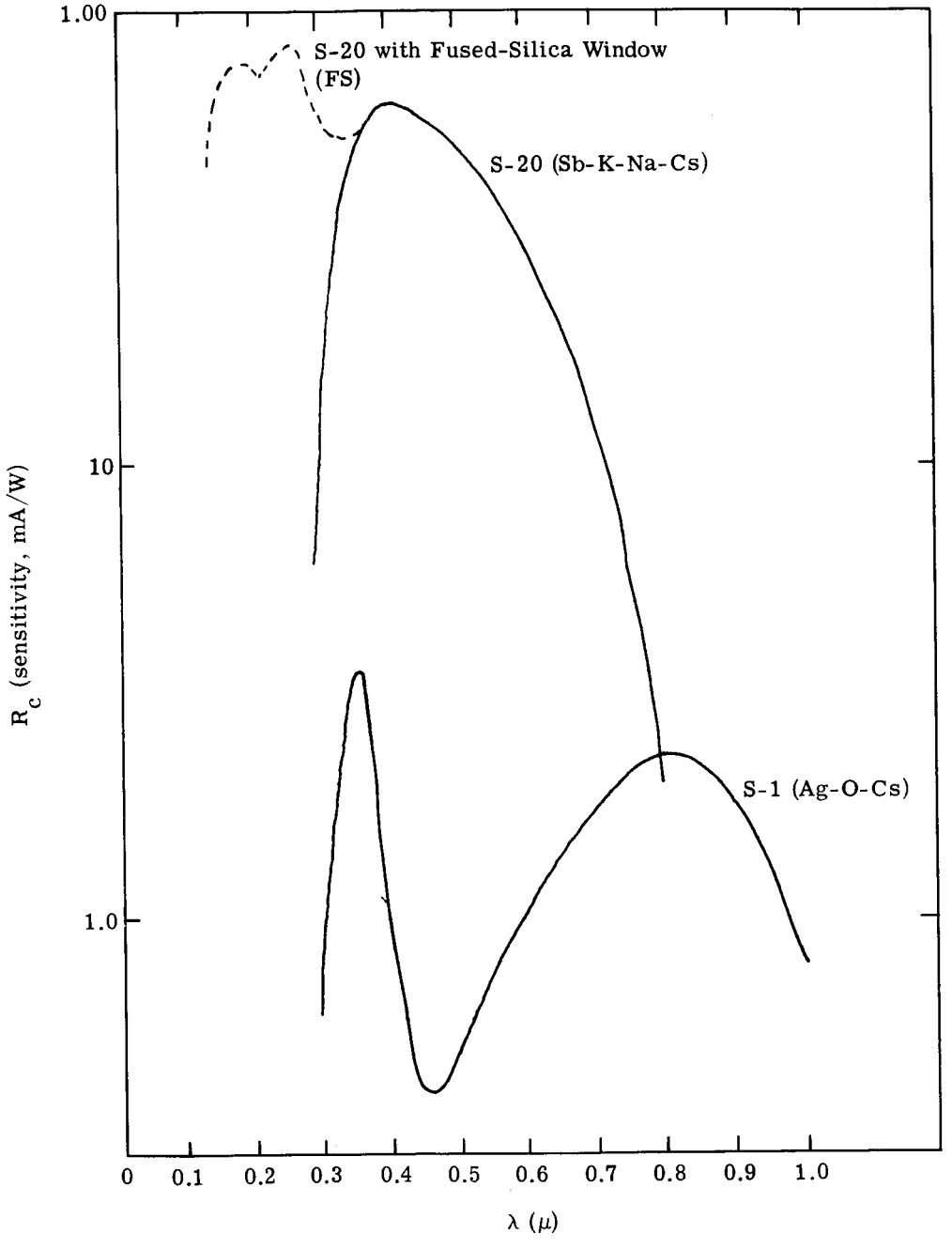

FIGURE 43. PHOTOMULTIPLIER SENSITIVITY

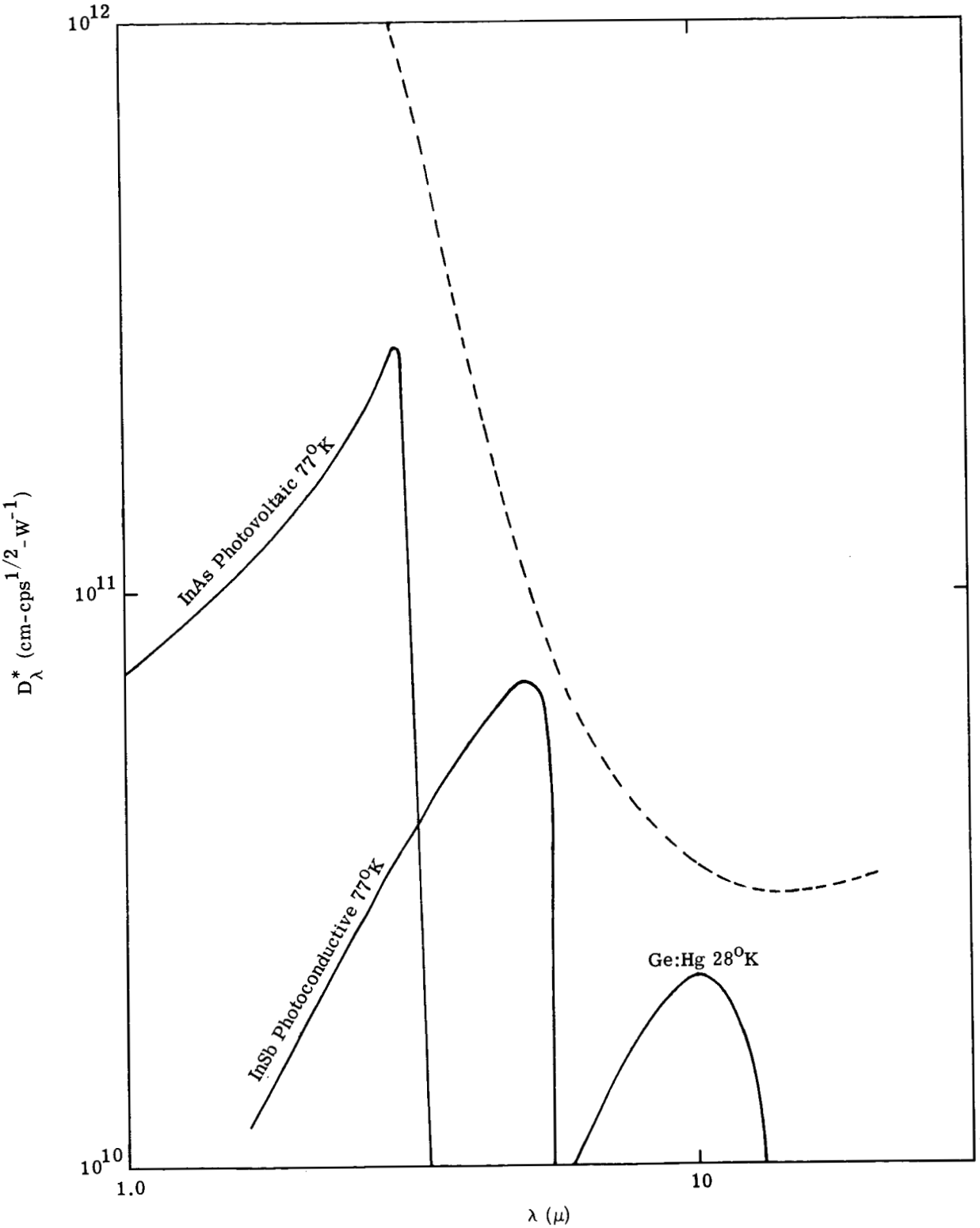

FIGURE 44. INFRARED-DETECTOR SPECTRAL DETECTIVITIES

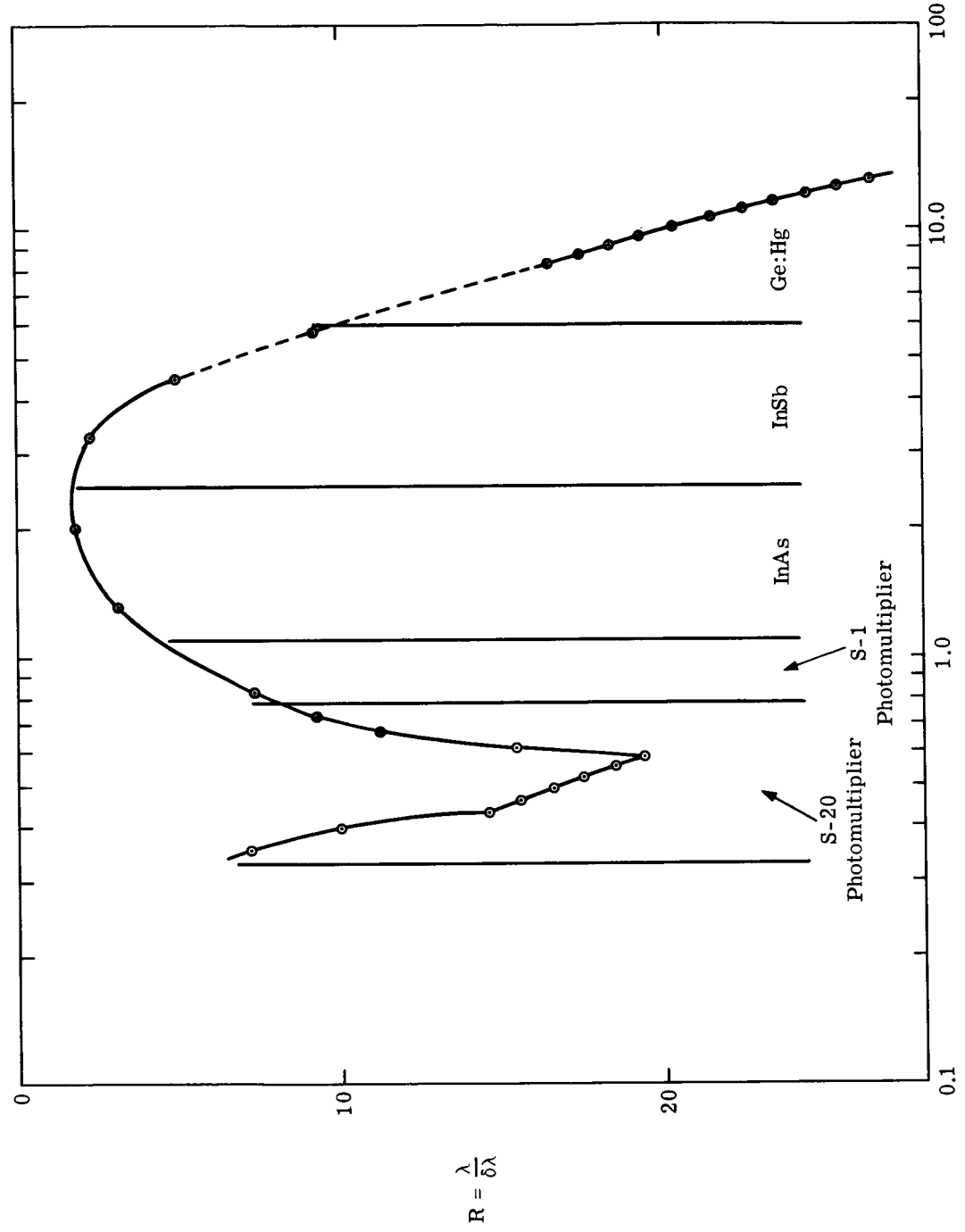

FIGURE 45. SPECTRAL RESOLUTION

TABLE VII. ESTIMATION OF OVERALL EFFICIENCIES

Wavelength Range (μ)	0.33-0.38	0.38-1.06	1.06-1.8	1.8-2.5	2.5-4	4-5	8-13.5
Reflectance (R)	0.63	0.96	0.97	0.98	0.98	0.99	0.99
R^6	0.064	0.79	0.85	0.87	0.91	0.92	0.97
Prism Efficiency (P)	0.7	0.73	0.75	0.78	0.8	0.8	0.8
Image-Slicer Efficiency (S)	0.8	0.5	0.55	0.47	0.28	0.32	0.99
Optical Efficiency ($\tau = R^6PS$)	0.036	0.29	0.35	0.32	0.20	0.24	0.78
Electrical Efficiency (σ)	0.7	0.7	0.7	0.7	0.7	0.7	0.5*
Overall Efficiency ($\sigma\tau$)	0.03	0.20	0.25	0.22	0.14	0.17	0.39

*This could be raised to 0.7 by using cooled preamplifiers, but this does not seem to be justified.

REFERENCES

1. M. R. Holter and W. L. Wolfe, Proc. IRE, Vol. 47, 1959, p. 1546.
2. D. S. Lowe and J. G. N. Braithwaite, Appl. Opt., Vol. 5, 1966, p. 893.
3. M. A. Romanova, Air Survey of Sand Deposits by Spectral Luminance, Consultants Bureau, New York, 1964.
4. N. A. Raspolozhenskii, Geodesy Aerophot., Vol. 6, 1964, p. 358.
5. R. R. Legault and F. C. Polcyn, in Proceedings of the Third Symposium on Remote Sensing of Environment, Report No. 4864-9-X, Institute of Science and Technology, The University of Michigan, Ann Arbor, February 1965, p. 813.
6. C. E. Molineaux, Photogrammetric Eng., Vol. 31, 1965, p. 131.
7. D. S. Lowe, F. C. Polcyn, and R. Shay, in Proceedings of the Third Symposium on Remote Sensing of Environment, Report No. 4864-9-X, Institute of Science and Technology, The University of Michigan, Ann Arbor, February 1965, p. 667.
8. R. J. P. Lyon and E. A. Burns, in Proceedings of the Second Symposium on Remote Sensing of Environment, Report No. 4864-3-X, Institute of Science and Technology, The University of Michigan, Ann Arbor, February 1963, p. 309.
9. J. Braithwaite, Dispersive Multispectral Scanning; A Feasibility Study, Report No. 7610-5-F, Willow Run Laboratories of the Institute of Science and Technology, The University of Michigan, Ann Arbor, March 1966.
10. F. E. Terman, Electronic and Radio Engineering, 4th ed., McGraw-Hill, 1965, p. 289.
11. T. G. Birdsall and W. W. Petersen, The Theory of Signal Detectability, Technical Report No. 13 EDG, The University of Michigan, Ann Arbor, June 1953.
12. D. Blackwell and M. A. Girshick, Theory of Games and Statistical Decisions, Wiley, 1954.

BIBLIOGRAPHY

Davenport, W. B., and W. L. Root, Random Signal and Noise, McGraw-Hill, 1958.

Lee, Y. W., Statistical Theory of Communication, Wiley, 1960.

DISTRIBUTION LIST

Copy No.	Addressee
1-10	National Aeronautics & Space Administration George C. Marshall Space Flight Center Huntsville, Alabama 35812
(1)	ATTN: PR-SC
(2)	ATTN: MS-IL
(3)	ATTN: MS-T
(4-5)	ATTN: MS-I
(6-10)	ATTN: R-ASTR-IMT (Harlan D. Burke)

UNCLASSIFIED

Security Classification

DOCUMENT CONTROL DATA - R&D

(Security classification of title, body of abstract and indexing annotation must be entered when the overall report is classified)

1. ORIGINATING ACTIVITY *(Corporate author)*
Willow Run Laboratories, Institute of Science and Technology,
The University of Michigan, Ann Arbor

2a. REPORT SECURITY CLASSIFICATION
Unclassified

2b. GROUP

3. REPORT TITLE

AN INVESTIGATIVE STUDY OF A SPECTRUM-MATCHING IMAGING SYSTEM

4. DESCRIPTIVE NOTES *(Type of report and inclusive dates)*
Final Report

5. AUTHOR(S) *(Last name, first name, initial)*

Lowe, Donald S., Braithwaite, John, and Larrowe, Vernon L.

6. REPORT DATE	7a. TOTAL NO. OF PAGES	7b. NO. OF REFS
October 1966	ix + 105	14

8a. CONTRACT OR GRANT NO.	9a. ORIGINATOR'S REPORT NUMBER(S)
NAS 8 21000	8201-1-F
b. PROJECT NO.	
c.	9b. OTHER REPORT NO(S) *(Any other numbers that may be assigned this report)*
d.	

10. AVAILABILITY/LIMITATION NOTICES
Libraries of contractors and of other qualified requesters may obtain additional copies of this report by submitting NASA Form 492 directly to: Scientific and Technical Information Facility, P. O. Box 5700, Bethesda, Maryland 20014.

11. SUPPLEMENTARY NOTES	12. SPONSORING MILITARY ACTIVITY
	National Aeronautics and Space Administration George C. Marshall Space Flight Center, Huntsville, Alabama

13. ABSTRACT

Techniques are discussed for the classification of remote objects and materials on the basis of the spectrum of the solar radiation they reflect and of the thermal radiation they emit. A specific system for optimizing and evaluating the most promising of these techniques is recommended and described. It consists of an analyzer, a processor, and an airborne data-collection subsystem. The airborne subsystem includes an optical-mechanical ground scanner with which has been integrated a multichannel spectrograph, a control console, and a multichannel tape recorder. This subsystem will collect multichannel spectral data from the strip of territory being overflown. (The video data in any one channel could be used to construct a monochromatic strip map.) These data are recorded on parallel channels, one for each spectral interval. The tapes are later fed to the analyzer, which performs a statistical analysis of selections of the data corresponding to particular classes of objects or materials. The reduced statistics can then be used as classification keys in the processor. By using keys corresponding to a target and appropriate backgrounds, the processor can then locate specific targets from new data obtained with the airborne subsystem. The output of the processor might be in the form of maps showing the distribution of the target(s) of interest or in the form of the statistics of such distributions.

DD FORM 1 JAN 64 1473

UNCLASSIFIED

Security Classification

14. KEY WORDS	LINK A		LINK B		LINK C	
	ROLE	WT	ROLE	WT	ROLE	WT
Spectrum matching Imaging Target location						

INSTRUCTIONS

1. ORIGINATING ACTIVITY: Enter the name and address of the contractor, subcontractor, grantee, Department of Defense activity or other organization *(corporate author)* issuing the report.

2*a*. REPORT SECURITY CLASSIFICATION: Enter the overall security classification of the report. Indicate whether "Restricted Data" is included. Marking is to be in accordance with appropriate security regulations.

2*b*. GROUP: Automatic downgrading is specified in DoD Directive 5200.10 and Armed Forces Industrial Manual. Enter the group number. Also, when applicable, show that optional markings have been used for Group 3 and Group 4 as authorized.

3. REPORT TITLE: Enter the complete report title in all capital letters. Titles in all cases should be unclassified. If a meaningful title cannot be selected without classification, show title classification in all capitals in parenthesis immediately following the title.

4. DESCRIPTIVE NOTES: If appropriate, enter the type of report, e.g., interim, progress, summary, annual, or final. Give the inclusive dates when a specific reporting period is covered.

5. AUTHOR(S): Enter the name(s) of author(s) as shown on or in the report. Enter last name, first name, middle initial. If military, show rank and branch of service. The name of the principal author is an absolute minimum requirement.

6. REPORT DATE: Enter the date of the report as day, month, year, or month, year. If more than one date appears on the report, use date of publication.

7*a*. TOTAL NUMBER OF PAGES: The total page count should follow normal pagination procedures, i.e., enter the number of pages containing information.

7*b*. NUMBER OF REFERENCES: Enter the total number of references cited in the report.

8*a*. CONTRACT OR GRANT NUMBER: If appropriate, enter the applicable number of the contract or grant under which the report was written.

8*b*, 8*c*, & 8*d*. PROJECT NUMBER: Enter the appropriate military department identification, such as project number, subproject number, system numbers, task number, etc.

9*a*. ORIGINATOR'S REPORT NUMBER(S): Enter the official report number by which the document will be identified and controlled by the originating activity. This number must be unique to this report.

9*b*. OTHER REPORT NUMBER(S): If the report has been assigned any other report numbers *(either by the originator or by the sponsor)*, also enter this number(s).

10. AVAILABILITY/LIMITATION NOTICES: Enter any limitations on further dissemination of the report, other than those imposed by security classification, using standard statements such as:

(1) "Qualified requesters may obtain copies of this report from DDC."

(2) "Foreign announcement and dissemination of this report by DDC is not authorized."

(3) "U. S. Government agencies may obtain copies of this report directly from DDC. Other qualified DDC users shall request through

_____."

(4) "U. S. military agencies may obtain copies of this report directly from DDC. Other qualified users shall request through

_____."

(5) "All distribution of this report is controlled. Qualified DDC users shall request through

_____."

If the report has been furnished to the Office of Technical Services, Department of Commerce, for sale to the public, indicate this fact and enter the price, if known.

11. SUPPLEMENTARY NOTES: Use for additional explanatory notes.

12. SPONSORING MILITARY ACTIVITY: Enter the name of the departmental project office or laboratory sponsoring *(paying for)* the research and development. Include address.

13. ABSTRACT: Enter an abstract giving a brief and factual summary of the document indicative of the report, even though it may also appear elsewhere in the body of the technical report. If additional space is required, a continuation sheet shall be attached.

It is highly desirable that the abstract of classified reports be unclassified. Each paragraph of the abstract shall end with an indication of the military security classification of the information in the paragraph, represented as *(TS)*, *(S)*, *(C)*, or *(U)*.

There is no limitation on the length of the abstract. However, the suggested length is from 150 to 225 words.

14. KEY WORDS: Key words are technically meaningful terms or short phrases that characterize a report and may be used as index entries for cataloging the report. Key words must be selected so that no security classification is required. Identifiers, such as equipment model designation, trade name, military project code name, geographic location, may be used as key words but will be followed by an indication of technical context. The assignment of links, rules, and weights is optional.